Alma Mater Studiorum – Università di Bologna

DOTTORATO DI RICERCA IN

Scienze Biomediche e Neuromotorie

Ciclo XXXIII

Settore Concorsuale: 05/D1

Settore Scientifico Disciplinare: BIO/09

Prenatal treatment with the flavonoid 7,8-DHF improves trisomy-linked proliferation defects in numerous brain regions of the Ts65Dn model of Down syndrome

Presentata da: Beatrice Uguagliati

Coordinatore Dottorato

Prof. Pietro Cortelli

Supervisore

Dott.ssa Sandra Guidi

Co-Supervisore

Prof.ssa Elisabetta Ciani

Esame finale anno 2020

TABLE OF CONTENTS

ABBREVIATION LIST

5-HT= Serotonin
7,8 DHF= 7,8-Dihydroxyflavone
Aβ= Amiloid β
AD= Alzheimer disease
ADNP = Activity dependent Neuroprotective protein
APP= Amiloid β (A4) Precursor Protein
ARNT= Aryl hydrocarbon receptor nuclear translocator
ASD= Autism spectrum disorder
BBB= Blood brain barrier
BDNF= Brain derived neurotrophic factor
BrdU= 5-Bromo-2-deoxyuridine
CA1= Conus Ammonis 1
CA2= Cornus Ammonis 2
CA3= Cornus Ammonis 3
CAM kinase= Ca2+-calmodulin-dependent protein kinase
cCX= Caudal neocortex
CNS= Central nervous system
CP= Cortical-plate
CREB = cAMP response element-binding protein
cSVZ= Caudal subventricuar zone
CX= Neocortex
DAG = 1,2-Diacylglycerol
DG= Dentate gyrus
DS= Down Syndrome
DYRK1A= Dual-specificity tyrosine-phosphorylated regulated kinase 1A.
E# =Embryonic day #
EGCG =Epigallo-catechin-3-gallate
ERK =Extracellular signal regulated kinase
GM= Grey matter
GW#= Gestational week #
HSA21= Human chromosome 21
HYP= Hypotalamus
ID= Intellectual disability
iNOS= Inducible nitric oxide synthase
IP3= inositol-1,4,5-triphosphate
IPSCs= Human pluripotent stem cells
LSD= Least significance difference
LTP= Long term potentiation

MAPK=Mitogen-activated protein kinase
Mmu= Murine chromosome
NAP= NAPVSIPQ peptide
NFAT= Nuclear factor of activated T cells
NT-3= Neurotrophin-3
NT-4/5= Neurotrophin-4/5
P= Postnatal day
p75NTR= Receptor p75
PI3K= PI3 kinase
PKC = Protein kinase C
PSD-95= Post-synaptic density protein 95
rCX= Rostral neocortex
ROS= Reactive oxygen species
rSVZ= Rostral subventricular zone
SAL= SALLRSIPA peptide
SGZ= Subgranular zone
SP= Sub-plate
STR= Striatum
SVZ= Subventricular zone
SYN= Synaptophysin
TH= Thalamus
Trk= Tropomyosin-related kinase
TrkB-FL = TrkB full length
VZ= Ventricular zone
WM= White matter

ABSTRACT

Down syndrome (DS) is a genetic condition due to the triplication of human chromosome 21. DS has a worldwide incidence of 1:700-1000 live births. The phenotype of DS has been linked to an extra copy of one or more of about 300 protein coding genes. Although DS has a high genetic complexity and a broad phenotypic variability, intellectual disability (ID) is the unavoidable hallmark and the most invalidating feature of DS. ID, that lifelong affects people with DS, is mainly due to neurodevelopmental alterations among which neurogenesis reduction appears to play a particularly prominent role. Mouse models that mimic human pathologies are becoming invaluable tools, because they can be exploited in order to clarify the mechanisms underpinning a given pathology and to examine the outcome of targeted therapies. The most studied DS mouse model is the Ts65Dn mouse whose phenotype largely mimics the human condition. Despite intense efforts of the scientific community, there are currently no therapies for DS. Considering the time course of brain development and that the bulk of neurogenesis takes place during the embryonic period, therapeutic interventions aimed at correcting brain developmental defects should be started prenatally. Pharmacological interventions during the extremely delicate embryonic periods may pose some caveats. Therefore, it is important that therapies are based on molecules with a safe profile. 7,8-DHF is a natural flavonoid present in fruits and vegetables, is able to cross the blood brain barrier, and specifically binds the TrkB receptor activating its downstream signaling cascade. We previously found that neonatal treatment with 7,8-DHF improves cellularity and restores dendritic pathology in the hippocampus of the Ts65Dn model of DS. Based on these premises the goal of the current study was to establish whether prenatal treatment with 7,8-DHF is able to rescue defective neurogenesis in Ts65Dn mouse brain. To this purpose Ts65Dn pregnant females were treated with 7,8-DHF from embryonic day 10 until delivery. On postnatal day 2 (P2) the pups were injected with BrdU and killed after 2 h. In P2 mice, we evaluated the number of proliferating (BrdU+) cells in various forebrain neurogenic niches. Namely the rostral and caudal subventricular zone, dentate gyrus, rostral and caudal neocortex, striatum, thalamus and hypothalamus. We found that in treated Ts65Dn mice the proliferation potency was improved or even restored in most of the examined regions. Moreover, treatment restored cellularity in layer II of the neocortex but not in the hippocampus. These results show that 7,8-DHF has a positive influence on prenatal neurogenesis and cortical cellularity in the Ts65Dn mouse model, but, unlike neonatal treatment, it has moderate effects on hippocampal cellularity. Since 7,8-DHF is orally bioavailable, and in view of his chemical nature and no reported side effects, maternal supplementation with this molecule

should be considered as a promising strategy for the improvement of overall brain development in DS.

INTRODUCTION

Down syndrome

Down syndrome (DS) OMIM 190685, a genetic condition due to the triplication of human chromosome 21 (HAS21), is the most common viable chromosomal abnormality in humans. DS has a relatively high incidence, occurring in 10-14 out 10000 live births in Europe and United States respectively (Dierssen, 2012). Approximately 0.45% of all human conceptions are trisomic for HAS21 (Ruparelia, 2013). DS is characterized by different and variable phenotypic traits, but intellectual disability (ID) is the common hallmark of this pathology. People with DS suffer of abnormalities in learning, memory, and language. Their cognitive profiles may be different in terms of both the severity of cognitive disability and the type of cognitive function affected. In the past decades, there has been a substantial improvement in the life expectancy for people with DS. The survival rate for children under one year of age has changed from less than 50% in the 1940s to a 4.4% in the 2000s. Thanks to appropriate early medical care and changes in the attitude of the community now people with DS can live longer (around 60 years of age). Moreover, their quality of life has also notably improved (Arumugam, 2016).

Etiology

The majority of DS cases (95%) are due to free trisomy 21 with a nondisjunction during meiosis (Bull, 2011). Non disjunction occurs because of aberrant cell division during the formation of ovum or sperm, resulting in an extra chromosome 21 (Arumugam, 2016). Nondisjunction is more likely in mothers, especially in older ones, but it can occur at any maternal age (Driscoll, 2009). Another genetic rearrangement that can cause DS is translocation (3-4%). In this condition, an additional copy of chromosome 21 is partially or fully translocated to another chromosome, usually chromosome 14 or 15 (Arumugam, 2016; Asim, 2015; Bull, 2011). The remaining 1-2 % of individuals with DS show mosaicism for trisomy 21, with both normal and trisomy 21 cell lines in the same individual. Mosaicism results when an error occurs during mitotic cell division soon after conception. Persons with mosaicism may be more mildly affected than persons with complete trisomy 21 or translocation (Asim, 2015; Bull, 2011; Pangalos, 1994; Papavassiliou, 2013). While nondisjunction and mosaicism mechanism are not usually inherited, some cases of DS that result from translocation are associated with a genetic risk that can increase the probability of DS offspring (Arumugam, 2016; Bull, 2011).

Clinical features

Although DS has a high genetic complexity and a broad phenotypic variability, due to allelic variation, genomic imbalance, epigenetic or environmental factors (Lott, 2010) there are various conserved features occurring in all individuals with DS. **Congenital heart disease** is one of the main clinical features that affects people with DS (Versacci, 2018). The most frequent heart defects in DS are atrioventricular septal defect, atrial septal defects, ventricular septal defect, and tetralogy of Fallot (Asim, 2015; Versacci, 2018). It must be noted that children with DS with an associated congenital heart disease have poorer neurodevelopmental outcomes, probably due to a reduced cerebral oxygen delivery (Baburamani, 2019). Individuals with DS present a large number of **gastrointestinal defects**, such as duodenal and anal stenosis and the most frequently occurring Hirschprung disease (Arumugam, 2016). Children with DS are more likely than other children to have some **hematological aberrations and disorders**. These include polycythemia, macrocytosis and a transient myeloproliferative disorder (Roizen, 2003). Individuals with DS are also 10-20 fold more likely to develop **leukemia**, usually during early childhood (Asim, 2015). Almost all children with DS suffer of **muscle hypotonia**, usually related to skeletal muscles, that could result in ligamentous laxity and lead to a delay in developmental milestones (Dey, 2013; Lott, 2012).

THE HUMAN CHROMOSOME 21

DS is a disorder of gene expression, as it is characterized by the presence of an additional copy of the HAS21. HSA21 is the smallest human chromosome. The length of 21q is 33.5 Mb and that 21p is 5-15 Mb (Asim, 2015). Sequencing of HSA21 was completed in the year 2000 within the Human Genome Project (Hattori, 2000). Overall, HSA21 is among the poorest chromosomes in terms of functional DNA elements per Mb and this could be the reason why DS is a viable condition in the postnatal period (Antonarakis, 2017). However, HSA21 is among the richest chromosomes for long non-coding RNA encoding genes and among the poorest for microRNA encoding genes. HSA21 is also poor for other non-coding RNA, long interspersed nuclear elements and short interspersed nuclear elements (Antonarakis, 2017). Nonetheless, HSA21 encodes several classes of non-coding RNA and the overexpression of some of them may contribute to different phenotypes of DS. The overexpression of protein coding genes and non-coding RNA affects several cellular functions and developmental process. Among the proteins encoded by HSA21, 23 proteins are involved in signal transduction and 31 proteins are transcription factors that may influence the expression of other

genes (Antonarakis, 2017). The advances in the functional exploration of the genome have helped to understand the phenotypic impact of the triplication of HSA21 regarding the molecular mechanism of the early onset of Alzheimer disease (AD) in DS, the molecular basis of the higher incidence of leukemia and the identification of HSA21 regions that harbor functional elements or causative genetic variation for certain DS typical phenotypes (see(Antonarakis, 2017)).

HUMAN BRAIN DEVELOPMENT

In this chapter, the ontogenesis of the human central nervous system (CNS) is briefly reviewed. According to the common nomenclature referring to gestation, the embryonic period starts at conception and lasts until the end of the seventh gestational week (GW) and the period from GW8 to delivery is called fetal period. Nonetheless, some authors use the term embryonic for periods extended beyond the seventh GW.

The development of the human CNS is a protracted and neatly orchestrated chain of specific ontogenetic events that begin during the third GW and extend to late adolescence and, conceivably, throughout the whole lifespan. Neurogenesis begins on embryonic day 42 (E42) and is completed by midgestation. By the end of the prenatal period major fiber pathways are complete. Postnatally, brain development continues, the brain size increases by four-fold during early childhood and reaches 90% of adult volume by the age of 6. Structural changes both in white matter (WM) and grey matter (GM) continue throughout childhood and adolescence, and these changes in structure parallel changes in functional organization that are also reflected in behavior. Both gene expression and environmental input are essential for normal brain development, and disruption of either can alter the neural outcomes (de Graaf-Peters, 2006; Stiles, 2010).

The prenatal brain

Two weeks after conception the embryo is an oval-shaped two-layered structure, with the upper layer containing epiblast cells that will differentiate into the three primary stem cells lines and the lower layer containing hypoblast cells that will form extraembryonic tissues. During gastrulation, GW3, neural stem cells start to differentiate from the stem cells lines as a result of complex molecular signaling, such as gene expression as well as environmental cues. Neural progenitors lay in the region of the embryo called neural plate. The subsequent folding of the neural plate will form a hollow tube, called neural tube, which is the first step in the establishment of the CNS. The neural progenitors located in the most rostral part of the neural tube will give rise to the brain, while the more caudal cells will give rise to the hindbrain and spinal cord (Stiles, 2010). As the brain grows and becomes more complex, the shape of the hollow cavity changes, forming the ventricular systems of the brain. The neural progenitors are located in the region that will become the ventricles of the brain, the ventricular zone (VZ). By the end of GW8 the shape of the nervous system undergoes drastic changes. The anterior part of the neural tube expands, forming three brain

vesicles. The most anterior one is called the prosencephalon, from which the telencephalon and the diencephalon will be arranged. The middle vesicle is the mesencephalon, precursor of midbrain structures, and the most posterior is the rhombencephalon, which will be further subdivided into the metencephalon and myelencephalon (Stiles, 2010).

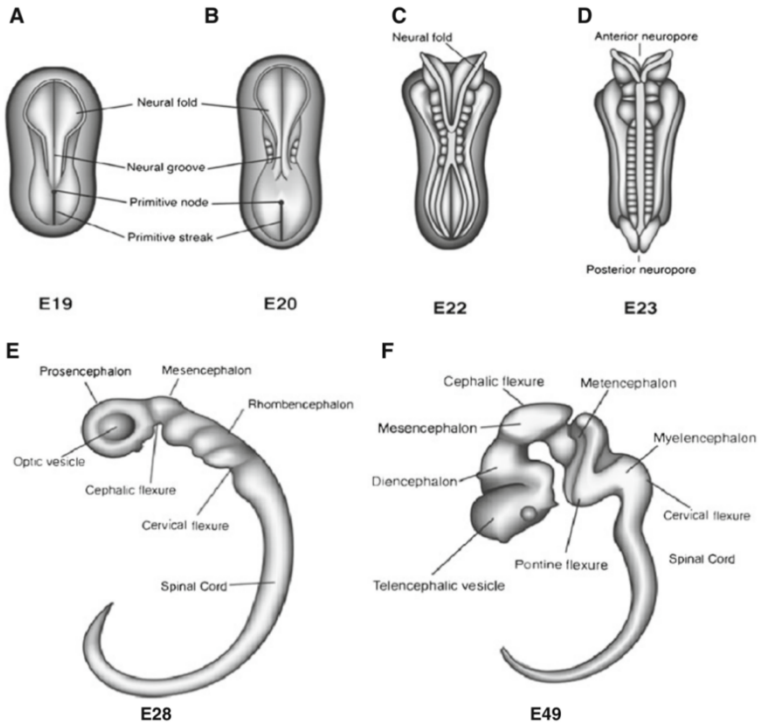

Fig. 1. Changes in the morphology of the embryo. *A. The emergence of the neural ridges on E19. B. Folding of the neural ridges and neural tube formation. C, D. Closure of the neural tube. E. Following the closure of the neural tube, the embryo begins to expand particularly in anterior regions. The primary vesicles are evident by E28. These include the Prosencephalon, Mesencephalon, and Rhombencephalon. F. By E49 the secondary vesicles emerge. The Prosencephalon differentiates into the Telencephalon and Diencephalon, and the Rhombencephalon into the Metencephalon and Myelencephalon. E=embryonic day. From (Stiles & Jernigan, 2010).*

From GW9 the fetal period begins and the gross morphology oh the brain undergoes dramatic changes. The brain from a lissencephalic structure gradually develops the characteristic pattern of sulcal and gyral folding. The first evidence of the future cortex is the formation of the preplate, a transient structure that contains various predecessor cells migrating to their final destination. The preplate is located between the proliferative zone and the pial surface, which is the outer surface of the developing brain. When migrating neuroblasts reach the preplate, their migration stops and the preplate is split into two layers: the future cortical layer I and the subplate. The subplate is a temporary target of afferent fibers originating from the thalamus, brainstem nuclei, and hemispheres and also acts as a reservoir for maturing neurons and transient synapses. It regresses

after 31 weeks, coinciding with the expansion of gyration, and completely disappears after birth (Girard, 2016).

At GW7, the germinal matrix can be divided into VZ, and an underlying subventricular zone (SVZ). Approximately from E25 to E42 the population of neural stem cells, located in the proliferative niches, divides in a symmetrical mode and from one neural progenitor the division produces two identical neural progenitor cells. From E42, the cell division gradually shifts to an asymmetrical mode and from one neural progenitor the division produces one neural progenitor and one neuron. The new progenitor remains in the proliferative niche and continues to divide, while the postmitotic neuron leaves the proliferative zone and migrates to the neocortex. In most areas of the human brain neurogenesis is completed by approximately E108 (de Graaf-Peters, 2006; Jessell, 2000; Stiles, 2010). Neurons arise in the VZ and SVZ and migrate radially to their definitive destination before or during differentiation. Early in development the distance neurons must traverse is small, thus they migrate using somal translocation; the neuron extends a basal process out of the VZ to the pial surface, the nucleus of the cell moves up trough cytoplasm of the basal process and reaches the pial surface. As development proceeds the distance becomes larger and neuron migration requires a special cell population, the radial glial cells. The radial glia cell extend a process from the VZ to the pial surface and the migrating neurons use the radial glia process as a scaffold to migrate into the developing cortical plate (Bystron, 2008; Jessell, 2000; Stiles, 2010).

During early brain development neural progenitor cells are able to produce any neuron type, but as development proceeds following intrinsic cell signaling, they became more restricted in the types of neurons they can produce. The selection of the neural fate depends on diverse cellular signaling and complex molecular interactions between neurons and glia cells regulate the cellular migration. Moreover, a relationship exists between the time a neuron is born and differentiates and its final destination. For example, the migration of the cells that are going to shape the cerebral cortex occurs in an inside-out order with the oldest neurons travelling to the deepest cortical layer, and the youngest neurons locating in the more superficial layers (de Graaf-Peters, 2006; Girard, 2016).

Once neurons have reached their target region they arborize and branch in order to establish appropriate connections with other neurons and become part of processing networks. Once the axon has reached its target, synapses are formed with the target cell (Jessell; Stiles, 2010). Dendritic development starts early during fetal life, accelerates from the third trimester, and remains active till the end of the first postnatal year. Several growth factors such as the brain-derived neurotropic factor (BDNF), nerve growth factor (NGF) and glia-derived growth factor influence the migration and

maturation of neurons that reaches the highest levels during the prenatal period when neurons first establish synaptic contacts. Finally, immediately before birth approximately 50% of all neurons are eliminated with the goal to increase efficiency of synaptic transmission and for the establishment of functional networks in the developing brain (Andersen, 2003; de Graaf-Peters, 2006; Girard, 2016; Stiles, 2010). In the human forebrain, neocortical neurons are generated during a restricted period that begins at approximately GW6 and is largely completed by GW18. By GW24, the size of the VZ and SVZ is considerably reduced and there is a marked decrease in proliferative activity. While, in the dentate gyrus (DG) and cerebellum the period of neurogenesis is prolonged in comparison with the other brain regions, neurogenesis begins at approximately GW 12 and is almost accomplished within the first postnatal year (Stagni, 2018a).

Neurons are thought as the fundamental unit of the CNS, but they are dependent on, interact with and are surrounded by glia cells. Similarly to neurogenesis, gliogenesis within the CNS occurs during embryonic development. The peak of gliogenesis takes place between GW20 and GW40, after the peak of neurogenesis has passed. Macroglia cells arise from neural progenitors in the VZ and SVZ, as neurons themselves, and then migrate to their final destination. The most prominent macroglial populations are oligodendrocytes, responsible for the formation of myelin, and astrocytes, which play a role in the regulation of the composition of extracellular environment, clearance of excess of neurotransmitters and modulation of formation and efficiency of synaptic connections (de Graaf-Peters, 2006).

Neurotransmitters and neuromodulatory substances play a fundamental role in the development on the nervous system, driving neuronal migration and differentiation and shaping synaptic circuitries. The major neurotransmitters are present from early prenatal stages onwards and their relative expression and concentration can change throughout pregnancy and postnatally. Nicotine acetylcholine receptors can be detected in different brain areas from GW6. After GW24 cholinergic innervation obtains a pattern of topographical relationship which can be compared to that of the human adult brain. The catecholaminergic system also emerges during early development, dopaminergic and noradrenergic cells can be found in several brain areas at GW8 and between GW22-26 dopaminergic and noradrenergic innervation becomes visible throughout the cerebral cortex. GABAergic cells originate in the ganglionic eminence. During early development the GABA inhibitory neurotransmitter acts as an excitatory transmitter; the switch from excitatory to inhibitory occurs during the last trimester of gestation. Glutamate receptors are found in the fetal cortex starting from GW10, with two different period of transient increased expression. The

serotoninergic innervation occurs very early and does not change after the fetal age (de Graaf-Peters, 2006; Girard, 2016).

The postnatal brain

As mentioned above, at advanced stages of embryogenesis the VZ decreases in size and is gradually replaced by the SVZ, that plays pivotal role in corticogenesis during the early postnatal period. However, after early infancy, the human SVZ shows little to no neurogenesis. The few existing neuroblasts found in the adult SVZ migrate to the olfactory bulbs at lower extent. Neurogenesis in the DG continues, at a slow rate, throughout the whole life. Granule neurons are generated in the subgranular layer from which they migrate to the nearby granular layer (Conover, 2017). Unlike neurogenesis, proliferation and migration of glial precursors continues for an extended period after birth and the process of differentiation and maturation of astrocytes and oligodendrocytes continues throughout childhood. The myelination process occurs in a linear way throughout childhood and adolescence. Glia cells contribute to the maintenance of axonal integrity and neuronal survival through the release of trophic factor. The length of axons and dendrites increases five to ten times during the first six postnatal months and dendritic growth of cortical neurons continues till the age of 5 years. In parallel to the axonal and dendritic development the number of synaptic connections increases. In the developing brain the number of connections is exaggerate both at the macroscopic level within the major brain areas that form transient connections through the brain, and at the microscopic level, with the number of synapses during the early postnatal period that doubles that observed in the adult brain (Foulkes, 2018; Girard, 2016; Stiles, 2010). During the preadolescence period, a second wave of neuronal rearrangement occurs with the pruning of synapses, receptors, and overproduced glia cells. Many factors concur to the retention and eliminations of connections, such as competition for resources and afferent input. The process of synapse production and elimination is different across brain regions and parallels the functional development of each region (Andersen, 2003; Khundrakpam, 2016; Stiles, 2010).

During adolescence, the human brain undergoes significant structural change also in terms of GM volume, surface area and cortical thickness, as well as WM volume and microstructure. The total volume of the WM increases during childhood and adolescence, probably reflecting increased myelination, leading to better connectivity as well as enhanced signal integration. In contrast, the volume of the cortical GM increases during early childhood but subsequently declines throughout adolescence, reflecting the initial synapse overproduction and the subsequent pruning. It is

interesting to note that the age of peak of GM density is associated with specific functional and cognitive development. It has been observed earliest in primary sensorimotor areas and latest in higher-order association areas (Girard, 2016; Khundrakpam, 2016).

As a physiological process, the human brain shows a progressive decline during aging. The brain shrinks during advanced age, with reductions in both GM and WM and an associated enlargement of the cerebral ventricles. GM volume begins to decrease after adolescence. The age-related reduction in the GM is most prominent in the temporal and frontal lobes (Mattson, 2018). The brain atrophy and the decline in GM volume in older adults is explained not only by neuronal death but also by a decrease in cells size, decreased number of connections between neurons, reduced complexity of dendrite arborization and length, and decreased dendritic spines. During advanced life stages, a reduction in WM volume also emerges. A 16% to 20% decrease in the volume of WM has been demonstrated in subjects older than 70 years in comparison with younger subjects (Harada, 2013).

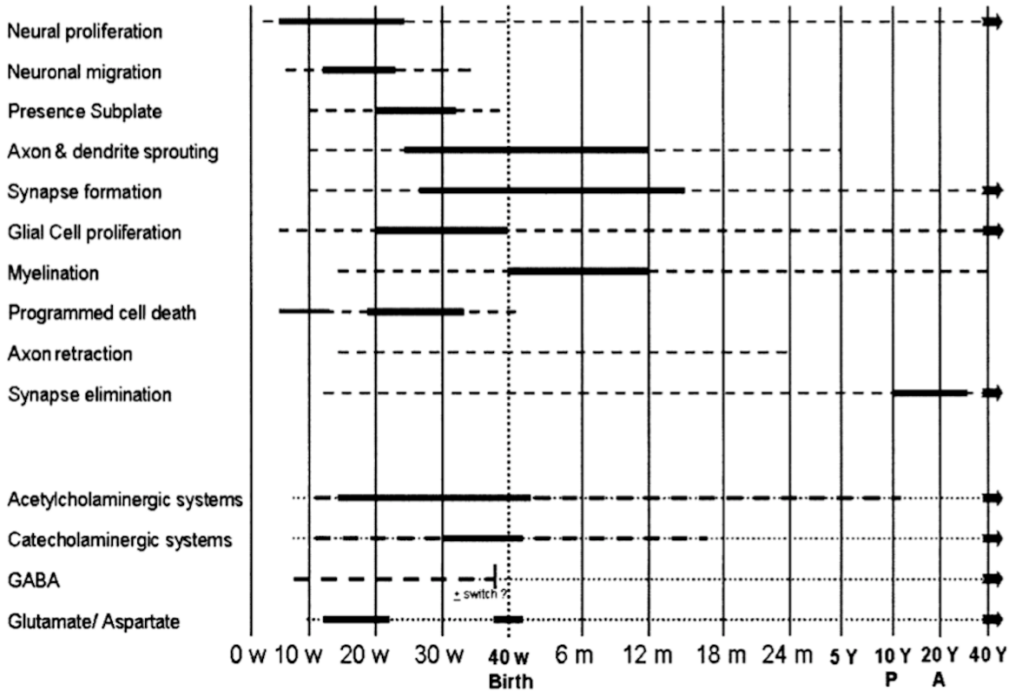

Fig. 2. Timing of neurobiological processes in the telencephalon during human ontogeny. *W= week, M= postanal months, Y= years, P= onset of puberty, A= onset of adulthood. The broken line means that the process is active, a bold line indicate that the process is very active. In the lower part, the development of various neurotransmitter system is represented, thin broken line means that the transmitter is present, a continuous bold line represents an overexpression of the transmitter. The increasing dot density in the catecholaminergic systems denote the gradual increase in dopaminergic activity. The bold broken line in the GABAergic systems reflects that GABA in early life exerts an excitatory function and later switches to its inhibitory function. From (de Graaf-Peters, 2006).*

BRAIN DEVELOPMENT IN DOWN SYNDROME

The prenatal brain

DS is characterized by brain hypotrophy and intellectual disability starting from early life stages. Several studies have focused on the neuroanatomical correlates of cognitive impairment in DS. This section summarizes information on neuroanatomical defects and neurogenesis alterations in the brain of individuals with DS, starting from early developmental stages.

Individuals with DS have an overall reduced brain volume and numerous brain regions appear to be smaller in comparison with controls (Stagni, 2018a). A pioneering study by Schmidt-Sidor in fetuses at GW15-22 found no gross differences in brain shape, weight and fronto-occipital length and no differences in the volume of the cerebellum and hippocampus (Schmidt-Sidor, 1990). This is in contrast with the hypotrophy of the DS brain reported in other following studies regarding the DS fetal brain. The absence of differences in Schmidt-Sidor's study may be attributable to the fact that fetuses were not stratified by age, which, may obscure differences between DS and non-DS fetuses. In fact, the evaluation of the brain of fetuses with DS during restricted time windows revealed a reduction in brain size starting from 4-5 month-old-fetuses (Guihard-Costa, 2006). A size reduction has been revealed in various brain structures such as the subiculum, hippocampus, inferior temporal region, and cerebellum of fetuses with DS at GW17-22 (Guidi , 2008; Guidi, 2011; Guidi, 2018; Stagni, 2018; Stagni, 2019). Moreover, in addition to weight and volume alterations, the fetal DS brain is brachycephalic due to a reduction in the length of the frontal lobe and an increase in the transparietal length (Guihard-Costa, 2006). It has been suggested that the neurodevelopmental abnormalities of DS arise from a decreased production of neurons during critical phases of brain development. Indeed, several studies reported a reduced number of neurons in several brain regions of fetuses and children with DS (Guidi , 2008; Stagni, 2018b; Stagni, 2018a). It has been proposed that aberrant copies of a single chromosome could alter the cell cycle and, thus, the proliferation rate during development. Accordingly, it has been hypothesized that in DS, an extra copy of chromosome 21 may affect the cell cycle of neuronal precursor cells during neurogenesis. In fact, in fetuses with DS (GW17-23) the number of proliferating cells is reduced in the DG of the hippocampus, hippocampus proper, parahippocampal gyrus, the germinal matrix of the inferior horn of the lateral ventricle, external granular layer of the cerebellum, in a region of the fifth cerebellar lobe that is the remnant of the cerebellar ventricular zone (Contestabile, 2007; Guidi, 2011), and in the frontal cortex (GW 18) (Lu, 2012). The analysis of the cell cycle of trisomic neural

progenitors has demonstrated an elongation of the G2 phase, which possibly accounts for the reduced proliferation rate found during neurogenesis in the DS brain (Contestabile, 2007; Guidi, 2008). In addition to having a reduced number of neurons, the cortex of fetuses with DS exhibits a delay in the emergence of lamination and has a disorganized appearance (Stagni, 2018a). An additional confirmation of defective neurogenesis in DS derives from *in vitro* studies showing that neuronal precursors isolated from DS fetal brains and cultured as neurospheres give rise to reduced numbers of neurons when differentiated (Lu, 2012). The reduced proliferation potency of the trisomic brain is worsened by a reduction in the acquisition of a neuronal phenotype accompanied by a relative increase in the acquisition of an astrocytic phenotype (Guidi, 2008). In addition to neurogenesis impairment, an increase in apoptotic cell death had been found in the DG and SVZ of fetuses with DS, suggesting that alterations of both neurogenesis and programmed cell death may concur to the hypocellularity found in DS brains (Guidi, 2008). However, the role of apoptosis remains unclear and the results from different studies are still contradictory. Upregulation of some pro apoptotic factors, downregulation of anti-apoptotic factors and apoptosis-associated proteins have been found in different cortical and cerebellar regions of DS fetuses (Helguera, 2005; Seidl, 2001). Although some studies reported an enhancement of apoptosis, the number of cells undergoing programmed cell death is very low, suggesting that this process does not have a prominent role in reducing the final neuron number in the DS brain (see (Stagni, 2018a)). Harmonious development of the CNS during prenatal development does not only require an accurate course of genetic schedules but also depends on appropriate signaling processes. Neurotransmitters and neuromodulatory substances have established roles in the maturation of the CNS. Neurochemical alterations of several neurotransmitter systems have been found in the fetal DS brain. In particular, the brain of DS fetuses shows reduced levels of i) GABA, that is the main responsible for the excitatory neurotransmission in the developing brain; ii) taurine, that acts as a neurotropic factor during brain development; iii) dopamine, that is fundamental for the establishment of synaptic contacts; and iv) serotonin (5-HT), that is crucial for neuronal proliferation, differentiation, migration and synaptogenesis (Whittle, 2007).

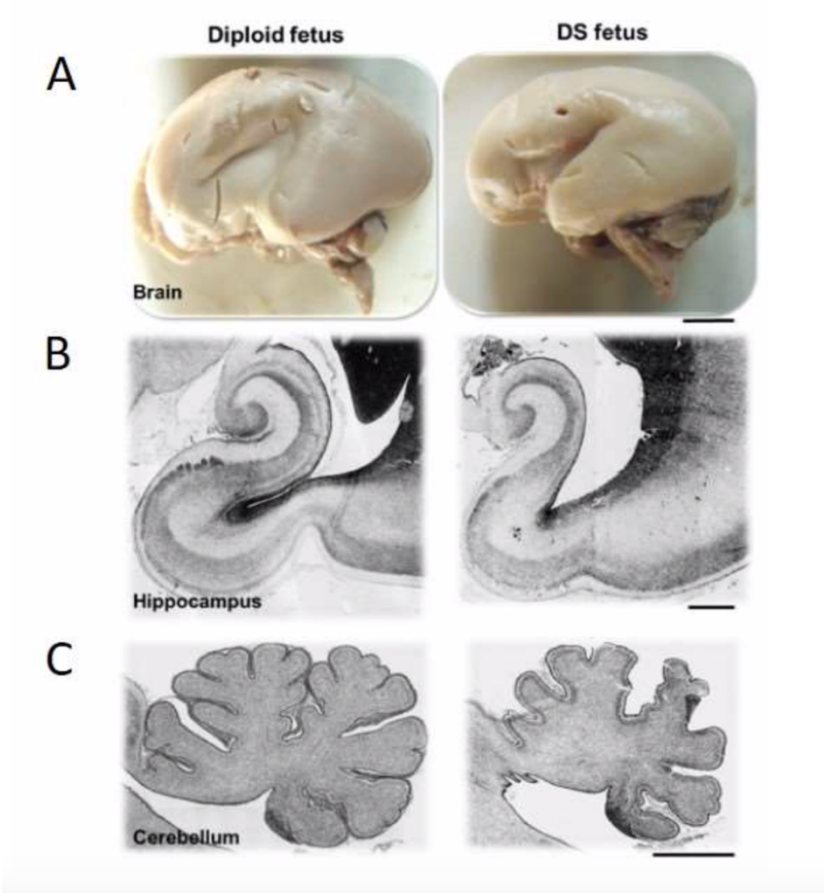

Fig. 3. Brain hypotrophy in DS fetuses. *A-C. Examples of brain (scale bar 1 cm), hippocampus (scale bar 1mm) and cerebellum (scale bar 2mm) of diploid and DS fetuses (GW17-21). DS= Down syndrome. From (Guidi, 2008; Guidi, 2011; Stagni, 2018).*

The postnatal brain

The shape alterations present during fetal life stages are retained in the brain of infants and children with DS. Morphometric studies in children with DS show architectonic abnormalities and reduced cellularity both in cortical and extracortical regions (Stagni, 2018a). The brains of children with DS have a reduced volume in comparison to typical children, both of the GM and WM. With the exception of the occipital lobes, all brain lobes have a reduced size, and volume reduction is also present in the hippocampus and cerebellum (see (Stagni, 2018a)). There is evidence for a reduced number of neurons in the cerebellar granule cell layer and in the cortex of children with DS (Baxter, 2000; Buxhoeveden, 2002). Moreover, the astrocytic hypertrophy and the increase in astrocyte number present in the DS brain during fetal life stages is maintained in adulthood (see (Stagni, 2018a)).

The sprouting of dendrites in the first postnatal period of the typical brain development contrasts with the progressive reduction that affects children with DS. Infants with DS begin their lives with

normal or even increased dendritic branching and abnormalities in cortical dendrites start to appear during the first year of age. The dendritic arborization and the number of dendritic spines poorly increase in children with DS and the dendritic atrophy seen in childhood progresses during adulthood, with marked reduction of dendritic branching, length, and spine density in elderly adults (Becker, 1986; Marin-Padilla, 1976; Takashima, 1981; Takashima, 1994). Given the role of dendrites and dendritic spines as essential structures for brain connectivity and plasticity, it is straightforward to postulate that alterations in these neuronal microcompartments may affect neuronal network activity.

During aging, brain atrophy superimposes on the pre-existing developmental alterations that characterize the brain of people with DS. MRI studies have reported atrophy of the medial temporal lobe, including hippocampus, amygdala, and of neocortical regions such as the corpus callosum and the parietal, frontal, and occipital cortices in aged non-demented DS patients, suggesting prodromal stages of AD-like pathology (Teipel, 2006). Decreased levels of excitatory neurotransmitters, monoamines, histamine, and 5-HT, as well as reduced activity of the histamine synthetase enzyme have been detected in various regions of the adult DS brain, suggesting profound alterations of neuronal network activity. Moreover, deficits in the cholinergic system, similar to those occurring in AD, have been demonstrated in the brain of adult with DS. Degeneration of basal forebrain cholinergic neurons and a decreased activity of choline acetyltransferase, that start during late adolescence and adulthood, have been observed in both DS and AD (Contestabile, 2008; Whittle, 2007).

NEUROLOGICAL DEFECTS IN DOWN SYNDROME

The neuroanatomical alterations that characterize the DS brain from the first embryonic stages of development to old age undoubtedly play a key role on the several neurological problems that affect people with DS. The trisomy of chromosome 21 is the most common genetic cause of intellectual disability and account for 15% of the population with ID (Ruparelia, 2013). DS people show altered cognitive and behavioral phenotypes with a delayed and incomplete acquisition of motor, linguistic and visuospatial abilities, impairments in learning and memory and neurobehavioral disorders (Bartesaghi, 2011). However, there is a great interindividual variability both in the nature and intensity of cognitive impairment (Rueda, 2012).

Intellectual capacity. The intelligence quotient (IQ) in people with DS lays usually in the moderately to severely retarded range (IQ=25-55) and Mental Age is rarely above of 8 years. However, few individuals with DS have been reported to have IQ in the normal range. It must be also remarked that IQ in adults with DS may be also influenced by the increased risk of early onset dementia (Vicari, 2006). It is estimated that among children affected by DS, 10% have profound intellectual disability, 70% severe, and 20% mild or none. Infancy is characterized by a delay in cognitive development and while there is an improvement in cognitive skills during infancy, the IQ plateaus or even decreases starting from adolescence (Dierssen, 2012; Lott, 2010). The behavioral phenotype associated with DS emerges in infancy and accumulates in early childhood, with impairments of speech, language, motor skills, cognition, and adaptive behavior.

Learning and memory impairment. Learning and memory problems in children with DS emerge in late infancy and become more noticeably during adolescence (Lott, 2010), when the acquisition of skills and the cognitive growth become slower (Grieco, 2015). Learning deficits involve both short-term and long-term memory domains. In particular, DS children perform worse than normal children in task requiring explicit type of memory, like verbal short-term memory, while they show normal learning ability in tasks that require implicit memory, indicating a functional dissociation between implicit and explicit memory. Moreover, they show difficulties in both long- and short-term spatial memory, mainly at the levels of encoding and retrieval, but they have normal performance in simple tasks like associative learning, (Godfrey, 2018; Grieco, 2015; Silverman, 2007). Starting from adolescence, deficits in verbal short term memory continue and specific working memory deficits became evident (Godfrey, 2018; Grieco, 2015). Both hippocampal- and prefrontal-related functions appear defective in individuals with DS. Furthermore, children with DS show impairments in distinct aspects of attention, and selective attention deficits persist through

adulthood. Deficit in attention and high processing demand together with impaired language comprehension and weakness in verbal information processing can contribute to adversely impact learning and memory performances in individual with DS (Grieco, 2015). All these defects are probably due to brain structural abnormalities, in particular at the level of the medial temporal lobe and prefrontal cortex (Lott, 2010).

Visuo-spatial abilities. Visuo-spatial short-term memory domain in individual with DS is usually consistent with their mental age. However, in recognition tasks, when memory demand increase or when visual and spatial demands are combined, the performance of DS children is impaired compared with mental age-matched controls (Vicari, 2006; Visu-Petra, 2007).

Linguistic abilities. Despite rare exceptions people with DS usually exhibit very poor linguistic capacities when compared with typical developing peers of the same mental age. Infants with DS show many of the normal features of paralanguage behavior, but they show slowest rates of development in grammatical morphology, a longer period of phonological errors and poorer intelligibility, although language comprehension is more advanced than syntax (Vicari, 2006).

Seizures. It is estimated that 5-13% of children with DS have seizures. Seizures occurrence in DS is bimodal, 40% of people develop seizure before 1 year of age, and another 40% develop seizure after the third decade of life (Lott, 2012; Roizen, 2003). Seizure, if uncontrolled, can impair cognitive function. Infantile spasm and myoclonic seizure in children have been linked to structural brain abnormalities, such as fewer inhibitory neurons, abnormal cortical lamination, and impaired dendritic morphology (Lott, 2010). Seizures in adult with DS are often associated with dementia and early onset of Alzheimer disease (Lott, 2010).

Autism spectrum disorder. In children with DS, ID together with the expression of other social and behavioral differences leads to a profile that carries increased risk for language impairment and other comorbid developmental disorders such as autism spectrum disorder (ASD). Current estimates suggest that approximately 7–19% of individuals with DS have comorbid ASD. Despite the relatively high prevalence of ASD in DS, the nature of this comorbidity is still poorly understood. This has led to discrepant findings regarding the prevalence rate and how to identify ASD in individuals with DS who carry their own phenotypic profile with potentially overlapping features of ASD (see (Channell, 2019)).

Dementia and Alzheimer's disease. Dementia resembling Alzheimer disease (AD) is among the most significant age-associated concerns in DS. By the age of 40 the brain of individuals with DS presents the characteristic signs of AD neuropathology, including senile plaques and neurofibrillary tangles,

and by the age of 65 the majority of people with DS are likely to develop dementia (Godfrey, 2018; Lott, 2012; Ruparelia, 2013). In trisomy 21 there is an overexpression of the gene for APP (Amiloid beta precursor protein) from which the amyloid beta protein derives and intraneuronal accumulation of amyloid beta appears to trigger the neurodegeneration cascade. Moreover, overexpression of DYRK1A (dual-specificity tyrosine-phosphorylated regulated kinase 1A), located on chromosome 21, through the hyperphosphorylation of tau that is responsible for the formation of neurofibrillary tangles, may also contribute to the early onset of neurofibrillary degeneration (Lott, 2012).

MOUSE BRAIN DEVELOPMENT

Mouse models that mimic human pathologies are invaluable tools, that are essential in order to identify the mechanisms underpinning a given pathology and to examine the outcome of targeted therapies. In this chapter, the events that take place during brain development in mice are briefly described, with a particular focus on prenatal neurogenesis.

The prenatal brain

In mammals the neural tube formation is a highly dynamic process that takes place early during embryogenesis, between GW3 and 4 in humans, and between E8.5 and E10.0 in mice (Massarwa, 2013). At E9.5, with the appearance of the cerebral vesicles from the dorsal surface of the rostral neurotube, the development of murine neocortex begins. Initially, the primordial neocortex is comprised of an apparently homogeneous pool of neural stem cells. Starting from E10.5 the first post mitotic neurons of the cortex, the Cajal-Retzius cells, arise. The bulk of neurogenesis in mice takes place at E11, when an active neuronal generation and migration of several neuronal populations occur in many brain regions (Sansom, 2009).

The VZ and SVZ are the two germinal regions of the embryonic mammalian brain. The progenitors of the neurons and glia forming the telencephalon emerge from the embryonic VZ/SVZ of the lateral ventricle. The VZ is the most active neurogenic niche during the early phase of brain development. Soon after the emergence of the first neurons from the VZ, a second proliferative population is discernable at the edges of the VZ, formed by the SVZ cells. The SVZ cell population expands rapidly and becomes the major brain neurogenic niche during the latter third of the prenatal development and peaks in size during early postnatal development (Brazel, 2003). Four distinct divisions of the SVZ can be distinguished in the forebrain during fetal development, the medial ganglionic eminence (MGE), the lateral ganglionic eminence (LGE), the caudal ganglionic eminence (CGE) and the fetal neocortical SVZ (SVZn). Each region is constituted by cell progenitors that generate diverse types of neurons and glia, which will populate different regions of the brain (Brazel, 2003) (Fig. 4). Both the MGE and LGE contribute to the development of several brain structures, including the neocortex, striatum, thalamus, septum, and olfactory bulb. The majority of the MGE progeny contributes to the neocortex, although some evidence suggests that the LGE may play a role in the neocortex formation too. It has been established that neocortical interneurons, Cajal-Retzius cells and GABAergic interneurons arise from the MGE progeny. Both the MGE and LGE contribute to the

formation of the striatum, during embryogenesis, although the major contribute is played by the LGE. The MGE have a key role also in the hippocampal neurogenesis, in particular the MGE is a primary source for hippocampal GABAergic interneurons. The CGE cells migrate to the hippocampus and cortex but also to the nucleus accumbens, bed nucleus of the stria terminalis, hippocampus, select nuclei of the amygdala, posterior striatum, and posterior globus pallidus (Brazel, 2003; Nery, 2002).

The cells that originate from ganglionic eminences contribute also to the gliogenesis of the developing brain. The onset of gliogenesis in the cortex commences after the bulk of neurogenesis has taken place, the appearance of the first differentiated astrocytes occurring around E18. Gliogenesis persists long after neurogenesis has ceased and continues during the postnatal period. The number of mature astrocytes peaks in the neonatal period, and differentiated oligodendrocyte are first seen postnatally (Miller, 2007). The cells of the VZ are direct descendants of the neural plate; they differentiate prenatally into radial glia cells, neurons, and astrocytes. The radial glia spans the width of the developing brain and with their projection serve as a guide for migrating neurons. Immature neurons settle into specific cortical laminae dictated by their birth date and, with the exceptions of the Cajal-Retzius cells, corticogenesis follows an inside-outside pattern, earlier born neurons settle into deeper laminae and later born neurons colonize more superficial layers (Brazel, 2003; Sansom, 2009). It has been suggested that VZ cells preferentially produce deep layer neurons of the neocortex, whereas SVZ cells are destined to produce neurons of the more superficial neocortical layers (Brazel, 2003; Sansom, 2009).

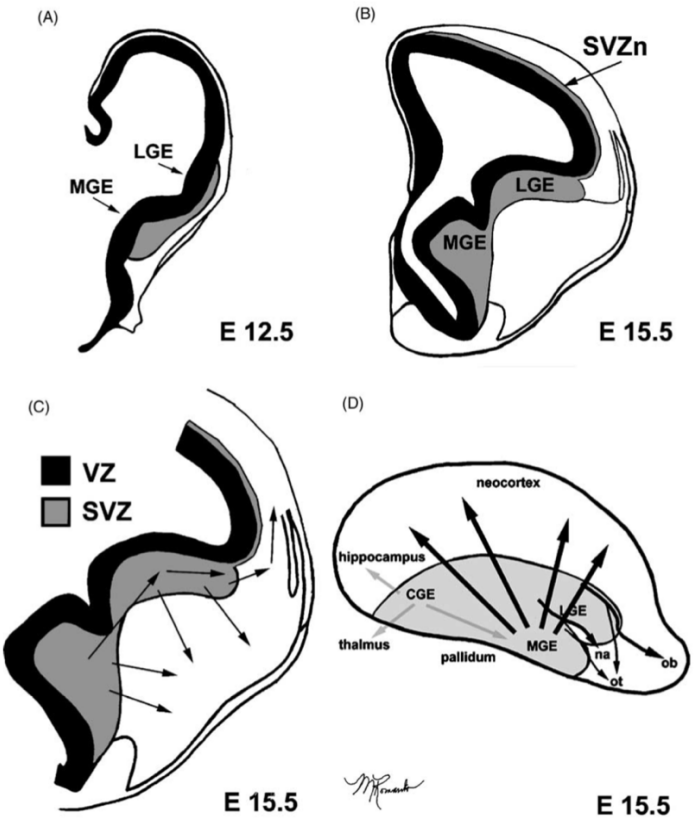

Fig. 4. Contribution of the ventricular zone, subventricular zone, medial ganglionic eminence, lateral ganglionic eminence, and caudal ganglionic eminence to early brain development. *A. Coronal view of the rodent forebrain germinal zones at E12.5. B. The MGE and LGE are prominent structures in E15.5 brain. C. Directional movements of MGE and LGE cells as they migrate. D. Sagittal view of the rodent brain at E15.5 shows directional movements from the MGE, LGE and CGE. CGE=caudal ganglionic eminence; E=embryonic day; LGE=lateral ganglionic eminence; MGE=mediall ganglionic eminence; SVZ=subventricular zone; VZ=ventricular zone. From (Brazel, 2003).*

The postnatal brain

While the bulk of neurogenesis in the mouse brain is a prenatal event, there are two exceptions for this rule, the hippocampal DG, and the cerebellum. The cerebellum appears on E10-12 as an evaginated thickening in the anterior part of the roof of the fourth ventricle (Miale, 1961). Cerebellar neurogenesis begins approximately at E15 and continues in the first two postnatal weeks. Purkinje cells and Golgi cells are generated prenatally, around E11-13 and E12-15, respectively (Fujita, 1967; Miale, 1961). Cerebellar granule cells arise at late embryonic stage and their neurogenesis continues until P15. Cells of molecular layer arise mainly during the first postnatal week (Fujita, 1967; Marzban, 2015; Miale, 1961). By P16 all cerebellar cells types are organized in layers, and the morphology and molecular domains are correlated with the localization of specific cerebellar circuits (Sillitoe, 2007). In the DG of the hippocampus neurogenesis begins during the embryonic period, at E10, but it is not accomplished at birth, it continues until puberty and, at slow

rate, is maintained for the whole life. Neurons forming the DG derive from the hippocampal neuroepitelium which will give rise to the postnatal subgranular zone (SGZ). The SGZ becomes thinner as the DG grows but the granule cell precursors that remain in the SGZ retain their neurogenic abilities in the adult brain. The first granule cells that form the DG are generated in the hippocampal neuroepitelium and migrate to the hilus. The new generated granule cells arise from the germinal zone of the DG and accumulate under the oldest cells. Therefore the DG is shaped in an outside-inside fashion, with the oldest granule cells being the most superficial cells and the youngest being the deeper cells (Altman 1990.; Altman, 1990b).

While neurogenesis, with the exceptions of the DG and cerebellum, is a prenatal event, neuron migration and maturation, as well as differentiation and maturation of astrocytes and oligodendrocytes, occur perinatally (Brazel, 2003; Miller, 2007; Stagni, 2015). Neurons migrate to the GM, WM and striatum using radial glia process as guide to the migration but also nascent WM tracts. Cells continue to divide as they migrate, and their differentiation is regulated by local signals they receive once they cease to migrate (Brazel, 2003). In the postnatal brain the SVZ has replaced the VZ as main source of brain cells and can be divided in a rostral and a dorsolateral part. Cells located in the anterior part of the SVZ are the major source of the rostral migratory stream (RSM) cells. They migrate to the olfactory bulb to become perigromerular and granule cells. In the anterior part of the SVZ, glial precursors also arise that will colonize the anterior part of the neocortex (Pino , 2017; Marshall, 2003). During the perinatal period, the dorsolateral part of the SVZ gives rise to neocortical and striatal glial cells and acts as a major source of GM and WM microglia. Cells born in the dorsolateral part of the SVZ in the perinatal period preferentially colonize the GM, while at the beginning of adolescence they increase their preference towards the WM. Indeed, in rats aged 2 days (P2), 80% of the cells belonging to the dorsolateral SVZ labeled with retrovirus migrate to the neocortex, 10% migrate to the WM, and the remaining cells migrate to either the striatum or to the border regions between WM and neocortex or striatum. In P14 rats, 80% of the labeled cells colonize the WM and the remaining cells migrate to the striatum or to the border region (Brazel, 2003; Levison, 1993).

After P7, the rodent brain starts to acquire the features of a more mature brain. Axons and dendrites arborize, and dendritic spines develop. Synapses mature over the first three postnatal weeks following a different time schedule in diverse brain regions. Oligodendrocytes differentiate and myelination occurs. A wave of functional rearrangement removes, by programmed apoptosis, a

large number of neurons and neuronal processes produced during early brain development (Brumwell, 2006; Rice, 2000).

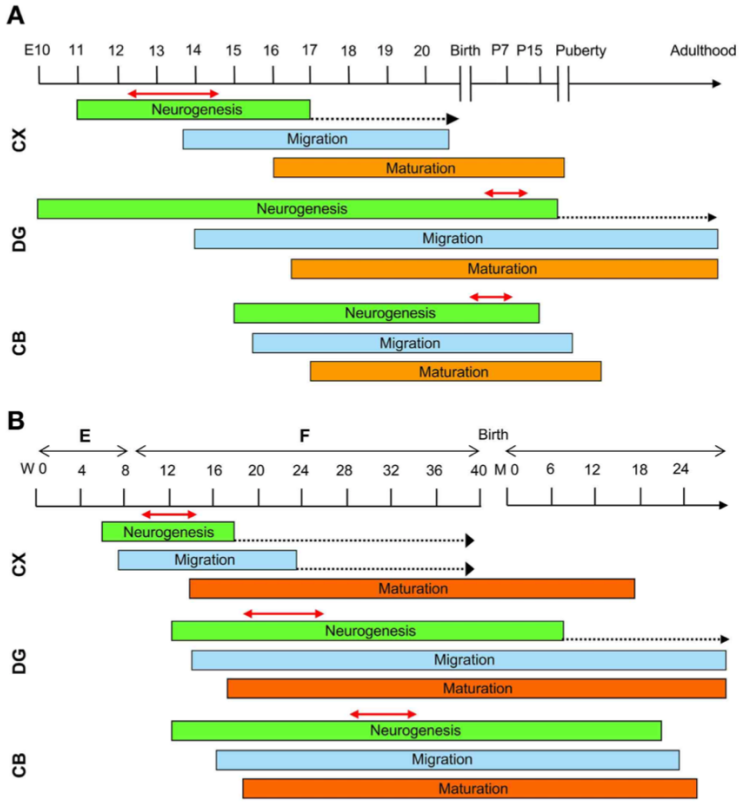

Fig. 5. Schematic representation of the timeline of brain development. *Timeline of neurogenesis, migration and maturation in the cortex, dentate gyrus and cerebellum of mouse (A) and humans (B) during brain development. Dotted arrows indicate a reduction in the rate of neurogenesisis. The double-headed red arrows delineate the period of maximum neurogenesis. CB=cerebellum; Cx=neocortex; DG=dentate gyrus; E=embryonic; F=fetal; M=month; P=postnatal; W=week.*

MOUSE MODELS FOR THE STUDY OF DS

Trisomy 21 is a complex genetic perturbation which makes it difficult to create models of this pathology. To date, various DS mouse models that replicate some aspects of the human condition have been created. The long arm of HSA21 contains 33.7 Mb and approximately includes ~160 encoding proteins with diverse functions, a large family of ~45 encoding apparently redundant keratin associated proteins, and several provisionally annotated microRNA (Gardiner, 2014). The comparative analysis of the chromosomes of human and laboratory mice revealed that the long arm of HSA21 is homologous to portions of three mouse chromosomes (Mmu): Mmu10, Mmu16 and Mmu17. The internal part of Mmu10 contains ~40 protein coding genes, the distal end of Mmu16 contains ~100 HSA21 orthologous protein coding genes and the internal part of Mmu17 contains ~20 protein-coding genes (Antonarakis, 2017; Das, 2011; Gardiner, 2014; Rueda, 2012). Two kinds of mouse models have been developed for investigating the molecular genetics of DS, trisomic and transgenic mouse models. Trisomic mouse models carry complete or segmental trisomy for Mmu10, Mmu16, Mmu17 and are able to mimic the genetic complexity of trisomy. Transgenic mouse models, on the contrary, have been generated to study the effect of cell-specific and stage-specific overexpression of a unique gene (Rachidi, 2008).

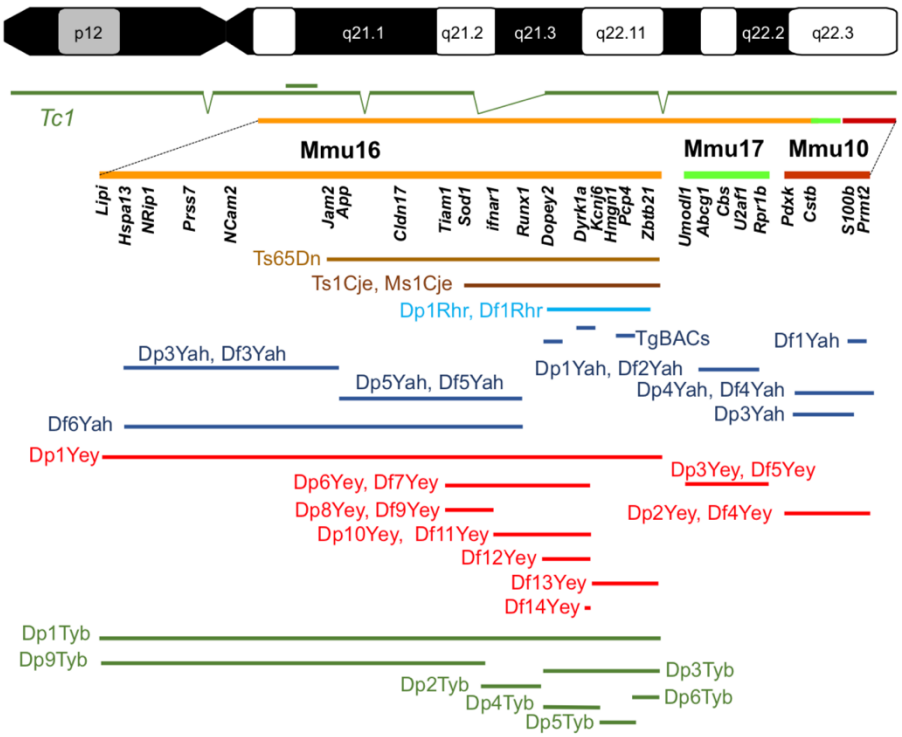

Fig. 6. Trisomic and transgenic mouse models of DS and their syntenic regions on HSA21. *Human chromosome 21 is depicted at the top of the figure, with the mouse genome orthologus region found on Mmu10 (red), Mmu16 (orange), Mmu17 (light green). A few known genes that are homologous to HSA21 genes in the DS critical region are listed below each chromosome. The transchromosomic Tc1 mouse model is shown in dark green, with deletions and a duplication (double bar) relative to HSA21 depicted. Below, the segment of the DS critical region encompassed in different mouse models for DS is illustrated. From (Herault, 2017).*

In the table below the most popular mouse models of DS generated during the last 30 years are briefly described. For more details the reader can refer to several reviews (Hamlett, 2015; Das, 2011; Gupta, 2016; Herault, 2017; Rachidi, 2008).

	Name	Type of mutation	Major Abnormalities	First reference
Model with triplication of the whole Mmu16	Ts16	Trisomic for the whole Mmu16	Decreased brain size; cellular hypoplasia; abnormal neural migration; enhanced oxidative stress; delayed development of sensory organs and skull ossification	(Cox et al., 1985)
Segmental trisomic mice	Ts1Cje	Trisomic for 81 genes located in the region of Mmu16 from *Sod1* to *Mx1*	Embryonic brain alterations; cerebellar volume reduction; abnormal craniofacial development; learning deficits	(Sago et al., 1998)
	Ts2Cje	Translocation of the distal region of Mmu16 onto Mmu12	Spine density reduction	(Villar et al., 2005)
	Ts65Dn	Trisomic for ~104 genes on Mmu16 orthologus to HSA21 genes. Plus an extra segment from Mmu17 with non-DS- related genes.	Decreased brain size; neurogenesis reduction; synaptic defects; dendritic pathology; neurotransmitter alterations; learning and memory deficits	(Davisson et al., 1990)
	Ms1Ts65	Trisomic for about 33 genes located in the region of MMu16 that starts from *App* to *Sod1*	Mild spatial learning deficits	(Sago et al., 2000)
	Ms1Rhr	Trisomic for the region of Mmu16 between Mrpl39 and Zpf29 with the deletion of the region *Cbr1 – Orf9*	Brain volume reduction	(Olson et al., 2004)
	Ts1Rh	Trisomic for the *Cbr1-Orf9* region, syntenic to the DS critical chromosomal region on HSA21	Brain volume reduction; synaptic structure abnormalities; learning and memory deficits	(Olson et al., 2004)
	Ts1Yah	Trisomic for 12 genes in the Mmu17 region syntenic to HSA21	Increased hippocampal LTP; defects in novel object recognition, open-field and Y- maze tests; enhancement of hippocampal-dependent spatial learning in the Morris water maze	(Pereira et al., 2009)

Models with the triplication of Mmu16, Mmu17 or Mmu10 and triplication of the three Mmu (10+16+17)	Dp(16)Yey	Duplication of the entire HSA21 syntenic regions on Mmu16	DS-related heart defects; decreased hippocampal LTP; impaired cognitive behavior	(Yu et al., 2010)
	Dp(10)Yey	Duplication of the entire HSA21 syntenic regions on Mmu10	DS-related heart defects; decreased hippocampal LTP; impaired cognitive behavior	(Yu et al., 2010)
	Dp(17)Yey	Duplication of the entire HSA21 syntenic regions on Mmu17	DS-related heart defects; decreased hippocampal LTP; impaired cognitive behavior	(Yu et al., 2010)
	Dp(10)1Yey/+; Dp(16)1Yey/+; Dp(17)1Yey/+	Duplication of the entire HSA21 syntenic regions on Mmu10, Mmu16, Mmu17	Learning and memory deficits and LTP impairment	(Yu, Li, et al., 2010)
Models with insertion of HSA21	Tc1	Almost complete HSA21 trisomy	Abnormal development of cognitive phenotypes; decreased LTP in the dentate gyrus; synapse loss; altered spine morphology; learning and memory deficits	(O'Doherty et al., 2005)
Transgenic mouse models	Tg*Sod1*	Trisomic for HSA21 *SOD1*	Neuromuscular junction defects, decreased serotonin level, neuronal degeneration in brainstem, learning defects	(Epstein et al., 1987)
	Tg*App*	Trisomic for HSA21 *APP*	Dystrophic neuritis associated with congophilic plaques; learning deficits	(Lamb et al., 1993)
	Tg*Ets2*	Trisomic for HSA21 *ETS2*	Neuronal cell apoptosis; brachycephaly; neurocranical and cervical skeletal defects	(Wolvetang et al., 2003)
	Tg*S100β*	Trisomic for HSA21 *S100β*	Abnormal dendritic development; astocytosis; learning and memory deficits	(Whitaker-Azmitia et al., 1997)
	Tg*Dyrk1a*,	Trisomic for HSA21 *DIRK1A*	Abnormal brain structure; increased brain weight and neuronal size; learning deficits	(Altafaj et al., 2001)
	Tg*Dscr1*	Trisomic for HSA21 *DSCR1*	Neurological phenotype; impaired working memory in null mice	(Fuentes et al., 2000)
	Tg*Sim2*	Trisomic for HSA21 *SIM2*	Altered behavior and learning deficits	(Chrast et al., 2000)

Table.1. Mouse model of DS. *List of trisomic and transgenic mouse model of DS.*

None of the mouse models of DS is able to fully replicate the trisomic human phenotype. To overcome this obstacle, a full trisomic mouse, carrying the duplications spanning the entire HSA21 syntenic regions has been created. The Dp(10)1Yey/+;Dp(16)1Yey/+;Dp(17)1Yey/+ has been obtained by sequential crossing of three different trisomic mice the Dp16, Dp17 and Dp10 (Yu, 2010). Unfortunately, the breeding of this mouse is time consuming and expensive, two generations of breading are required to obtain each mouse and final yields are much lower than expected. Consequently, for preclinical evaluation with behavioral testing, the generation of a sufficient number of mice is impracticable for most laboratories (Gupta, 2016).

The Ts65Dn mouse model of DS

In this work we have exploited the most widely used mouse model of DS, the Ts65Dn. The Ts65Dn mouse was created from the translocation of the distal region of Mmu16 onto the centrometer of Mmu17. This region of Mmu16 covers the genes *Mrpl39* to *Zfp295* and contains 132 genes orthologous to HSA21 (Davisson, 1990). It must be noted that the Ts65Dn carries three copies of an extra segment (arising from Mmu17) with non-DS related genes, including ∼35 protein-coding genes, 15 non-protein-coding genes and 10 pseudogenes (Herault, 2017). Thus, some of these genes may contribute to the phenotypic impairment of this strain. A detailed characterization of the Ts65Dn mouse model revealed several phenotypes similar to those seen in human trisomy 21. These mice show craniofacial abnormalities, reduced somatic growth, delayed brain development, and defective brain growth and maturation. In addition, this model shows age-related atrophy and degeneration of the basal forebrain cholinergic neurons which resembles the neuropathology of Alzehimer disease that is frequently observed in people with DS (Aziz, 2018; Bartesaghi, 2011; Dierssen, 2012; Duchon, 2011; Rueda., 2012; Stagni, 2018a).

Neuroanatomical alterations of the prenatal brain in the Ts65Dn mouse

Ts65Dn embryos are characterized by a reduction in body and brain weight in comparison with euploid littermates. Data regarding brain volume during embryonic development are inconsistent. It has been reported that at E13.5, E14.5, and E16.5 Ts65Dn mice have a reduced medial-lateral length of the telencephalon (Chakrabarti, 2007), while a study from Aziz et al. found no difference

in the mediolateral brain length but a decrease in rostro-caudal brain length at P15.5 (Aziz, 2018). Moreover, Ts65Dn mice from E13.5 to E18.5 show a reduced thickness of the intermediate zone, which contains migrating neurons and axon tracts, of the sub-plate/cortical plate (SP/CP), containing migrating and differentiating neurons, but no differences in the thickness of the VZ and SVZ, which contain neural precursor cells. At E18.5 Ts65Dn mice recover the brain weight and the size defects of the telencephalon; in addition, all neocortical layers have the same thickness in Ts65Dn and euploid mice, indicating a probable delay during early brain development (Chakrabarti, 2007).

During the prenatal period, a widespread reduction of 5-Bromo-2-deoxyuridine (BrdU)-positive cells in the pallium of Ts65Dn embryos, a poor generation of neurons by the germinal zone, an abnormal migration of new generated neurons into the SP/CP, and a reduction in the size of the pyramidal cell layer of the CA1 hippocampal region have been reported (Chakrabarti, 2007). In contrast with the impaired neurogenesis observed in the neocortex of Ts65Dn embryos, the neuronal precursors located in the MGE, a region that produces inhibitory neurons, exhibit faster proliferation rate. This is of particular interest because it shows that proliferation defects, in the developing trisomic brain, do not involve all brain regions and may provide an explanation for the largest inhibitory weight observed in Ts65Dn mice (Chakrabarti, 2010). No difference in the number of apoptotic cell has been found during the prenatal period in the neocortex of Ts65Dn (Chakrabarti, 2007).

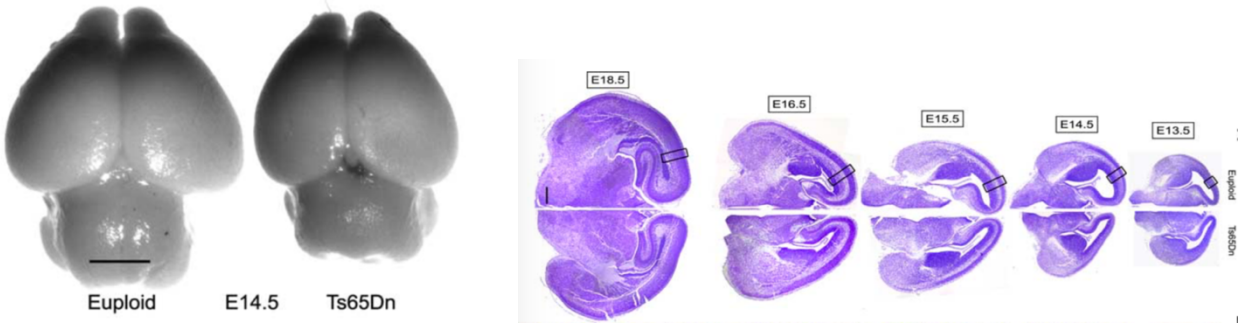

Fig. 7. The embryonic brain of Ts65Dn mice. *A. Hypotrophy of the Ts65Dn forebrain at midgestation (E14.5) (scale bar 1 mm). B. Nissl- stained images of coronal sections from euploid (upper part) and Ts65Dn (lower part) mice taken from matched sections at the levels of the future sensorimotor cortex from E13.5 to E18.5 (scale bar 200μm). E= embryonic day. From (Chakrabarti, 2007).*

Neuroanatomical alterations of the postnatal brain in the Ts65Dn mouse

Infancy.

Data regarding differences in brain weight and volume between euploid and Ts65Dn mice during the early postnatal period are contradictory. According to some studies, Ts65Dn mice have a reduced brain weight at P2 and P15 compared to euploid mice (Guidi, 2014; Stagni, 2016). On the contrary, other studies do not report differences between Ts65Dn mice and euploid littermates at P8, P15 and P22 (Belichenko, 2004; Bianchi, 2010; Chakrabarti, 2007). Moreover, while some studies show that Ts65Dn mice have differences in the volume of the DG at P2 and P15, and in the size of cerebellum at P2, P6, P14 (Contestabile, 2007;Contestabile, 2008; Roper, 2006), other studies report no volume defects in the cortex, DG, striatum and cerebellum at P2, P6, P10 and P22 (Belichenko, 2004; Holtzman, 1996; Lorenzi, 2006). The reason for these discrepancies may be related to the use of different protocols for brain excision, and/or differences in the number and sex of animals used, and/or different quantification methodologies (Stagni, 2018).

One hallmark of the Ts65Dn mouse model in the perinatal period is the widespread brain cell paucity associated with proliferation deficits (Stagni, 2018). At P2, this mouse model exhibits a reduced cellularity in the neocortex, DG, hippocampus, striatum, thalamus, hypothalamus, mesencephalon and in the Purkinje cell layer, external and internal granular layer of the cerebellum (Contestabile, 2007; Guidi., 2014; Roper, 2006). A reduced cellularity in the DG has been documented also at later stages, P6 and P15 (Bianchi, 2010; Lorenzi, 2006), and a lower number of neurons has been observed in the perirhinal cortex at P15 (Roncacé, 2017).

At P0 Ts65Dn mice show a reduced mitotic potency of the cerebellar granule precursors. At P2, Ts65Dn mice have fewer BrdU-positive cells in the neocortex, SVZ, DG, striatum, thalamus, hypothalamus, mesencephalon, pons and in the external granular layer of the cerebellum compared to the euploid littermates (Contestabile, 2009; Guidi, 2014). Deficits in proliferating cells have been observed at P15 in the striatum, neocortex, SVZ and DG (Bianchi, 2010; Contestabile, 2009), while at P6 and P30 reductions in proliferating cells are found only in the DG and in the cerebellar granular layer (Contestabile, 2009; Roper, 2006). The defective proliferation potency observed in the brain of Ts65Dn mice has been attributed to an elongation of the cell cycle, with the G1 and G2 phases being those mainly impaired (Contestabile, 2009).

A reduced number of glutamatergic neurons in the neocortex and a concomitant increase in the number of inhibitory interneurons both at cortical levels and in the hippocampal field CA1 has been demonstrated in P8 and P15 Ts65Dn mice (Chakrabarti, 2010). At variance with other brain regions,

no differences have been observed in the number or size of the basal forebrain cholinergic neurons at P2, P10, P22 (Holtzman, 1996), indicating that defects in this brain region arise later during the development of Ts65Dn mouse brain.

Conflicting results have been reported regarding apoptosis in different brain areas of Ts65Dn pups. An increased apoptotic death has been found in the cortex at P0 (Lu, 2012) and in the external granular layer of the cerebellum at P2 (Contestabile, 2009). In contrast, no difference in the number of apoptotic cell has been described in the neocortex, hippocampus, SVZ and cerebellum of young mice (Stagni, 2018).

During early phases of postnatal brain development, defects in dendritic arborization and in spine density affect the brain of Ts65Dn mice, similarly to individual with DS. In particular, it has been shown that neurons in the DG exhibit a reduced spine density at P12, P15, and P21 (Belichenko, 2004; Stagni , 2017) and a reduced number of dendritic branches at P15 (Emili et al., 2020).

Adolescence

At P45 Ts65Dn mice have a reduced brain weight when compared to controls in addition to a reduced volume of the neocortex, DG, hippocampal fields CA1 and CA3, and cerebellum (Bianchi, 2010; Guidi, 2014). The defects in cytoarchitecture and the reduced number of proliferating cells displayed in early infancy by Ts65Dn pups are retained in adolescent mice. In particular, there is evidence for a lower number of granule cells in the DG and a reduce thickness of the terminal field of mossy fibers in hippocampal field CA3 (Bianchi, 2010; Stagni, 2013). In addition, P30 and P45 Ts65Dn mice have a lower number of Brdu- and Ki67-positive cells in both the DG and SVZ in comparison with controls (Bianchi, 2010; Chakrabarti, 2010). In P45 Ts65Dn mice, the granule neurons of DG have a reduced total dendritic length, a lower branch number and a decreased mean length of each branch, in addition to absence of branches of higher order (Guidi, 2014). Moreover, the dendritic tree of the pyramidal neurons of hippocampal field CA3 exhibits a reduced number of dendritic spines (Stagni, 2013).

The defects in dendritic architecture that characterize trisomic mice are accompanied by altered expression of presynaptic and postsynaptic proteins in the neocortex, DG, and fields CA1 and CA3 of the hippocampus. In particular, an evaluation of the number of immunoreactive puncta for synaptophysin (SYN) (a marker of presynaptic terminal) and postsynaptic density protein (PSD-95) (a marker of postsynaptic terminals) in the brains of Ts65Dn mice aged 45 days demonstrated a reduction in the number of immunoreactive puncta (Stagni, 2016).

Similarly to individual with DS, Ts65Dn mice show abnormalities in phenotype acquisition, namely a reduction in the number of cells that differentiate into neurons and an increase in the number of cells with an astrocytic phenotype. Although the absolute number of astrocytes in Ts65Dn and euploid mice is similar, Ts65Dn mice have a higher ratio of astrocyte over total cell number, due to a reduced number of neurons (Guidi, 2014).

Adulthood

Ts65Dn mice aged three months exhibit normal brain weight and volume, normal hippocampal volume but a reduction in the DG volume and cerebellar volume, when compared to euploid mice (Aldridge, 2007; Holtzman, 1996; Lorenzi, 2006; Necchi, 2008; Olson, 2007). it has been reported that mice aged 20-28 weeks have a reduction in the volume of the hippocampal field CA2, but a normal volume has been measured in the other regions of the hippocampus (Insausti, 1998).

The distinctive reduction in cell number that characterizes the brain of the Ts65Dn mouse during all developmental stages is also detectable in adult mice. At three months of age, Ts65Dn mice display a reduced cell density and a lower number of granule neurons in the DG, but no differences have been found in the number of neurons populating the hippocampal fields CA1 and CA3 (Lorenzi, 2006; Stagni, 2015). A reduction in the number of granule neurons has been also found in older mice, aged 20-28 weeks (Insausti, 1998). In Ts65Dn mice aged 2-3 months a significant decrease in the density of BrdU- and Ki67-positive cells has been observed in the SVZ, DG and in the motor cortex but not in the corpus callosum, a route taken by migratory neurons (Stagni, 2015; Belichenko, 2011). At 1.5-4.5 months, trisomic mice display a significant cellular reduction in layers V and VI of the perirhinal cortex, with a further increase in the damage reported at P15 (Roncacé, 2017). At 8-10 weeks and 10 months the density of cerebellar granule cells and Purkinje cells is reduced (Olson , 2007). Moreover, at 10 months Ts65Dn mice have a normal cerebellar cortical layering but the thickness of the molecular layer and granular layer of the vermis are reduced in size (Necchi, 2008). Ts65Dn mice aged 4-5 months display a higher density of calretinin-positive cells (inhibitory neurons) in the somatosensory cortex compared to the euploid counterparts, suggesting a higher level of inhibition (Pérez-Cremades, 2010).

The defects in dendritic arborization and dendritic spine density observed at P15 and P45 in the DG of Ts65Dn mice have been also detected in older mice, aged 3 months and 13-17 months (Dang, 2014; Stagni, , 2015; Velazquez, 2013). Defects in dendritic arborization have also been found in neocortical pyramidal cells of mice aged 10 weeks (Benavides-Piccione, 2004).

In line with the reduction in synaptic proteins found in adolescent mice, an alteration in the expression of presynaptic and postsynaptic proteins has been reported in the brain of Ts65Dn mice aged 3 months (Fernandez, 2007). Ts65Dn mice exhibit an increased colocalization of synaptophysin with the inhibitory presynaptic proteins GAD65 and VGAT, suggesting an increase in the inhibitory weight (Belichenko, 2007). In agreement with the synaptic alterations found in the trisomic brain of Ts65Dn mice, long term potentiation (LTP) in the hippocampal DG (Kleschevnicov, 2004) and in the perirhinal cortex (Roncacé, 2017) is severely impaired.

Data regarding the increased number of astrocytes in the hippocampal region of adult Ts65Dn are inconsistent. A larger number of astrocytes has been reported in the hippocampus of 3 months old Ts65Dn mice in comparison with euploid mice, although this difference did not reach statistical significance (Holtzman, 1996). However, another study shows that Ts65Dn mice aged 4 months have a lower percentage of Brdu/GFAP-positive cells (cells that had acquired an astrocytic phenotype) in the DG when compared with euploid mice (López-Hidalgo, 2016). Finally, cell culture experiments show that Ts65Dn oligodendrocytes exhibit impaired maturation and lower viability, in agreement with the defect in myelination observed in fetuses and children with DS (see(Olmos-Serrano, 2006)).

In addition to the neurodevelopmental defects reported above Ts65Dn mice undergo age-related neurodegeneration. The proliferation potency and cellularity defects seen in the SVZ and hippocampus of Ts65Dn mice is observed also at older ages, suggesting that these defects characterize the Ts65Dn mice brain during the whole life span (Corrales, 2014; López-Hidalgo, 2016; Martínez-Cué, 2013). Ts65Dn mice aged 14 months show a reduction in the number of BrdU-positive cells in the SVZ and RMS (Guidi, 2016). In 5-8 month-old Ts65Dn mice, the number of basal forebrain cholinergic neurons is reduced (Ash, 2014; Contestabile, 2006; Cooper, 2001). During aging, Ts65Dn mice exhibit low brain levels of choline acetyltransferase, neurotrophic growth factor, neurotrophic tyrosine kinase receptor type 1 in the basal forebrain cholinergic neurons, and loss of tyrosine hydroxylase in the locus coeruleus. These defects are relevant to premature cognitive decline and development of AD (Kelley, 2016; Rueda, 2012).

Behavioral alterations during the life span of the Ts65Dn mouse model

The distinctive alterations in the brain of Ts65Dn mice during the whole life span translate into functional alterations and behavioral impairments starting from early life stages. Similarly to the hypotonia and delay in achieving developmental milestones found in newborns with DS, Ts65Dn pups exhibit deficits in achieving both early and late developmental milestones in the open field and

motor-based developmental task. Ts65Dn perform worst in surface righting, negative geotaxis, cliff aversion, open field and air righting task compared with euploid littermates. However, they exhibit a similar performance in the forelimb grasp, ear twitch, eye opening and auditory startle responses (Aziz, 2018).

Young adult and adult mice show significant hyperactivity in setting that elicit caution and lack of movement in euploid animals, such as the open field and plus maze tests, but do not exhibit deficits in sensory capabilities and coordinated behavior, i.e. olfactory sensitivity, visual abilities, orienting reactions, forelimb strength, postural skills, coordination, climbing, locomotion, motor coordination and balance deficits (Bartesaghi 2011; Rueda, 2012). However, Ts65Dn mice perform worst in learning an operant conditioning paradigm and in tests that require the integrity of the hippocampal system such as spontaneous alternation (T maze), contextual memory (fear-conditioning test), spatial learning, long-term memory and cognitive flexibility (Morris water maze test; radial arm maze test), non-spatial short- and long-term declarative memory (novel object recognition) (see (Bartesaghi, 2011; Rueda, 2012)). This evidence suggests that in Ts65Dn mice, similarly to individuals with DS, declarative memory which, in rodents is delineated along spatial and recognition memory domains, is impaired. Furthermore, it is important to note that, similarly to humans with DS, the Ts65Dn mouse shows a cognitive decline with age (Hunter, 2003), indicating a strong correlation with the onset of AD-like pathology.

THERAPIES FOR DS

In the last two decades the number of studies focusing on pharmacotherapies for DS has grown exponentially (Stagni, 2015). The knowledge of the gene content of HSA21, the efforts to understand signaling, metabolic and developmental pathways that are dysregulated in DS, the availability of several mouse models that mimic DS, the generation of trisomic human pluripotent stem cells (iPSCs) and their differentiation in various cell types and tissue, the awareness of the numerous neurodevelopmental alterations that affect the DS brain has made possible a cautious enthusiasm for attempting to treat individuals with DS using drugs that appear to be effective in DS mouse models (Antonarakis, 2017; Antonarakis, 2020). However, most of the pharmacological attempts to improve trisomy-related brain defects were conducted in adult mice. It is important to note that neurodevelopmental defects in DS (and Ts65Dn mice as well) are already present at fetal life stages (Stagni, 2015). In view of the time course of brain development neonatal and, even better, prenatal therapies can have the largest impact. Early therapeutic interventions may be able to potentially affect the development of the whole brain, exerting widespread effects in terms of the phenotypic features they are able to rescue and of the duration of their effects (see (Stagni, 2015)). The Ts65Dn mouse model has been extensively exploited for preclinical studies of experimental pharmaceutical therapies during all developmental stages, from prenatal intervention to therapies targeted to the comorbidity between DS and AD. This section will focus on neonatal and prenatal therapies in the Ts65Dn mouse model of DS, with a specific section dedicated to therapies with natural compounds. For a detailed description of preclinical studies in the Ts65Dn mouse at adult life stages (summarized in Table 2) the reader can refer to several comprehensive reviews (Gardiner, 2014; Stagni, 2015; Vacca, 2019).

Phenotype	Treatment	Mechanism	Age (M)	Treatment duration	Outcome	Long-term effect	References
L/M (MWM)	Donepezil (Class A)	AChE inhibitor	4	7 w	**Failed**	NA	Rueda et al., 2008a
L/M (SA)	Physostigmine (Class A)	AChE inhibitor	4 10 16	Acute Acute Acute	Rescued **Failed** **Failed**	NA NA NA	Chang and Gold, 2008
Olfactory learning	Galantamine (Class A)	AChE inhibitor	3–6	Acute	Rescued	NA	de Souza et al., 2011
L/M (NOR, TM)	Pentylentetrazole (Class A)	Antagonist of $GABA_A$ R	3–4	17 d	Rescued	**Yes (at 2 m)**	Fernandez et al., 2007
L/M (MWM)	Pentylentetrazole (Class A)	Antagonist of $GABA_A$ R	4	7 w	Rescued	NA	Rueda et al., 2008a
L/M (NOR)	Pentylentetrazole (Class A)	Antagonist of $GABA_A$ R	2–3	2 w	Rescued	**Yes (at 8 d)**	Colas et al., 2013
L/M (NOR)	Pentylentetrazole (Class A)	Antagonist of $GABA_A$ R	12–15	2 w	Rescued	**Yes (at 8 d)**	Colas et al., 2013
L/M (MWM)	RO4938581 (Class A)	$GABA_A$ α5 negative allosteric modulator	3–4	6 w	Rescued	NA	Martínez-Cué et al., 2013
L/M (NOR, MWM, CFC)	CGP55845 (Class A)	Antagonist of $GABA_B$ R	2–3	3 w	Rescued	NA	Kleschevnikov et al., 2012
L/M (MWM, CFC)	Ethosuximide (Class A)	Inhibits KCNJ6/GIRK2 channel, a $GABA_B$-coupled ion channel	4.5–5	10 w	**Failed**	NA	Vidal et al., 2012
L/M (MWM, CFC)	Gabapentin (Class A)	Modulator of GABA synthesis	4.5–5	10 w	**Failed**	NA	Vidal et al., 2012
L/M (CFC, nesting behavior)	L-DOPS (Class A)	NA pro-drug	6	Acute	Rescued	**No (at 2 w)**	Salehi et al., 2009
L/M (NOR, CFC, TM)	Xamoterol (Class A)	β1 receptor agonist	9–12	Acute	Rescued	NA	Faizi et al., 2011
L/M (NOR, SA)	Clozapine-N-oxide (agonist of hM3Dq, administered via adeno virus into Locus Coeruleus) (Class A)	DREADD design in order to stimulate NA neurons of Locus Coeruleus	14	Acute	Rescued	NA	Fortress et al., 2015
L/M (SA)	L-DOPS (Class A)	NA pro-drug	11	2 w	Rescued	NA	Fortress et al., 2015
L/M (CFC)	Memantine (Class A)	Antagonist of NMDA R	4–7	Acute	Rescued	NA	Costa et al., 2008; Ahmed et al., 2015
L/M (WRAM, NOR)	Memantine (Class A)	Antagonist of NMDA R	4	6 m	Improved	**No (at 1 w)**	Lockrow et al., 2011
L/M (MWM)	Memantine (Class A)	Antagonist of NMDA R	9	8–9 w	Rescued	NA	Rueda et al., 2010
L/M (YM)	RO25-6981 (Class A)	Antagonist of NMDA R (GluN2B)	3–6	Acute	**Failed**	NA	Hanson et al., 2013
L/M (YM, BM)	RO25-6981 (Class A)	Antagonist of NMDA R (GluN2B)	3–6	2 w	**Failed**	NA	Hanson et al., 2013
L/M (NOR, YM)	Fluoxetine (Class A)	Inhibits serotonine reuptake	> 2 m	8 w	Rescued	NA	Begenisic et al., 2014
L/M (MWM)	Fluoxetine (Class A)	Inhibits serotonine reuptake	5–7	4 w	**Failed**	NA	Heinen et al., 2012
L/M (YM, NPR, NOR)	JZL184 (Class A)	Inhibitor of monoacylglycerol lipase that increases levels of 2-arachidonoylglycerol	11	4 w	**Failed** (YM, NPR) Rescued (NOR)	NA	Lysenko et al., 2014
L/M (MWM)	NAPVSIPQ+SALLRSIPA (fragments of ADNP and ADNF) (Class B)	Neuroprotection against oxidative stress	10	9 d	Rescued	**No (at 10 d)**	Incerti et al., 2011
L/M (MWM)	Peptide six (fragment of CNTF) (Class B)	Neurotrophic factor	11–15	30 d	Improved	NA	Blanchard et al., 2011
L/M (TM)	Estrogen (Class B)	Protects basal forebrain cholinergic neurons	11–15	2 m	Improved	NA	Granholm et al., 2002

Phenotype	Treatment	Mechanism	Age (M)	Treatment duration	Outcome	Long-term effect	References
L/M (MWM, PM)	Melatonin (Class B)	Free radical scavenger	5–6	5 m	Improved	NA	Corrales et al., 2013
L/M (WRAM)	Vitamin E (Class B)	Antioxidant	4	4–6 m	Improved	NA	Lockrow et al., 2009
L/M (MWM)	Piracetam (Class B)	Nootropic	1.3	4 w	**Failed**	NA	Moran et al., 2002
L/M (MWM)	SGS-111 (Class B)	Analog of Piracetam. Nootropic	4–6	6 w	**Failed**	NA	Rueda et al., 2008b
L/M (WRAM)	Minocycline (Class B)	Anti-inflammatory	7	3 m	Improved	NA	Hunter et al., 2004
L/M (MWM, NOR, CFC)	Lithium (Class C)	Mood stabilizer. Interferes with GSK3β signaling	5–6	4 w	Rescued	NA	Contestabile et al., 2013
L/M (MWM)	DAPT (Class D)	Gamma-secretase inhibitor	4	Acute	Rescued	NA	Netzer et al., 2010
L/M (MWM, NOR)	Epigallocatechin-3-gallate (EGCG) (Class D)	Inhibitor of DYRK1A kinase	3	1 m	Rescued	NA	De la Torre et al., 2014
LTP	Pentylentetrazole (Class A)	$GABA_A$ R antagonist	3–4	17 d	Rescued	**Yes (at 2 m)**	Fernandez et al., 2007
LTP	RO4938581 (Class A)	$GABA_A$ α5 negative allosteric modulator	3–4	6 w	Rescued	NA	Martínez-Cué et al., 2013
LTP	CGP55845 (Class A)	Antagonist of $GABA_B$ R	2–3	3 w	Rescued	NA	Kleschevnikov et al., 2012
LTP	Picrotoxin (Class A)	Antagonist of $GABA_A$ R	3–4	Acute	Rescued	Acute (slices)	Kleschevnikov et al., 2004
LTP	Picrotoxin (Class A)	Antagonist of $GABA_A$ R	4–6	Acute	Rescued	Acute (slices)	Costa and Grybko, 2005
LTP	RO25-6981 (Class A)	Antagonist of NMDA R (GluN2B)	3–6	2 w	Rescued	**Yes (at 2–4.5 w)**	Hanson et al., 2013
LTP	Fluoxetine (Class A)	Inhibits serotonine reuptake	> 2	8 w	Rescued	NA	Begenisic et al., 2014
LTP	JZL184 (Class A)	Inhibitor of monoacylglycerol lipase/Endocann System	11	4 w	Improved	NA	Lysenko et al., 2014
LTP	Melatonin (Class B)	Free radical scavenger	6–6.5	5–5.5 m	Rescued	NA	Corrales et al., 2014
LTP	Lithium (Class C)	Mood stabilizer. Interferes with GSK3β signaling	5–6	4 w	Rescued	NA	Contestabile et al., 2013
LTP	Epigallocatechin-3-gallate (EGCG) (Class D)	Inhibitor of DYRK1A kinase	2–5	Acute	Rescued	Acute (slices)	Xie et al., 2008
Neurogenesis (DG)	RO4938581 (Class A)	$GABA_A$ α5 negative allosteric modulator	3–4	6 w	Rescued	NA	Martínez-Cué et al., 2013
Neurogenesis (DG)	Farmoterol (Class A)	β2 Receptor agonist	5–6	15 d	**Failed**	NA	Dang et al., 2014
Neurogenesis (DG)	Fluoxetine (Class A)	Inhibits serotonin reuptake	2–5	24 d	Rescued	NA	Clark et al., 2006
Neurogenesis (DG)	Peptide six (fragment of CNTF) (Class B)	Neurotrophic factor	11–15	30 d	Rescued	NA	Blanchard et al., 2011
Neurogenesis (DG)	Melatonin (Class B)	Free radical scavenger	6–6.5	5–5.5 m	Rescued	NA	Corrales et al., 2014
Neurogenesis (DG)	Lithium (Class C)	Mood stabilizer. Interferes with GSK3β signaling	5–6	4 w	Rescued	NA	Contestabile et al., 2013
Neurogenesis (SVZ)	Lithium (Class C)	Mood stabilizer. Interferes with GSK3β signaling	12	1 m	Rescued	NA	Bianchi et al., 2010a
Neurogenesis (DG)	P7C3 (Class E)	Proneurogenic drug	1–2.5	3 m	Improved	NA	Latchney et al., 2015
Dendritic hypotrophy	Farmoterol (Class A)	β2 Receptor agonist	5–6	15 d	Rescued	NA	Dang et al., 2014
Connectivity	Peptide six (fragment of CNTF) (Class B)	Neurotrophic factor	11–15	30 d	Rescued	NA	Blanchard et al., 2011
Neurodegeneration	Estrogen (Class B)	Protects basal forebrain cholinergic neurons	11–15	2 m	Rescued	NA	Granholm et al., 2002
Neurodegeneration	Estrogen (Class B)	Protects basal forebrain cholinergic neurons	9–15	2 m	Rescued	NA	Granholm et al., 2003
Neurodegeneration	Minocyclin (Class B)	Anti-inflammatory	7	3 m	Prevented	NA	Hunter et al., 2004
Neurodegeneration	Vitamin E (Class B)	Antioxidant	4	4–6 m	Prevented	NA	Lockrow et al., 2009

Table. 2. Therapies administered at adult life stages in the Ts65Dn mouse model of DS. *The outcome "Rescued" means that in treated Ts65Dn mice the examined phenotype became similar to that of untreated euploid mice. The outcome "Improved" means that in Ts65Dn mice treatment ameliorated but did not rescue the examined phenotype. The text in bold in the column "Outcome" highlights treatments that were ineffective (Failed) and the text in bold in the column "Long-term effect" highlights treatments that either had (Yes) or did not have (No) a long-term effect. ADNF, Activity Dependent Neurotrophic Factor; ADNP, Activity Dependent Neuroprotective Protein; BM, Barnes Maze; CFC, Contextual Fear Conditioning; CNTF, Ciliary Neurotrophic Factor; d, day; DG, dentate gyrus; m, month; MWM, Morris Water Maze; NA, not available; NOR, Novel Object Recognition; NPR, Novel Place Recognition; PM, Plus Maze; SA, Spontaneous Alternation Task; SVZ, subventricular zone; TM, T Maze; w, week; WRAM, Water Radial Arm Maze; YM, Y Maze. From (Stagni, 2015).*

NEONATAL THERAPIES IN THE Ts65Dn MOUSE MODEL

Therapies targeted to transmitter systems

Fluoxetine

Fluoxetine is an antidepressant belonging to the selective serotonin reuptake inhibitor class. Fluoxetine inhibits the serotonin transporter and thus retards the reuptake of 5-HT and in this way the neurotransmitter can persist longer in the synaptic cleft enhancing its action on the postsynaptic neuron. Neonatal treatment with fluoxetine in Ts65Dn mice from P3 to P15 restored number of proliferating cells in the DG, total number of granule cells, dendritic pattern, and hippocampal connectivity. Furthermore, one month after treatment cessation Ts65Dn mice showed normal learning in hippocampus dependent memory (Bianchi, 2010; Guidi, 2013; Stagni, 2013). In a subsequent study it has been found that adult mice (3.month-old) treated neonatally with fluoxetine exhibit restored hippocampal neurogenesis, no dendritic pathology and restored hippocampus dependent memory (Stagni, 2015).

Clenbuterol

Clenbuterol is a long-acting β-adrenergic agonist, clinically used as a bronchodilator. A recent study that examined the effects of neonatal treatment with β-adrenergic agonists in the Ts65Dn mouse model showed that trisomic mice treated with clenbuterol (from P3 to P15) have increased proliferation rate of granule precursor cells, restoration of granule cell density, and a complete rescue of dendritic pathology, in terms of dendritic complexity and spine density, in DG granule neurons (Emili, 2020).

Salmeterol

Salmeterol is a long-acting β-adrenergic agonist. The same study mentioned above (Emili, 2020) also examined the effect of salmeterol. Ts65Dn mice treated in the neonatal period (from P3 to P15) with salmeterol did not exhibit an increase in neurogenesis but exhibited increased spine density, increased dendritic length and increased number of branches of granule neurons, when compared to the untreated counterparts (Emili, 2020). A comparison of the effects of clenbuterol and salmeterol showed that clenbuterol was more effective than salmeterol, most likely due to its better pharmacokinetic properties.

Therapies targeted to perturbed signaling pathways

SAG 1.1

SAG 1.1 is a derivative of chlorobenzo [*b*] thiophene, which was identified as a Sonic hedgehog agonist. A single dose of SAG 1.1 in P0 Ts65Dn mice rescued at P6 the number of cells in the granule cell layer of the cerebellum, and this positive effect was still present after 4 months. Moreover, SAG was able to restore hippocampal LTP and enhance Ts65Dn mice performance in hippocampal dependent memory test (Das, 2013).

ELND006

ELND006 is a selective inhibitor of the γ-secretase enzyme and thereby it reduces the formation of amyloid precursor protein intracellular domain (AICD), a small peptide deriving from the processing of APP that negatively affects neurogenesis. Treatment with ELND006 in Ts65Dn neonate (P3-P15) was able to restore neurogenesis in SVZ and DG, number of granule cells, synapse development, and lowered the level of various gene transcriptionally regulated by AICD (Giacomini, 2015). Furthermore, one month after treatment cessation the pool of proliferating cells in the DG, the total number of granule neurons as well as the number of pre- and postsynaptic terminals in the stratum lucidum of CA3 hippocampal field were still restored (Stagni, 2017).

Others

Cyclosporin A

Cyclosporin A (CASA) is an FDA approved immunosuppressant. A recent study demonstrated that neonatal treatment (from P3 to P15) with CSA in Ts65Dn mice was able to restore proliferation of neuronal precursors cells in SVZ and SGZ, total number of hippocampal granule cells and dendritic spines of granule neurons (Stagni, 2019).

PRENATAL THERAPIES IN THE Ts65Dn MOUSE MODEL

Therapies targeted to transmitter systems

Choline

Choline is a vitamin-like nutrient and a precursor of acetylcholine, a fundamental brain neurotransmitter. Several studies investigated the effects of maternal choline supplementation in Ts65Dn mice. Pregnant dams were treated with an enriched choline diet (4.5-fold than normal)

throughout pregnancy and until litters weaning. In the adult offspring choline supplementation was able to restore hippocampal neurogenesis, reduce the loss of BFCNs and rescue learning and memory impairment in hippocampal dependent spatial cognition (Ash, 2014; Kelley, 2015; Moon, 2010; Velazquez, 2013). Moreover, maternal choline supplementation was able to normalize adult offspring gene expression, in particular it was able to regulate aberrant expressions of genes involved in GABAergic neurotransmission, endosomal-lysosomal pathways, autophagy and kinase activity in CA1 pyramidal neurons (Alldred, 2019). Another study with maternal choline supplementation demonstrate that treatment was able to normalize the expressions of aberrant genes related to the cytoskeleton, AD, cell death, presynaptic function, immediate early, G protein signaling and cholinergic neurotransmission in BFCN (Kelley, 2019).

Fluoxetine

Based on the strong a positive effect of neonatal treatment with fluoxetine on brain development, pregnant Ts65Dn female were treated with fluoxetine from E10 to delivery. At P2 the offspring exhibited restored neurogenesis and cellularity throughout the forebrain, midbrain, and hindbrain. Importantly, at P45 the prenatally-treated mice exhibited restored number of proliferating neuronal precursors, normal number of pre- and postsynaptic terminals, no deficits in dendritic arborization and restoration of cognitive performances (Guidi, 2014).

Therapies targeted to perturbed signaling pathways

Cilostazol

Cilostazol is a selective inhibitor of phosphodiesterase (PDE) 3 that promotes the clearance of amyloid β and it has been demonstrated to rescues cognitive deficits in an AD mouse model (Maki, 2014). A recent study showed that early intervention (from pregnancy to adulthood) with cliostazol food-supplementation was able to ameliorate cognitive deficits and hyperactivity in Ts65Dn mice (Tsuji, 2020).

Others

Neuropeptides

Neuropeptides are small proteinaceous substances produced and released by neurons and acting on neural substrates. Two active peptides derived from the neurotrophic factors activity-dependent

neuroprotective protein (ADNP) and activity-dependent neurotrophic factor (ADNF), NAPVSIPQ (NAP) and SALLRSIPA () respectively, have been administered to pregnant dams from E8 to E12. Ts65Dn offspring treated prenatally achieved developmental milestones at the same time as euploid littermates. In addition, prenatal treatment prevented the activity-dependent neurotrophic factor decrease and the downregulation of glial fibrillary acidic protein in the TS65Dn brains (Toso, 2008). Furthermore, adult Ts65Dn mice treated prenatally showed increased levels of NMDA receptor subunits NR2A and NR2B and of GABA receptor subunits GABA Aβ3 (Vink, 2009) and performed better in a hippocampus-dependent memory test (Incerti, 2012).

CLINICAL TRIALS IN DOWN SYNDROME

Pharmacological studies in people with DS began in the 1960s. Early studies were often based on case reports and were typically small, single-center trials, sometimes open label, making it difficult to assume valid conclusions regarding their efficacy (Hart, 2017). Clinical trials in DS initially focused on AD and successively moved to investigate early pharmacological interventions and to target the pediatric population. The exploiting of translational research and, in particular the usefulness of the Ts65Dn mouse model for the study of DS, made it possible to target specific molecular mechanisms within the brain and to address cognitive and functional deficits associated with DS (Hart, 2017).
The majority of the clinical trials carried out in people with DS showed moderate to no effects. It must be observed that in the history of clinical trials in DS the majority of studies conducted so far have focused on adolescent or adult population (see table 2). While the initial focus on this age range is required to establish the safety of a pharmacological intervention, these studies have had a limited success in demonstrating their efficacy. This emphasize the need of studying the potential effects of early pharmacological intervention on brain development and cognitive outcome in infants with DS (Hart, 2017). It has been well established that an early pharmacotherapeutic intervention is capable to rescue brain developmental defects in mouse model of DS. Considering the timeline of human brain development when acting on prevention it is necessary to exploits the windows of opportunity of the developing brain to improve the neurodevelopmental alterations that characterize the DS brain (Stagni, 2015).

The table below summarizes registered clinical trials using pharmacological interventions targeting specific aspects of neurobiology, neurochemistry, neuroplasticity or connectivity within the brain.

Drug	Mechanism	Identification number	Outcome	Reference
Donepezil	Reversible inhibitor of acetylcholinesterase	NCT00570128	Safe and well tolerated in both children and adults with DS. No significant benefit on cognitive outcomes.	(Kishnani, 2010; Kishnani., 2009)
Rivastigmine	Inhibitor of acetylcholinesterase and butyrylcholinesterase	NCT00748007	Improves expressive language in children and adolescent with DS. No significant effect on adaptive function, executive function, language and memory.	(Spiridigliozzi, 2016)
Phentylenetetrazole	GABA antagonist	ACTRN12612000652875	Under investigation in youg adults and adolescents with DS.	Anzctr.org.au
Basmisanil	GABA α5 negative allosteric modulator	NCT02024789	No significant impact on cognition or adaptive behavior in young adults and adolescent with DS.	(Hart, 2017)
Memantine	Low affinity NMDA-antagonist	NCT01112683	Amelioration in hippocampus dependent functions in young adults with DS.	(Boada, 2012)
Memantine	Low affinity NMDA-antagonist	NCT00240760	No improvement in cognition and adaptive function in individual with DS over age 40.	(Hanney, 2012)
Memantine	Low affinity NMDA-antagonist	NCT00240760	Ongoing phase II clinical trial in young adults with DS is trying to assess whether a 16-week treatment with memantine will have an effect on learning and memory.	Clinicaltrials.gov
ELND005	Amyloid-anti-aggregation agent	NCT01791725	Safe and tolerated in young adults with DS. No differences in cognitive or behavioral measures.	(Rafii, 2017)
ACI-24	vaccine targeting αβ protein	NCT0273845	Under investigation in adults with DS.	Clinicaltrials.gov
Glulisine	Rapid-acting insulin	NCT02432716	Safe in adult with DS. No significant effects on memory and cognition.	(Rosenbloom, 2020)
Nicotine	CNS stimulant	NCT01778946	Under investigation as a treatment for cognitive decline in adults with DS.	Clinicaltriasl.gov

Table. 3. Registered clinical trials in DS.

PRECLINICAL AND CLINICAL STUDIES WITH NATURAL COMPOUNDS

This section is focused on neonatal and prenatal preclinical studies and on clinical trials exploiting natural compounds to target specific aspects of the trisomic brain

Neonatal therapies with natural compounds

Eppigallocatechin-3-gallate

Epigallocatechin-3-gallate (EGCG) is a flavonoid present in green tea leaf extracts that, among other activities, is able to specifically inhibits DYRK1A. Early postnatal administration of EGCG (from P3 to P15) restored hippocampal neurogenesis, total number of granule neurons, and pre- and postsynaptic proteins levels in the hippocampus and cortex of Ts65Dn mice. However, one month after treatment cessation the effects were no longer present and behavioral testing of hippocampus dependent learning and memory showed no improvement, indicating a lack of long lasting effects of EGCG (Stagni, 2016).

7,8-dihydroxyflavone

7,8-dihydroxyflavone (7,8-DHF) is a natural flavonoid that mimics the action of BDNF because it is able to bind with high affinity and specificity the tropomyosin-related kinase receptor B (TrkB). Neonatal administration of 7,8-DHF (from P3 to P15) in Ts65Dn mice induced an increase in the number of neural precursor cells in the DG, restoration of granule cell number, dendritic spine density, and levels of SYN. Moreover, a prolonged treatment from P3 to P50 was able to improve learning and memory defects of Ts65Dn mice (Stagni, 2017). However, in another study neonatal treatment (from P3 to P15) did not show learning and memory improvement one month after treatment cessation, indicating that the positive effects of 7,8-DHF in the trisomic brain do not outlast the end of the treatment.

Prenatal therapies with natural compounds

Epigallocatechin-3-gallate

Epigallocatechin-3-gallate (EGCG) a flavonoid that showed interesting results when administered postnatally in Ts65Dn mice, was also tested prenatally. Treatment with EGCG from gestation to adulthood was able to suppress an imbalanced expression of an alternative splicing product of tau, regulated by DIRK1A, and to rescue anxiety and memory deficits in Ts65Dn adult mice (Yin, 2017).

Moreover, it has been shown that prenatal treatment with EGCG at E7 and E8 was able to modulate deficiencies in neural crest cells, peripheral nervous tissue ,and to normalize craniofacial phenotypes in the Ts65Dn mouse model of DS (McElyea, 2016).

α-Tocopherol

α-Tocopherol is the most active biological form of vitamin E. α-Tocopherol enriched diet was administered to pregnant Ts65Dn dams during the entire pregnancy and lactation period, and to the newborn until 12 weeks of age. The chronic supplementation of vitamin E was able to increase the granule cells density, to reduce the products of lipidic peroxidation in the DG, to reduce anxiety levels and to improve spatial learning and memory in Ts65Dn mice (Shichiri, 2011).

Oleic acid

Oleic acid is a monounsaturated acid of the ω-9 series. It is present endogenously in the organism and can also be obtained from the diet. Pregnant Ts65Dn female were treated from E10 to P2 with oleic acid and the outcome was examined in the progeny at P2 and at P30.P45. Administration of oleic acid increased the volume of the granule cell layer, the number and density of granule cells and the number of proliferating cells in the DG of P2 Ts65Dn mice. Moreover, prenatally treated mice tested at P30-P45 showed better cognitive abilities, as assessed with the Morris Water Maze test, and a higher density of PSD95 (García-Cerro, 2020).

Linolneic acid

α-Linolenic acid is an essential polyunsaturated fatty acid (PUFA) of the ω-3 series, which has to be obtained from the diet. The same study mentioned above (García-Cerro, 2020) also examined the effects of prenatal treatment with linolenic acid. Pregnant Ts65Dn female were treated from E10 to P2. At P30-45 Ts65Dn mice treated prenatally demonstrated higher density of PSD95 and better learning and memory performances compared to the untreated counterpart (García-Cerro, 2020).

Clinical trials with natural compounds

Epigallo-catechin-3-gallate (EGCG) is a flavonoid derived from green tea leaves and a well know DYRK1A inhibitor. A randomized, placebo-controlled pilot study tested the effects of green tea extract with a mean EGCG oral dose 9 mg/kg/day on cognition in adolescent with DS and found that three months of treatment with green tea extracts is effective in improving recognition and working memory (De la Torre, 2014) (ClinicalTrials.gov identifier NCT01394796). A phase II clinical trial in adolescent with DS, with an association therapy with green tea extracts and cognitive training for

12 months, showed a positive effects on visual recognition memory, inhibitory control, and adaptive behavior (de la Torre, 2016) (ClinicalTrials.gov identifier NCT01699711). However, phase III clinical trial with a larger population is needed to assess the long term efficacy of EGCG and cognitive training (Hart, 2017).

Antioxidants. Mitochondria are the most susceptible target of reactive oxygen species and mitochondrial DNA control region mutations occur in individuals with DS who suffer from dementia (Lott, 2011). A two-year randomized, double-blind, placebo-controlled clinical trial assessed whether a combination of antioxidants and mitochondrial cofactor could lead to stabilization or improvement in cognitive functioning in adults with DS and AD-like dementia. However, this study determined that antioxidant supplement was ineffective as treatment for dementia in individuals with DS and AD (Lott, 2011) (ClinicalTrials.gov identifier NCT00056329).

Folinic acid, is a vitamer of vitamin B9. As several genes involved in folate metabolism are located on HSA21 and folate deficiency has been linked to ID, folinic acid was investigated as pharmacotherapy for DS. A randomized control trial in children with DS with an association therapy of folinic acid an antioxidant found no effects on brain development and long term communication abilities (Ellis, 2008) (ClinicalTrials.gov identifier NCT00378456). More recently, a double-blind, placebo-controlled, single center trial in infants with DS who followed a folinic acid therapy revealed an improvement in global development. This effect was larger in a sub-analysis of subjects taking concomitant thyroid hormone (Blehaut, 2010) (ClinicalTrials.gov identifier NCT01576705). However, a recent 4-arm, placebo-controlled trial with folinic acid and thyroid hormone aimed at evaluating improvement in psychomotor development in toddlers with DS did not support this evidence (Mircher, 2020) (ClinicalTrials.gov identifier NCT01576705).

FLAVONOIDS AND THE BRAIN

Flavonoids are a large group of polyphenolic compounds containing a basic flavan nucleus with two aromatic rings (the A and the B rings) interconnected by a three-carbon-atom heterocyclic ring (the C ring). Flavonoids are the most common group of polyphenolic compounds found ubiquitously in fruits and vegetables (Perez-Vizcaino, 2018). They are constituted of two aromatic rings, bound together by three carbon atoms that form an oxygenated heterocycle. Flavonoids can be subdivided into 6 subclasses depending on the structure of the heterocycle: flavonols, flavones, isoflavones, flavanones, anthocyanidins, and flavanols (Manach, 2004).

These molecules are well known for their antioxidant properties, but they are also capable of several different beneficial effects on health. Flavonoids are able to reduce cardiovascular diseases and high blood pressure and to have antiallergic, anti-inflammatory, hepatoprotective and antidiabetic effects (Terahara, 2015). They are currently under investigation for the prevention of cancer and chronic diseases through their action as free radical scavenger, the ability to block lipid peroxidation chain reaction and the chelating action with metal ions (Terahara, 2015).

Furthermore, several studies recognized flavonoids as promising plant-based bio actives with neuroprotective properties, able to suppress neuroinflammation and potentially improve cognitive functions both in animals and humans (Pérez-Hernández, 2016; Rendeiro,2015). They are able to ameliorate cerebral arteries vascularization, modulate receptor function and interact with signaling pathways for neuronal function and survival, promote the expression of genes and proteins involved in synaptic plasticity and neuronal repair, modulate LTP, affect aspects crucial for neuronal communication such as spine density, stimulate neuronal regeneration and induce neurogenesis (Rendeiro, 2015; Spencer, 2009).

Flavonoids and neuroinflammation

Neuroinflammation is closely related to the pathogenesis of neurodegenerative diseases. The majority of events linked to neuroinflammation, such as transcriptional and post-transcriptional regulation of inducible nitric oxide synthase (iNOS) and cytokines in activated microglia and astrocytes, are controlled by upstream MAPK signaling. Some flavonoids, i.e. quercetin and flavonoids present in blueberry, are able to reduce the iNOS expression triggered by neuroinflammation, inhibit cyclooxygenase expression, NADPH oxidase activation and reactive

oxygen species (ROS) generation, through inhibition of MAPK signaling cascades (Calis, 2019; Spencer, 2009).

Flavonoids and neurodegeneration

There is a growing body of evidence suggesting that flavonoids may be able to delay the progression of neurodegenerative diseases such as AD and Parkinson's disease (Spencer, 2009). One example are Gingko biloba extracts that protect hippocampal neurons against NO and β-amyloid induced neurotoxicity (Luo, 2002). Flavonoids are also effective in blocking oxidant induced neuronal injury, modulating protein and lipid kinase signaling cascades such as PI3K/Akt, tyrosine kinase, PKC and MAPK signaling pathways (Spencer, 2007; Williams, 2004). Actions on these pathways are able to affect neuronal functioning through the phosphorylation of target molecules changing caspase activity and/or gene expression. Moreover, some flavonoids such as hesperetin and its active metabolites are able to inhibit oxidant-induced neuronal apoptosis through the activation of pro-survival pathways and inhibition of pro-apoptotic pathways (Spencer, 2009).

Flavonoids and learning and memory

Several lines of evidence suggest that fruits and vegetables-derived flavonoids are capable to promote beneficial effects on learning and memory (see (Spencer, 2009)). Although the precise site of their interaction with signaling pathways remains unknown, they are able to act in numerous different ways; binding to ATP sites on enzymes and receptors, modulating kinases activity, affecting the function of phosphatases, preserving Ca^{2+} homeostasis and preventing Ca^{2+}-dependent activation of kinases in neurons, modulating transcription factor activation and binding to promoter sequences (Spencer, 2009). Through these actions flavonoids are able to induce morphological changes that can influence memory acquisition, consolidation and storage, i.e. the flavonoid induced improvement in neuronal spine density and morphology, two crucial factors for learning and memory (Spencer, 2009). Flavonoids are well known for their ability to prevent cerebrovascular diseases, including those associated with stroke and dementia (Commenges, 2016). Efficient cerebral blood flow is vital for optimal brain functioning. Flavonoids trough their action on endothelial function and peripheral blood flow, are able to increase cerebrovascular blood flow and consequently brain functions. Moreover, flavonoids vascular action seems to facilitates adult

hippocampal neurogenesis, the new hippocampal cells clustered near blood vessels proliferate in response to vascular growth factors (Spencer, 2009).

7,8-DIHIDROXYFLAVONE

The 7,8-dihydroxyflavone (7,8-DHF) is a flavone substituted by hydroxy groups at positions 7 and 8. It is naturally present in *Godmania aesculifolia, Tridax procumbens* and the primula leaves. This flavonoid was identified as a high affinity TrkB agonist among 2000 biologically active compounds by screening of the Spectrum Collection Library (Jang, 2010). 7,8-DHF is able to cross the BBB, bind TrkB receptor, provokes receptor dimerization, phosphorylation and activation of its downstream signaling cascades. Structural-activity relationship (SAR) study suggests that the catechol group is essential for 7,8-DHF activity, in particular the presence of 8-hydroxy group in the A ring is necessaryl for the TrkB stimulatory effect (Liu, 2010).

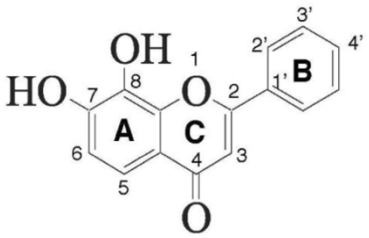

Fig.8. 7,8-dihydroxyflavone chemical structure. *From* (X. Liu et al., 2010).

Pharmacology of 7,8-DHF

The *in vivo* investigation of 7,8-DHF pharmacokinetics profile determined that 7,8-DHF in mice has a half-life of about 134 min in plasma after oral gavage of 50 mg/Kg (which is 10-fold the widely used therapeutic dose). The plasma concentration peaked at 10 min with 70 ng/ml and was still detectable after 8 hours (5 ng/ml). 7,8-DHF is able to cross the BBB and the brain concentration peaked at 10 min with a 50 ng/g, at 4 hours is 7 ng/g and at 6 h is below the quantitative limits (Liu, 2013). 7,8-DHF, as all the catechol-containing compound undergo glucuronidation, sulfation and methylation. From chromatographic analysis of plasma samples major metabolites were detected in addition to the parent drug including 7-metoxy-8-hydroxyflavone (7M8H-flavone), 7-hydroxy-8-metoxyflavone (7H8M-flavone). The *in vivo* agonistic effects exerted by 7,8-DHF might mainly result from the activity of 7,8-DHF and its metabolite 8M7H-flavone (Liu, 2013). The plasma concentration of both the methylated metabolites are low compared to the parent compound suggesting that glucuronidation but not methylation may be that main metabolic route. Moreover, 8M7H-flavone

possess higher half-life compared to the 7M8H-flavone, indicating that 8M7H-flavone is more metabolically stable (Liu, 2013). The oral administration of 7,8 DHF in mice elicits robust TrkB activation, suggesting that this molecule is orally-bioavailable (Liu, 2010). Both the methylated 7,8-DHF metabolites are able to activate TrkB receptor in the mouse brain and in primary neurons (Liu, 2013). However, the presence of the catechol group makes 7,8-DHF susceptible to fast metabolism, including sulfation, glucuronidation, methylation (Liu,2012). For this reason several prodrugs of 7,8-DHF has been synthetized and tested in order to improve the bioavailability of the parent drug.

In vitro experiment showed that 7,8-DHF treatment did not inhibit human embryonic kidney (HEK)293 cells proliferation at a dose up to 50 µM. However, at 100 µM 7,8-DHF it exerted an antiproliferative effect. Neuronal cell death assay revealed that 7,8-DHF is non-toxic for primary cortical neurons up to 5 µM (Liu, 2010). An *in vivo* study showed no pathological changes induced by 7,8-DHF in kidney, liver, lung, muscle, spleen, cortex, hippocampus, heart, intestine and testis in mice treated with 5 mg/kg/day for 3 weeks compared to the vehicle treated counterparts (Liu, 2010). Moreover, from complete blood count (CBC) analysis there was no difference between 7,8-DHF-treated and control mice (Liu, 2010). This is consistent with the results of another long-term experiment where female mice receiving ~ 2.4 µg 7,8-DHF/day for 20 weeks displayed normal CBC values (Chan, 2015). Additionally, 5 mg/kg/day treatment in neonate and young mice did not induce side effects on the body weight (Stagni, , 2017). Taken together these data in mice show that chronic treatment with 7,8-DHF does not exert toxic effects.

The TrkB receptor

The binding of BDNF to the TrkB receptor, causes receptor dimerization and autophosphorylation of the intracellular tyrosine residues (Y705/6), the formation of the phosphorylated-TrkB receptor (Rantamäki, 2019) and BDNF/Trk receptor complex translocation toward cellular membrane lipid rafts (i.e., microdomains rich in cholesterol and sphingolipids) (Suzuki, 2004). Thus, ligand-induced TrkB translocation into lipid rafts represents a signaling mechanism selective for synaptic modulation by BDNF in the central nervous system (Suzuki, 2004). Phosphorylated-TrkB leads to activation of three interconnected intrinsic intracellular cascades (Cunha, 2010 ; Chao, 2003) Phosphatidylinositol 3-kinase (PI3K), mitogen-activated protein kinase (MAPK) and phospholipase Cγ (PLCγ) (Gonzalez, 2016; Huang, 2003; Minichiello, 2009).

The TrkB receptor is capable of autophosphorylation and activation of downstream cascades independent of its ligand (BDNF). Activation of TrkB receptors in the absence of BDNF occurs *via*

trans-activation mechanism, which involves specific G protein coupled receptors (GPCR), such as the A2α adenosine receptor (A2αR) (Pradhan, 2019). In addition to TrkB transactivation by A2aRs, the transactivation of TrkB also occurs via other mechanisms such as epidermal growth factor, dopamine 1 receptors, pituitary adenylate cyclase-activating polypeptide, H_2O_2, and zinc (Huang, 2008).

7,8DHF- TrkB- dependent signaling

Similarly to BDNF 7,8-DHF specifically binds the TrkB receptor extracellular domain, in a different site in comparison with BDNF, with a binding constant Kd of =320 nM. It acts as a selective TrkB agonist, mimicking the physiological actions of BDNF (Jang, 2010; Liu, 2014).
7,8-DHF induces TrkB phosphorylation at Tyr515, Tyr706, and Tyr816 (X. Liu et al., 2014). The 7,8-DHF induced phosphorylation of TrkB leads to activation of several pathways, MAPK, PI3/Akt, and ERK1/2 in a time frame that comparable to BDNF and in a dose-dependent manner (Jang, 2010; Liu, 2016; Liu, 2010, 2014, 2013). After receptor internalization, the formation of signaling endosomes and ubiquitination/degradation had an important role in signal transduction. The action of BDNF in stimulating TrkB internalization and early endosomes delivery in the first 10 min is more potent than 7,8-DHF. On the contrary 7,8-DHF produces a more robust endocytic response at 60 minutes. TrkB ubiquitination by BDNF occurs 10 min after stimulation and its ubiquitination signals correlates with its phosphorylation pattern. While BDNF-induced TrkB phosphorylation peaks at 10 min, decreases at 60 min and ended at 180 min, 7,8-DHF-triggered TrkB phosphorylation lasts for more than 3 h, without inducing TrkB ubiquitination or degradation (Liu, 2014). These findings support the idea that bot 7,8-DHF and BDNF activate TrkB but different mechanisms and a different time-course.

7,8 DHF-TrkB independent signaling

A recent study in cell assays failed to confirm that 7,8-DHF activates the TrkB receptor (Boltaev, 2017). This discrepancy may be due to the use of different cell model, culture condition and duration of treatment. However, it must be taken into account that 7,8-DHF may induce transactivation of the TrkB receptor without binding to it. Different studies suggest that some effects of 7,8-DHF, in particular the antioxidant effects, do not require the TrkB receptor (see(Barriga, 2017; Ryu, 2014; Huai, 2014)). In addition, there is evidence for the direct uptake of flavonoids and their metabolites into the cytosol of several cell types, including cells of CNS (Ferrara, 2019; Mukai, 2011; Spencer,

2004). If this also happen for 7,8-DHF, the cell uptake will provide the possibility of a TrkB-independent modulation of signalling (Williams, 2004). In addition, as an antioxidant 7,8-DHF might exert a direct action within the cell which may contribute to its antioxidant effects (Han, 2014).

RATIONALE AND GOAL OF THE STUDY

Intellectual disability and brain hypotrophy are two of the main hallmarks of DS. The reduced brain volume typical of infants with DS can be attributed to neurogenesis impairment. Neurogenesis defects can be traced back to early gestational periods in fetuses with DS (Stagni, 2018a). Similarly to individuals with DS, the brain of Ts65Dn mouse is affected by reduced neurogenesis from early embryonic stages and defective neuronal proliferation is retained throughout the whole life span (Stagni, 2018a). While most of the brain neurons are generated during the prenatal period, there is the notable exception of those in the hippocampal dentate gyrus and cerebellum whose generation continues postnatally (Brazel, 2003). Previous studies in the Ts65Dn mouse showed that pharmacological interventions during the neonatal period are able to ameliorate the defective hippocampal neurogenesis that characterizes DS (Stagni, 2015). Considering that the bulk of neurogenesis takes place prenatally, therapeutic intervention aimed at correcting brain development should be started during the embryonic period.

Very few studies have examined the effects of prenatal pharmacotherapy in DS mouse models so far. A pioneering study demonstrated that embryonic treatment with fluoxetine was able to restore the trisomy-linked defects of brain development in the Ts65Dn mouse model (Guidi, 2014). Although prenatal administration of fluoxetine appears to be free of side effects in mice, the use of this molecule in humans may pose some caveats. From this perspective, 7,8-DHF, a natural molecule typically present in fruits and vegetables may be an ideal candidate for prenatal treatment. The natural flavonoid 7,8-DHF is able to cross the BBB and specifically binds the TrkB receptor activating its downstream signaling cascade (Liu, 2010). It has been demonstrated that 7,8-DHF was able to promote neurogenesis in the DG of adult mice (Liu, 2010), increase dendritic spine density in various rats brain regions among which amygdala, hippocampus and prefrontal cortex (Zeng, 2012), exert neurotrophic effects in various developmental disorders (Liu, 2013). Furthermore 7,8-DHF showed no side effects on somatic development, which is of particular relevance in the perspective of fetal treatment (Stagni, 2017).

Based on these premises, in this study we wanted to investigate whether prenatal treatment with 7,8-DHF, similarly to treatment with fluoxetine, was able to rescue defective neurogenesis in Ts65Dn brain.

MATERIALS AND METHODS

Colony

Ts65Dn mice were generated by mating B6EiC3Sn a/A-Ts(17^16)65Dn females with C57BL/6JEiJ x C3H/HeSnJ (B6EiC3Sn) F1 hybrid males. This parental generation was provided by Jackson Laboratories (Bar Harbor, ME, USA). To maintain the original genetic background, the mice used in this study were of the first generation of this breeding. Animals were genotyped as previously described (Reinholdt, 2011). The day of birth was designated as postnatal day zero (P0). The animals' health and comfort were controlled by the veterinary service. The animals had access to water and food *ad libitum* and lived in a room with a 12:12 h light/dark cycle. Experiments were performed in accordance with the European Communities Council Directive of 24 November 1986 (86/609/EEC) for the use of experimental animals and were approved by Italian Ministry of Public Health. In this study, all efforts were made to minimize animal suffering and to keep the number of used animals to a minimum.

Experimental protocol

Ts65Dn females (n= 14) were bred with C57BL/6JEi x C3SnHeSnJ (B6EiC3Sn) F1 males (n= 8). Conception was determined by examining the vaginal plug. Pregnant females received a daily subcutaneous injection of either 7,8-DHF (7,8-DHF, Sigma Aldrich) 5 mg/kg in vehicle (PBS with 2% DMSO) (n= 7) or vehicle (n= 7) from E10 to the day of delivery (E20/21), i.e. during the critical time windows when the majority of brain neurons are born. Hereafter the progeny of females that received 7,8-DHF will be called "treated mice" whereas the progeny of females that received the vehicle will be called "untreated mice". On P2 the progeny of treated and untreated females received an intraperitoneal injection of BrdU (150 μg/g body weight) (Sigma Aldrich) in TrisHCl 50 mM 2 hours before being killed, in order to label proliferating cells. The body weight was recorded prior to sacrifice. After sacrifice, the brain was excised and weighed.

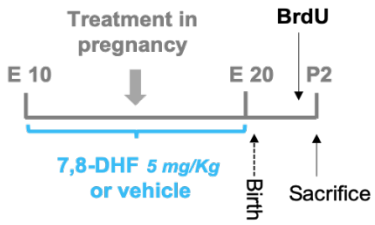

Fig.9. Experimental protocol. *Ts65Dn pregnant female received a daily subcutaneous injection of ether 7,8-DHF (5 mg/kg) or vehicle from E10 to delivery. The littermates at P2 received an intraperitoneal injection of BrdU and were killed after 2 hours.*

	Males	Females	Total
Eu+Veh	5	4	9
Ts65Dn+Veh	7	2	9
Eu+7,8-DHF	4	4	8
Ts65Dn+7,8-DHF	3	8	11

Table.4. Number of embryonically treated mice used in the study. *7,8-DHF, 7,8-dihydroxyflavone; Eu, Euploid; Veh, Vehicle.*

Histological procedures

P2 animals were decapitated and the brain was removed. The rostral brain (forebrain plus mesencephalon) was separated from the hindbrain (cerebellum, pons and medulla), cut along the midline and fixed by immersion in Glyo-Fixx (Thermo Electron) for 24 h and then dehydrated through a series of ascending ethanol concentrations. Each hemisphere was embedded in paraffin, cut in series of 8-µm-thick coronal sections that were attached to polylysine coated slides. The right hemisphere was used for BrdU immunohistochemistry, the left hemisphere was used for Nissl-staining.

BrdU immunohistochemistry. One out of 20 sections (n=15-19 sections) from the rostral brain was incubated with a primary rat anti-BrdU antibody (diluted 1:200; Biorad) and a mouse monoclonal anti-NeuN (Neuronal-specific nuclear protein), a marker of mature neurons (diluted 1:250, Chemicon, Billerica, MA, USA). Detection was performed with a Cy3-conjugated anti rat secondary antibody for BrdU immunohistochemistry (diluted 1:200; Jackson Immunoresearch) and a FITC-conjugated anti-mouse IgG (1:100; Sigma-Aldrich) for NeuN immunohistochemistry.

Nissl-method. One out of 20 sections (n=15-19) from the rostral brain of P2 mice were stained with Toluidine Blue according to the Nissl method.

Measurements

Number of BrdU-positive cells. BrdU-positive cells were sampled in the SVZ, DG, neocortex (CX), striatum (STR), thalamus (TH), and hypothalamus (HYP) of P2 mice. The brain coordinates (BC) reported below for these regions refer to the "Atlas of the developing mouse brain" (Paxinos et al., 2007). Since cells that are going to populate the telencephalon arise from different regions of the VZ/SVZ (Brazel et al., 2003), we evaluated the effects of treatment in two different rostro-caudal regions of the SVZ. The region that stretches from the rostral horn of the lateral ventricle to the beginning of the hippocampal formation (BC: 2.19-3.15 mm) named here rostral SVZ (rSVZ) and the region that stretches from the beginning to the end of the hippocampal formation (BC: 3.27-4.84 mm) named here caudal SVZ (cSVZ). In the neonatal DG, cells are scattered throughout the hilus, SGZ and granule cell layer, we evaluated the number of BrdU-positive cells in all these layers along the whole rostro-caudal extent of the hippocampal formation (BC: 3.27-4.84 mm). For simplicity, the layers in the DG where cells were counted will be called hereafter SGZ. In the CX, BrdU-positive cells were separately evaluated in the rostral cortex (rCX), namely the CX overlying the rSVZ (BC: 2.19-3.15 mm) and in the caudal cortex (cCX), namely the portion of the CX overlying the cSVZ (BC: 3.27-4.84 mm). In the STR cells were counted in sections that encroached the rSVZ (BC: 2.19-3.15 mm). In the TH and HYP cells were counted in sections comprised between the BC 3.27-4.23 and the BC 2.67-3.87 mm, respectively.

BrdU-positive cells were detected using a fluorescence microscope (Eclipse; objective: x 20, 0.5 NA). Quantification of BrdU-labeled nuclei was conducted in every 20th section. All BrdU-labeled cells located in the region of interest were counted using a modified unbiased stereology protocol that has previously been reported to successfully quantify BrdU labeling (Kempermann, 2002; Malberg, , 2000; Tozuka, 2005). The total number of BrdU-labeled cells per animal was determined and multiplied by 20 (the inverse of the section sampling fraction = 1/20) to obtain the total estimated number of cells per each region of interest.

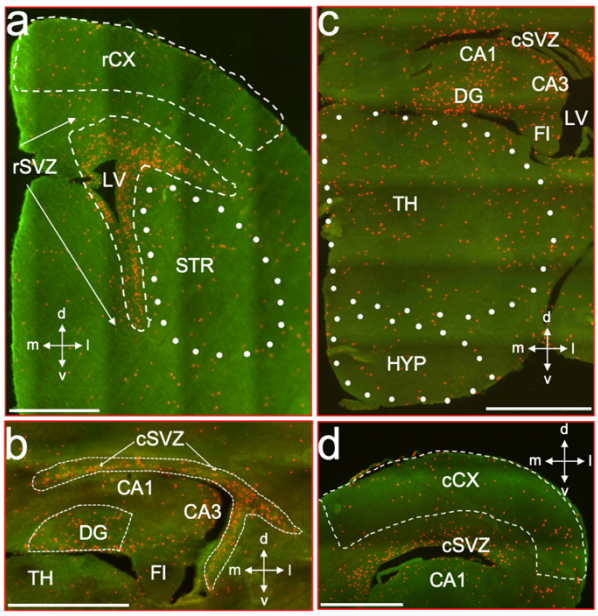

Fig.10. Brain regions where proliferating cells were sampled. *a-d: Examples of coronal sections from the brain of P2 mice. Sampled region in the rostral cortex, rostral subventricular zone, striatum (a), caudal subventricular zone, dentate gyrus (b), thalamus, hypothalamus (c), caudal cortex, caudal SVZ (d). BrdU-positive cells (red) were counted in the areas enclosed by stippled lines or dots. Calibration bars = 500 μm. CA1, hippocampal field; CA3, hippocampal field; CX, cortex; cCX, caudal cortex; cSVZ; caudal subventricular zone; d, dorsal; DG, dentate gyrus; FI, fimbria; HYP, hypothalamus; l, lateral; LV, lateral ventricle; m, medial; rCX; rostral cortex; SVZ, subventricular zone; rSVZ, rostral subventricular zone; TH, thalamus; v, ventral.*

Stereology. Stereology was conducted in every 20th Nissl-stained section. The volume of the granule cell layer of the DG, pyramidal layer of field CA1, cell numerical density (De) and number of neurons in the DG and CA1 were estimated as previously described (Bianchi, 2010). Counting frames (disectors) with a side length of 15 μm and a height of 8 μm spaced in a 100 μm square grid (fractionator) were used. The De in layers II and VI of the cCX overlying hippocampal field CA1 was evaluated using counting frames with a side length of 15 μm (in layer II) and 20 μm (in layer VI) and a height of 8 μm spaced in a 100 μm square grid. In layer II cells were counted in the portion of the layer close to layer I, in layer VI cells were counted in the portion of the layer close to the subcortical plate. The thickness of the cCX overlying field CA1 was measured by tracing radial lines across the cellular layers II-VI at 4-5 locations. Cell density was expressed as number of cells/mm^3.

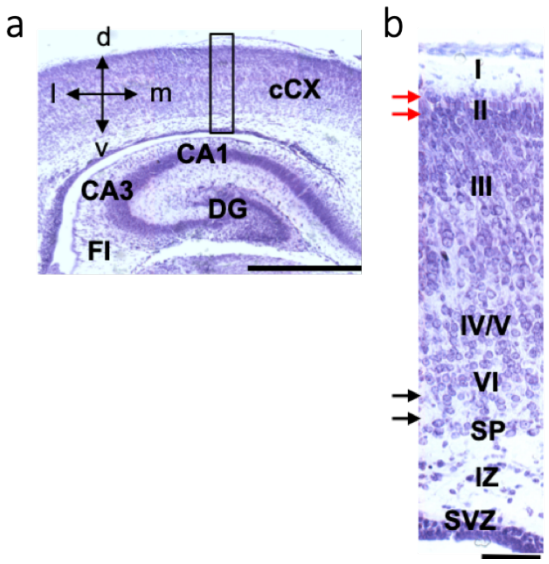

Fig.11. Example of the neocortex and hippocampal region where stereology was conducted. *(a) Nissl-stained coronal section encroaching the cCX and the hippocampal formation. (b) Higher magnification of the region enclosed in the rectangle in (a) showing the cortical layers (ordinal numbers). Red arrows indicate the regions where cells were counted in layer II, black arrows indicate the regions where cells where counted in were layer VI. Calibration in (a) = 500 μm. Calibrations in (b) = 50 μm. 7,8-DHF, 7,8-dihydroxyflavone; CA1, hippocampal field; CA3, hippocampal field; cCX, caudal cortex; d, dorsal; DG, dentate gyrus; Eu, euploid; FI, fimbria; IZ, intermediate zone; l, lateral; m, medial; SP, subplate; SVZ, subventricular zone; TH, thalamus; v, ventral; Veh, vehicle.*

All measurements were carried out by an experimenter blinded to the study code.
The number of mice used for the analysis of BrdU-positive cells and stereology in the regions of interest is reported in Table 5. Note that the number of mice used for individual measurements may vary in different regions due to technical reasons (rupture of some sections or poor staining quality).

BrdU immunohistochemistry

ROI	rSVZ	cSVZ	DG	rCX	cCX	STR	TH	HYP
ME	Tot	Tot	Tot	Tot	Tot	Tot	Tot	Tot
Eu+Veh	8	9	9	9	9	9	9	9
Ts65Dn+Veh	7	7	6	7	6	7	7	7
Eu+7,8-DHF	8	8	6	8	8	8	8	8
Ts65Dn+7,8-DHF	9	10	11	9	11	10	9	9

	Nissl staining								
ROI	cCX L II	cCX L VI	cCX	DG	DG	DG	CA1	CA1	CA1
ME	De	De	Thick	Vo	De	Tot	Vo	De	Tot
Eu+Veh	7	7	7	6	6	6	6	5	5
Ts65Dn+Veh	6	7	8	6	5	5	6	5	5
Eu+7,8-DHF	5	5	5	5	5	5	5	5	5
Ts65Dn+7,8-DHF	6	8	8	8	8	8	8	5	5

Table.5. Number of mice used for the evaluation of proliferation potency and stereology in the examined regions. *The numbers in each column indicate the number of mice used for the measurements (ME), indicated in the corresponding row, in the different regions of interest (ROI), indicated in the corresponding row. Sections processed for BrdU immunohistochemistry were used to evaluate the total number of proliferating cells. Nissl-stained sections were used for stereology. 7,8-DHF, 7,8-dihydroxyflavone; CA1, hippocampal field; cCX, caudal cortex; cSVZ, caudal subventricular zone; De, cell density; DG, dentate gyrus; Eu, euploid; HYP, hypothalamus; L II, layer two; L VI, layer sixth; rCX, rostral cortex; rSVZ, rostral subventricular zone; STR, striatum; Thick, thickness; TH, thalamus; Tot, total cell number; Veh, Vehicle; Vo, volume.*

Statistical analysis

Results are presented as mean ± standard error of the mean (SE). Data were analyzed with the IBM SPSS 22.0 software. Before running statistical analyses, we checked data distribution and homogeneity of variances for each variable using the Shapiro-Wilk test and Levene's test, respectively. If the data were normally distributed and variance was homogeneous, statistical analysis was carried out using a two-way ANOVA with genotype (euploid, Ts65Dn) and treatment (vehicle, 7,8-DHF) as factors. *Post hoc* multiple comparisons were then carried out using Fisher's least significant difference (LSD) test. If the data were not normally distributed and variance was heterogeneous, transformations were made to achieve normality. If the transformed data did not achieve normality, statistical analysis was carried out using the Kruskal-Wallis test followed by the Mann–Whitney U test. Based on the "Box plot" tool available in SPSS Descriptive Statistics, in each analysis we excluded the extremes, i.e., values that were larger than 3 times the IQ range [$x \geq Q3 + 3 * (IQ)$; $x \leq Q1 - 3 * (IQ)$]. The number of mice included in individual analyses is reported in the legends of figures. A probability level of $p \leq 0.05$ was considered to be statistically significant.

Abbreviations

The list reports the abbreviations used in the Results and Discussion

cCX caudal cortex

cSVZ caudal subventricular zone

CX neocortex

HYP hypotalamus

rSVZ rostral subventricular zone

rCX rostral cortex

SGZ subgranular zone

STR striatum

TH thalamus

RESULTS

General results

Effects of embryonic treatment with 7,8-DHF on abortion rate, perinatal death, and litter size.

The Ts65Dn mouse is the most widely used mouse model of DS. However, this strain is fragile and difficult to maintain. Males are sterile and female are generally poor mothers. Moreover, although loss of both euploid and trisomic mice occurs during the latter stage of gestation and between birth and weaning, trisomic mice are lost disproportionately (Roper, 2006). In view of this reason we deemed it important to evaluate whether prenatal treatment with 7,8-DHF affects the abortion rate and the number of pups per litter. Ts65Dn female treated with 7,8-DHF during pregnancy did not exhibit higher abortion rate in comparison to the untreated counterpart (Table 6).

Treatment		Abortion	
	n	Mean	SE
Vehicle	7	0.00	0.00
7,8-DHF	7	0.14	0.14
p		n.s.	

Table.6. Effects of embryonic treatment with 7,8-DHF on abortion rate. *Pregnancy outcome for Ts65Dn females treated with vehicle (n=7) or 7,8-DHF (n=7) from gestational day 10 to delivery. The number of spontaneous abortions is expressed as the mean of total pregnancies of each group. Data are mean ± SE. n.s, not significant (Kruskall-Wallis test).*

The number of mice per litter and their survival rate was similar between treated and untreated mice (Table 7).

Treatment		Litter size		Postnatal death	
	n	Mean	SE	Mean	SE
Vehicle	7	5.50	0.74	4.08	4.08
7,8-DHF	7	5.71	0.68	8.84	5.73
p		n.s.		n.s.	

Table.7. Effects of embryonic treatment with 7,8-DHF on perinatal death and litter size. *Litters of females treated with vehicle (n=7) or 7,8-DHF (n=7) from gestational day 10 to delivery. Litter size is expressed as mean of individual litters. Postnatal death is expressed as the mean of the percentage of deaths over numbers of births. Data are mean ± SE (two-tailed t-test, for litter size; Kruskall-Wallis test for postnatal death).*

These results indicated that prenatal treatment with 7,8-DHF has no adverse effects on pregnancy and pups viability.

Effect of embryonic treatment with 7,8-DHF on body and brain weight in Ts65Dn and euploid mice.

To establish the global effect of prenatal treatment with 7,8-DHF we evaluated the body and brain weight of P2 mice. A two-way ANOVA on the body weight showed no genotype x treatment interaction, a main effect of genotype [$F(1,33) = 11.089$, $p = 0.002$] and no main effect of treatment.

A *post hoc* Fisher's LSD test showed no difference in the body weight between untreated euploid and untreated Ts65Dn but that treated Ts65Dn mice had a reduced body weight in comparison with treated euploid mice. This finding is in line with the reduced body weight that characterizes the Ts65Dn mouse model (Guidi, 2014; Roper, 2006). Treatment with 7,8-DHF had no effect on body weight both in euploid and Ts65Dn mice (Table 8).

	n	Mean	SE		n	Mean	SE	
								p
Eu+ Veh	9	1.87	± 0.09	Eu+7,8-DHF	8	2.02	±0.07	n.s.
Ts65Dn+Veh	9	1.68	± 0.16	Ts65Dn+7,8-DHF	11	1.53	±0.06	n.s
p	n.s					**<0.01**		

Table.8. Effects of embryonic treatment with 7,8-DHF on body weight. *Body weight of P2 mice used in the current study. The mice received either vehicle (Veh) or 7,8-DHF during the embryonic period E10-E20/21. The p value in the row below the two genotypes refers to the comparison between untreated euploid (Eu+Veh) and Ts65Dn (Ts65Dn+Veh) mice and treated euploid (Eu+7,8-DHF) and (Ts65Dn+7,8DHF) mice. The p value in the column on the right refers to the comparison between untreated and treated mice of the same genotype. Data are mean ± SE (Fisher's LSD test after two-way ANOVA). 7,8-DHF, 7,8-dihydroxyflavone; Eu, euploid; n, number of mice; n.s, not significant; SE, standard error; Veh, vehicle.*

A two-way ANOVA on the brain weight showed no genotype x treatment interaction, no main effect of genotype, and no main effect of treatment. In absolute terms the brain weight of Ts65Dn mice was smaller in comparison with their untreated counterparts (see Table 8) which is in agreement with data from the literature (Belichenko 2004; Guidi, 2014; Stagni, 2017). Taken together, these results suggest that treatment with 7,8-DHF do not negatively affects body growth and brain development.

	n	Mean	SE		n	Mean	SE	
								p
Eu+ Veh	9	0.12	± 0.01	Eu+7,8-DHF	8	0.12	0.01	n.s.
Ts65Dn+Veh	9	0.11	± 0.01	Ts65Dn+7,8-DHF	11	0.10	0.01	n.s
p	n.s					n.s.		

Table.9. Effects of embryonic treatment with 7,8-DHF on brain weight. *Brain weight of P2 mice used in the current study. The mice received either vehicle (Veh) or 7,8-DHF during the embryonic period E10-E20/21. The p value in the row below the two genotypes refers to the comparison between untreated euploid (Eu+Veh) and Ts65Dn (Ts65Dn+Veh) mice and treated euploid (Eu+7,8-DHF) and (Ts65Dn+7,8DHF) mice. The p value in the column on the right refers to the*

comparison between untreated and treated mice of the same genotype. Data are mean ±SE (Fisher's LSD test after two-way ANOVA). 7,8-DHF, 7,8-dihydroxyflavone; Eu, euploid; n, number of mice; n.s, not significant; SE, standard error; Veh, vehicle.

Widespread neurogenesis in P2 mice

In the mouse brain 90% of the cell population of the SVZ is dividing at E16, whereas the majority of the cells in the VZ are leaving the cell cycle. Neurons that are going to populate the neocortex, the hippocampus, the striatum, thalamus and hypothalamus are mainly born between the embryonic period E10-E19 (Brazel, 2003; Nery, 2002). Indeed, with the exception of DG and cerebellum (the latter not under investigation in this study) neurogenesis is mainly a prenatal event. In the DG, unlike other brain regions, neurogenesis starts around E10 but most of the granule neurons (80%) are generated in the postnatal SGZ (Altman,1975; Brazel, 2003). In P2 mice we observed numerous neural precursor cells in the SVZ and SGZ. In addition, proliferating cells were also scattered throughout the neocortex, striatum, thalamus, and hypothalamus. In order to establish the possible efficacy of a prenatal treatment with 7,8-DHF on the proliferation potency of neural precursor cells and their progeny, in embryonically treated P2 mice we evaluated the number of BrdU-positive cells in the rostral and caudal part of the SVZ, rostral and caudal part of the neocortex, SGZ, striatum, thalamus and hypothalamus.

Effect of embryonic treatment with 7,8-DHF on the proliferation potency in the rSVZ of Ts65Dn and euploid mice.

Although cells arising from the rSVZ and cSVZ can populate the entire cortical mantle, it appears that cells arising from the rSVZ preferentially distribute to the rCX and cells arising from the cSVZ preferentially distribute to the cCX (Brazel, 2003). For this reason, we evaluated the effect of embryonic treatment in these two different rostro-caudal regions of the SVZ separately.

A two-way ANOVA on the number of BrdU-positive cells in the rSVZ showed a genotype x treatment interaction [$F(1,27) = 5.109$, $p = 0.032$], a main effect of genotype [$F(1,27) = 17.750$, $p = 0.001$], and no main effect of treatment. A *post hoc* Fisher's LSD test showed that untreated Ts65Dn mice had a reduced proliferation potency (-34%) compared with untreated euploid mice. Ts65Dn mice treated with 7,8-DHF have an increased (+25%) number of BrdU-positive cells in comparison with their untreated counterparts. Although Ts65Dn mice treated with 7,8-DHF showed a significant

increment in the number of BrdU-positive cells, this effect was not a restoration because treated Ts65Dn mice still had fewer BrdU-positive cells in comparison with euploid mice. In euploid mice treatment had no effect on the number of BrdU-positive cells in the rSVZ.

	df	F	Sign.
genotype	1	17,750	**,000**
treatment	1	,910	,349
genotype x treatment	1	5,109	**,032**
Error	27		

Table.10. *The table reports the results of the two-way ANOVA on the effect of 7,8-DHF on the number of BrdU positive cells in the rSVZ of euploid and Ts65Dn mice. df, degree of freedom; sign, significance.*

	Number of BrdU-positive cells
	p
Eu+Veh/ Ts65Dn+Veh	**<.001**
Eu+Veh/Ts65Dn+7,8-DHF	**.022**
Ts65Dn+Veh/Ts65Dn+7,8-DHF	**.029**
Eu+Veh/Eu+7,8-DHF	.370
Eu+7,8-DHF/Ts65Dn+Veh	**.002**
Eu+7,8-DHF/Ts65Dn+7,8-DHF	.173

Table.11. *The table reports the p value of the Fisher's LSD test after two-way ANOVA on the effect of 7,8-DHF on the number of BrdU positive cells in the rSVZ of euploid and Ts65Dn mice. 7,8-DHF, 7,8-dihydroxyflavone; Eu, euploid; Veh, vehicle.*

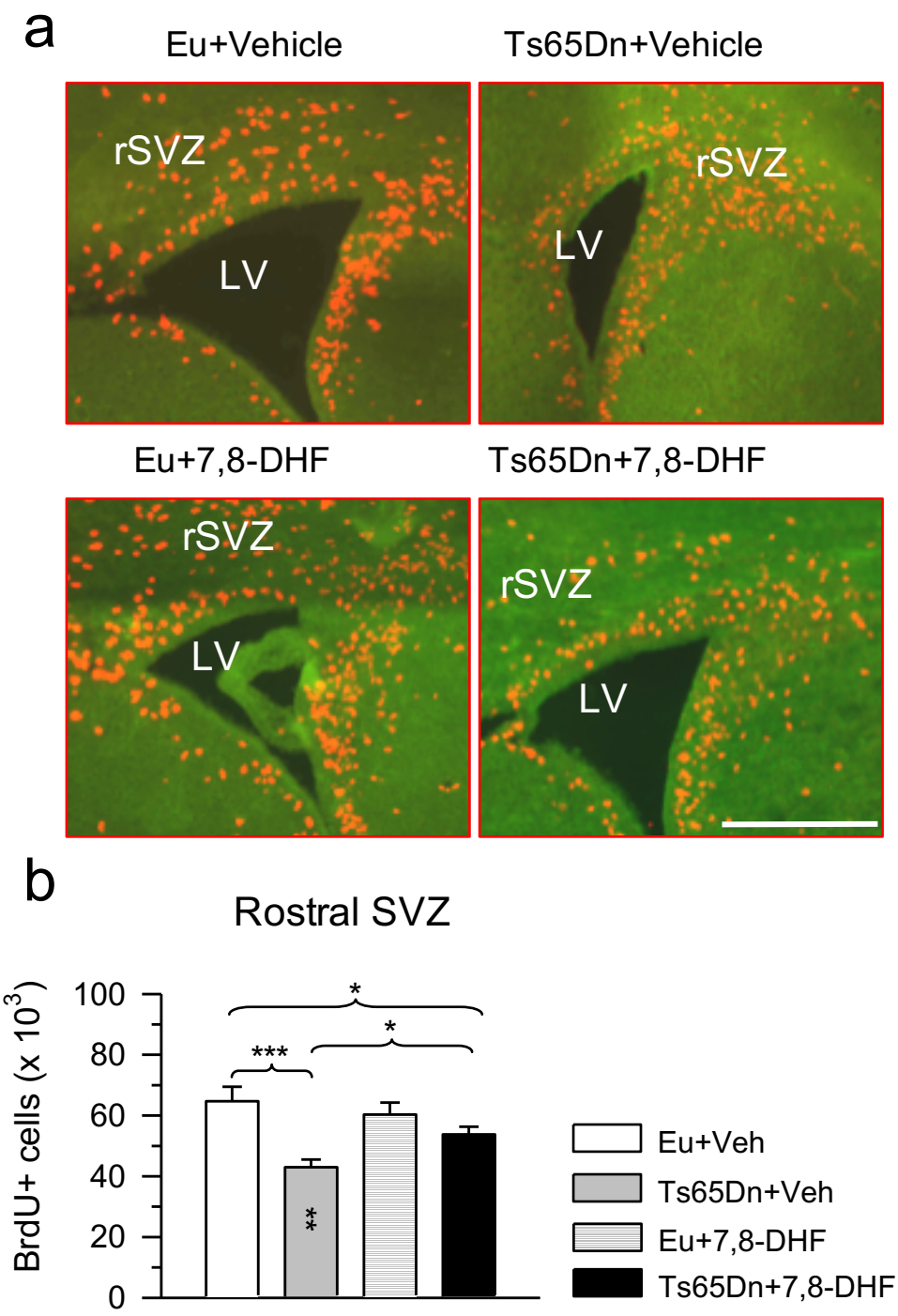

Fig.12. Effect of embryonic treatment with 7,8-DHF on neural precursor proliferation in the rostral subventricular zone of P2 Ts65Dn and euploid mice. *A) Examples of sections immunostained for BrdU and NeuN from the rSVZ of an animal of each experimental group. Calibration=200μm. B) Total number of BrdU positive cells in the rSVZ of untreated euploid (n=8) and Ts65Dn (n=7) mice and euploid (n=8) and Ts65Dn (n=9) mice treated with 7,8-DHF. Values (mean ± SE) represent totals for one hemisphere. * p < 0.05; ** p < 0.01; *** p < 0.001 (Fisher's LSD test after two-way ANOVA).*

Black asterisks in the gray bar indicate a difference between untreated Ts65Dn mice and treated euploid mice. 7,8-DHF, 7,8-dihydroxyflavone; Eu, euploid; LV, lateral ventricle; rSVZ, rostral subventricular zone; Veh, vehicle.

Effect of embryonic treatment with 7,8-DHF on the proliferation potency in the cSVZ of Ts65Dn and euploid mice.

A two-way ANOVA on the number of BrdU-positive cells in the cSVZ showed no genotype x treatment interaction, a main effect of genotype [F (1,30) = 17.181, p < 0.001], and a main effect of treatment [F(1,30) = 15.286, p < 0.001]. A *post hoc* Fisher's LSD test showed that untreated Ts65Dn mice had a reduced number of proliferating cells (-32%) in comparison with untreated euploid mice. In Ts65Dn mice treated with 7,8-DHF the number of BrdU-positive cells underwent an increase (+45%) in comparison with their untreated counterparts. A comparison of untreated euploid mice and Ts65Dn mice treated with 7,8-DHF showed no difference between groups indicating that treatment had restored the number of proliferating cells in the cSVZ. Treated euploid mice showed an increase in the number of BrdU-positive cells (+29%) in comparison with that of the untreated counterpart.

	df	F	Sign.
genotype	1	17,181	**,000**
treatment	1	15,286	**,000**
genotype x treatment	1	,007	,935
Error	30		

Table.12. *The table reports the results of the two-way ANOVA on the effect of 7,8-DHF on the number of BrdU positive cells in the cSVZ of euploid and Ts65Dn mice. df, degree of freedom; sign, significance.*

	Number of BrdU positive cells
	p
Eu+Veh/ Ts65Dn+Veh	**.007**
Eu+Veh/Ts65Dn+7,8-DHF	.861
Ts65Dn+Veh/Ts65Dn+7,8-DHF	**.009**
Eu+Veh/Eu+7,8-DHF	**.011**
Eu+7,8-DHF/Ts65Dn+Veh	**<.001**
Eu+7,8-DHF/Ts65Dn+7,8-DHF	**.006**

Table.13. *The table reports the p value of the Fisher's LSD test after two-way ANOVA on the effect of 7,8-DHF on the number of BrdU positive cells in the cSVZ of euploid and Ts65Dn mice. 7,8-DHF, 7,8-dihydroxyflavone; Eu, euploid; Veh, vehicle.*

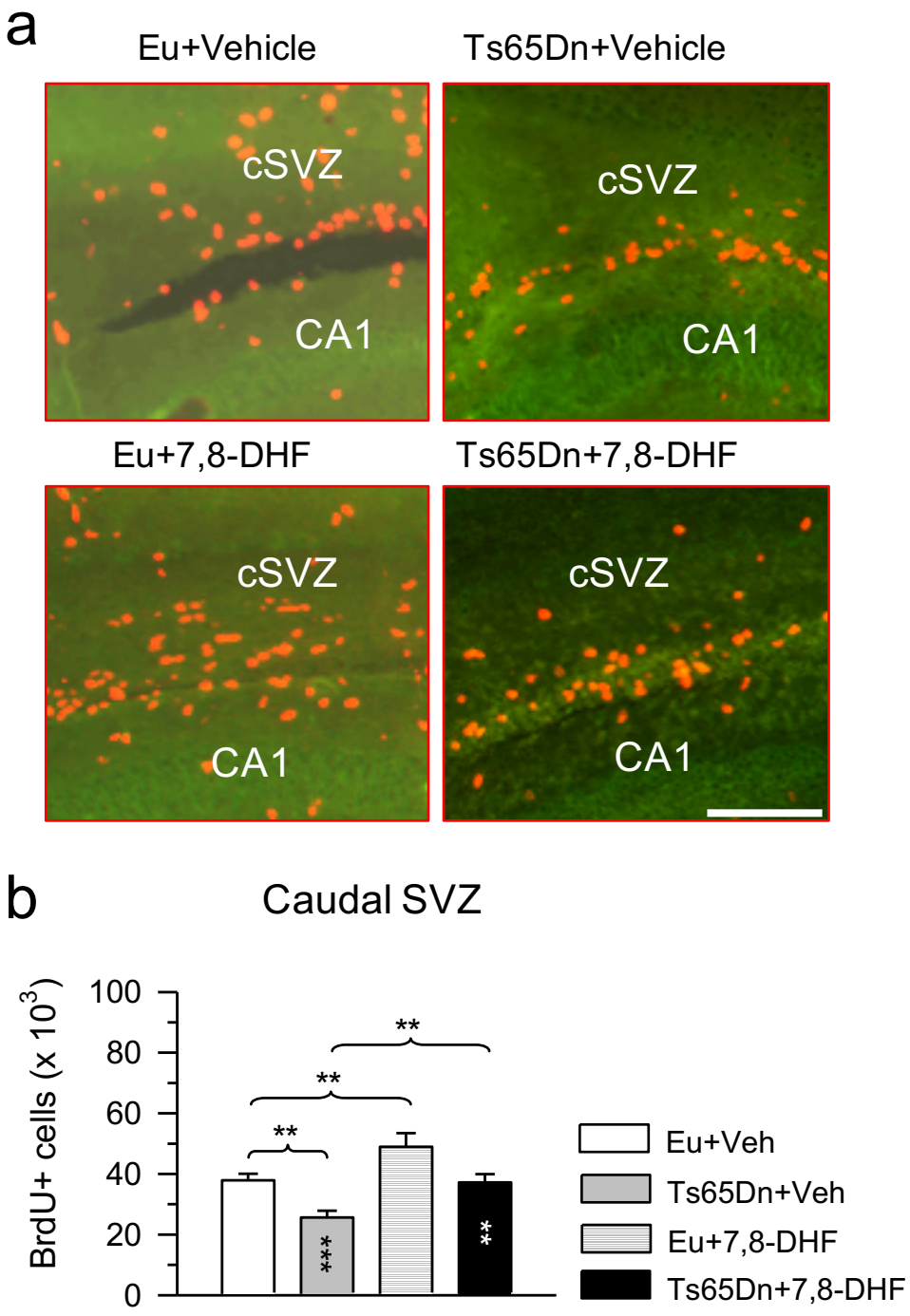

Fig.13. Effect of embryonic treatment with 7,8-DHF on neural precursor proliferation in the caudal subventricular zone of P2 Ts65Dn and euploid mice. *A) Examples of sections immunostained for BrdU and NeuN from the cSVZ of an animal of each experimental group. Calibration=100μm. B) Total number of BrdU positive cells in the cSVZ of untreated euploid (n=9) and Ts65Dn(n=7) mice and euploid (n=8) and Ts65Dn (n=10) mice treated with 7,8-DHF. Values (mean ± SE) represent totals for one hemisphere. ** p < 0.01; *** p < 0.001 (Fisher's LSD test after two-way ANOVA). Black asterisks in the gray bar indicate a difference between untreated Ts65Dn mice and treated euploid mice. White asterisks in the black bar indicate a difference between treated Ts65Dn mice and treated euploid mice. 7,8-DHF, 7,8-dihydroxyflavone; CA1, hippocampal field; cSVZ, caudal subventricular zone; Eu, euploid; Veh, vehicle.*

Effect of embryonic treatment with 7,8-DHF on the proliferation potency in the dentate gyrus of Ts65Dn and euploid mice.

While in the adult brain proliferating cells of the dentate gyrus are located in the SGZ, during the neonatal period proliferating cells are scattered throughout all layers of the DG. For this reason, we evaluated the number of proliferating cells located in the hilus, SGZ, and granule cell layer, along the whole rostro-caudal extent of the hippocampus.

A two-way ANOVA on the total number of BrdU-positive cells in the DG showed no genotype x treatment interaction, a main effect of genotype [F (1,28) = 13.068, p = 0.001], and no main effect of treatment. A *post hoc* Fisher's LSD test showed that in untreated Ts65Dn mice the number of proliferating cells was lower (-25%) compared with untreated euploid mice. The number of proliferating cells in treated Ts65Dn mice underwent an increase (+21%) and became similar to that of untreated euploid mice. Treatment showed no effect on the number of proliferating cells in the DG of euploid mice.

	df	F	Sign.
genotype	1	3,017	,093
treatment	1	13,068	**,001**
genotype x treatment	1	2,200	,149
Error	28		

Table.14. *The table reports the results of the two-way ANOVA on the effect of 7,8-DHF on the number of BrdU positive cells in the DG of euploid and Ts65Dn mice. df, degree of freedom; sign, significance.*

	Number of BrdU positive cells
	p
Eu+Veh/ Ts65Dn+Veh	**.001**
Eu+Veh/Ts65Dn+7,8-DHF	.138
Ts65Dn+Veh/Ts65Dn+7,8-DHF	**.028**
Eu+Veh/Eu+7,8-DHF	.861
Eu+7,8-DHF/Ts65Dn+Veh	**.002**
Eu+7,8-DHF/Ts65Dn+7,8-DHF	.136

Table.15. *The table reports the p value of the Fisher's LSD test after two-way ANOVA on the effect of 7,8-DHF on the number of BrdU positive cells in the DG of euploid and Ts65Dn mice. 7,8-DHF, 7,8-dihydroxyflavone; Eu, euploid; Veh, vehicle.*

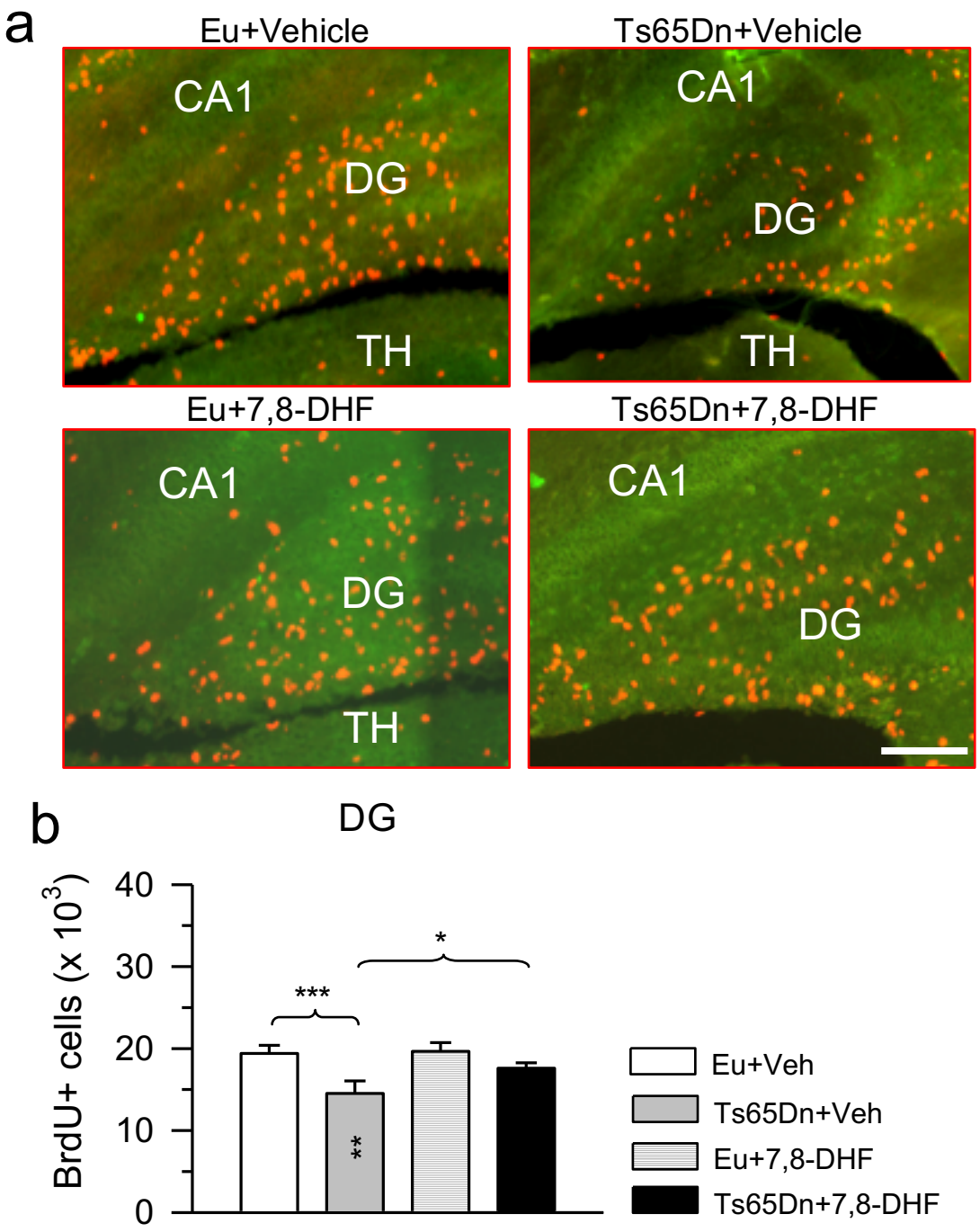

Fig.14. Effect of embryonic treatment with 7,8-DHF on neural precursor proliferation in dentate gyrus of P2 Ts65Dn and euploid mice. *A) Examples of sections immunostained for BrdU and NeuN from the DG of an animal of each experimental group. Calibration=100μm. B. Total number of BrdU positive cells in the hilus+granule cell layer of the DG of untreated euploid (n=9) and Ts65Dn(n=6) mice and euploid (n=6) and Ts65Dn (n=11) mice treated with 7,8-DHF. Values (mean ± SE) represent totals for one hemisphere. * p < 0.05; ** p < 0.01; *** p < 0.001 (Fisher's LSD test after two-way ANOVA). Black asterisks in the gray bar indicate a difference between untreated Ts65Dn mice and treated euploid mice. 7,8-DHF, 7,8-dihydroxyflavone; CA1, hippocampal field; DG, dentate gyrus; Eu, euploid; TH, thalamus; Veh, vehicle.*

Effect of embryonic treatment with 7,8-DHF on the proliferation potency in the rostral neocortex of Ts65Dn and euploid mice.

We separately evaluated cells located in the cortex overlying the rSVZ and cells located in the cortex overlying the cSVZ. A two-way ANOVA on the total number of BrdU-positive cells in the rostral neocortex showed no genotype x treatment interaction, a main effect of genotype [F (1,31) = 12.667, p = 0.001] and a main effect of treatment [F (1,31) = 8.315, p = 0.007]. A *post hoc* Fisher's LSD test showed that the number of proliferating cells in untreated Ts65Dn mice was lower (-39%) in comparison with untreated euploid mice. In treated Ts65Dn mice the number of proliferating cells underwent an increase (+45%) in comparison with their untreated counterparts and became similar to that of untreated euploid mice. In euploid mice prenatal treatment had no effect on the number of BrdU-positive cells.

	df	F	Sign.
genotype	1	12,667	**,001**
treatment	1	8,315	**,007**
genotype x treatment	1	,357	,555
Error	31		

Table.16. *The table reports the results of the two-way ANOVA on the effect of 7,8-DHF on the number of BrdU positive cells in the rCX of euploid and Ts65Dn mice. df, degree of freedom; sign, significance.*

	Number of BrdU-positive cells
	p
Eu+Veh/ Ts65Dn+Veh	**.004**
Eu+Veh/Ts65Dn+7,8-DHF	.620
Ts65Dn+Veh/Ts65Dn+7,8-DHF	**.017**
Eu+Veh/Eu+7,8-DHF	.124
Eu+7,8-DHF/Ts65Dn+Veh	**<.001**
Eu+7,8-DHF/Ts65Dn+7,8-DHF	.054

Table.17. *The table reports the p value of the Fisher's LSD test after two-way ANOVA on the effect of 7,8-DHF on the number of BrdU positive cells in the rCX of euploid and Ts65Dn mice. 7,8-DHF, 7,8-dihydroxyflavone; Eu, euploid; Veh, vehicle.*

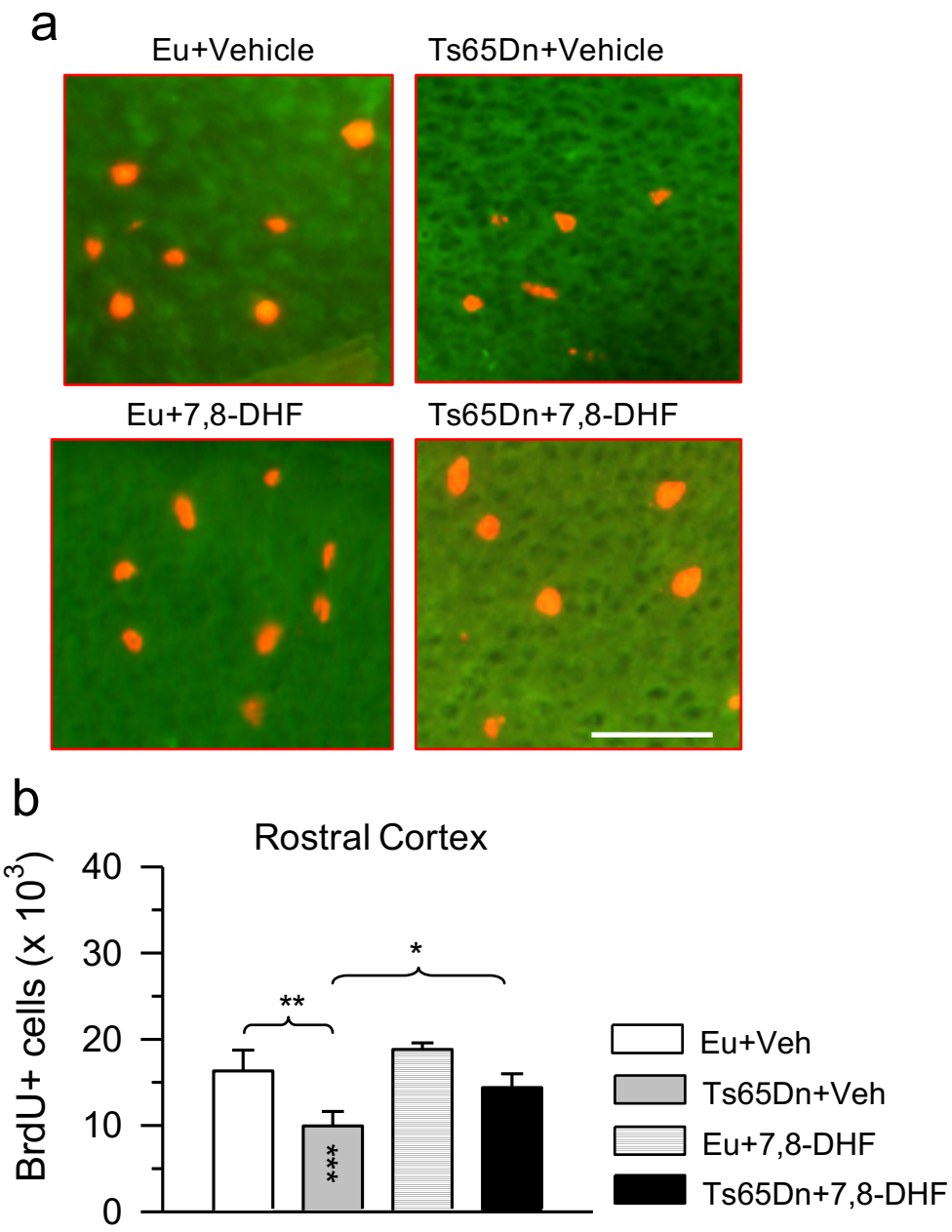

Fig.15. Effect of embryonic treatment with 7,8-DHF on proliferating cells in the rostral neocortex of P2 Ts65Dn and euploid mice. *A) Examples of sections immunostained for BrdU and NeuN from the rCX of an animal from each experimental group. Calibration bar = 50 μm. B) Total number of BrdU-positive cells in the rCX of untreated euploid (n= 9) and Ts65Dn (n=7) mice and euploid (n=8) and Ts65Dn (n=9) mice treated with 7,8-DHF. Values (mean ± SE) in represent totals for one hemisphere. * p < 0.05; ** p<0.01; *** p < 0.001 (Fisher's LSD test after two-way ANOVA). Black asterisks in the gray bar indicate a difference between untreated Ts65Dn mice and treated euploid mice. 7,8-DHF, 7,8-dihydroxyflavone; Eu, euploid; Veh, vehicle.*

Effect of embryonic treatment with 7,8-DHF on the proliferation potency in the caudal neocortex of Ts65Dn and euploid mice.

A two-way ANOVA on the total number of BrdU-positive cells in the caudal neocortex showed no genotype x treatment interaction, a main effect of genotype [$F(1,29) = 20.417$, $p < 0.001$] and no main effect of treatment. A *post hoc* Fisher's LSD test showed that untreated Ts65Dn mice displayed fewer proliferating cells (-45%) in comparison with untreated euploid mice. In treated Ts65Dn mice the number of BrdU-positive cells did not increase in comparison with their untreated counterparts.

	df	F	Sign.
genotype	1	20,417	**,000**
treatment	1	3,454	,073
genotype x treatment	1	,023	,880
Error	29		

Table.18. *The table reports the results of the two-way ANOVA on the effect of 7,8-DHF on the number of BrdU positive cells in the cCX of euploid and Ts65Dn mice. df, degree of freedom; sign, significance.*

	Number of BrdU-positive cells
	p
Eu+Veh/ Ts65Dn+Veh	**.006**
Eu+Veh/Ts65Dn+7,8-DHF	**.043**
Ts65Dn+Veh/Ts65Dn+7,8-DHF	.239
Eu+Veh/Eu+7,8-DHF	.164
Eu+7,8-DHF/Ts65Dn+Veh	**<.001**
Eu+7,8-DHF/Ts65Dn+7,8-DHF	**.002**

Table.19. *The table reports the p value of the Fisher's LSD test after two-way ANOVA on the effect of 7,8-DHF on the number of BrdU positive cells in the cCX of euploid and Ts65Dn mice. 7,8-DHF, 7,8-dihydroxyflavone; Eu, euploid; Veh, vehicle.*

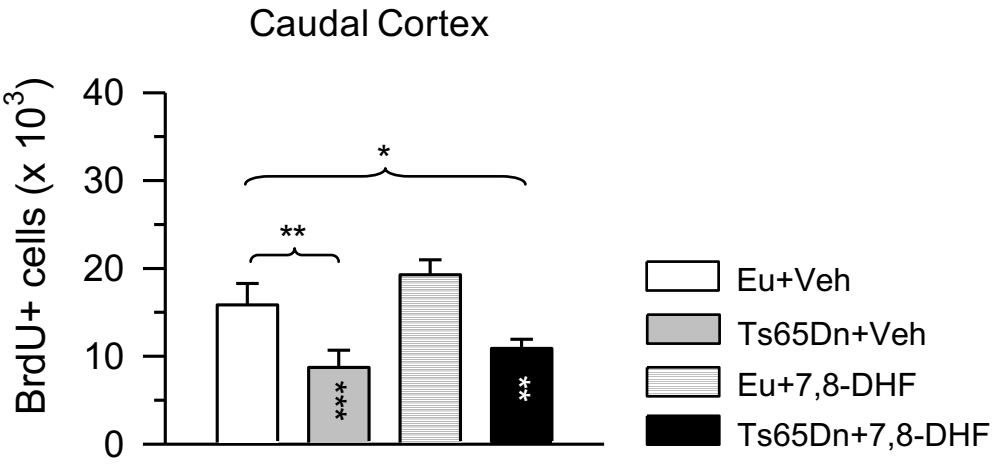

Fig.16. Effect of embryonic treatment with 7,8-DHF on proliferating cells in the caudal neocortex of P2 Ts65Dn and euploid mice. *Total number of BrdU-positive cells in the cCX of untreated euploid (n= 9) and Ts65Dn (n=6) mice and euploid (n=8) and Ts65Dn (n=11) mice treated with 7,8-DHF. Values (mean ± SE) represent totals for one hemisphere. * p < 0.05; ** p < 0.01; *** p < 0.001 (Fisher's LSD test after two-way ANOVA). Black asterisks in the gray bar indicate a difference between untreated Ts65Dn mice and treated euploid mice. White asterisks in the black bar indicate a difference between treated Ts65Dn mice and treated euploid mice. 7,8-DHF, 7,8-dihydroxyflavone; Eu, euploid; Veh, vehicle.*

Effect of embryonic treatment with 7,8-DHF on the proliferation potency in the striatum of Ts65Dn and euploid mice

Part of the cells arising from the LGE during the embryonic period migrate to constitute the striatum. A two-way ANOVA on the total number of BrdU-positive cells in the striatum showed no genotype x treatment interaction, a main effect of genotype [$F(1,30) = 16.564$, $p < 0.001$], and a main effect of treatment [$F(1,30) = 8.493$, $p = 0.007$]. A *post hoc* Fisher's LSD test showed that untreated Ts65Dn mice had fewer proliferating cells (-36%) in comparison with untreated euploid mice. Treatment increased the number of BrdU-positive cells (+40%) in Ts65Dn mice in comparison with their untreated counterparts and, although this effect was only marginally significant, the number of BrdU-positive cells became similar to that of untreated euploid mice. Euploid mice showed an increase (+28%) in the number of BrdU-positive cells in comparison with untreated euploid mice.

	df	F	Sign.
Genotype	1	16,564	**,000**
treatment	1	8,493	**,007**
genotype x treatment	1	,034	,855
Error	30		

Table.20. *The table reports the results of the two-way ANOVA on the effect of 7,8-DHF on the number of BrdU positive cells in the STR of euploid and Ts65Dn mice. df, degree of freedom; sign, significance.*

	Total number of BrdU-positive cells
	p
Eu+Veh/ Ts65Dn+Veh	**.012**
Eu+Veh/Ts65Dn+7,8-DHF	.391
Ts65Dn+Veh/Ts65Dn+7,8-DHF	.065
Eu+Veh/Eu+7,8-DHF	**.035**
Eu+7,8-DHF/Ts65Dn+Veh	**<.001**
Eu+7,8-DHF/Ts65Dn+7,8-DHF	**.004**

Table.21. *The table reports the p value of the Fisher's LSD test after two-way ANOVA on the effect of 7,8-DHF on the number of BrdU positive cells in the STR of euploid and Ts65Dn mice. 7,8-DHF, 7,8-dihydroxyflavone; Eu, euploid; Veh, vehicle.*

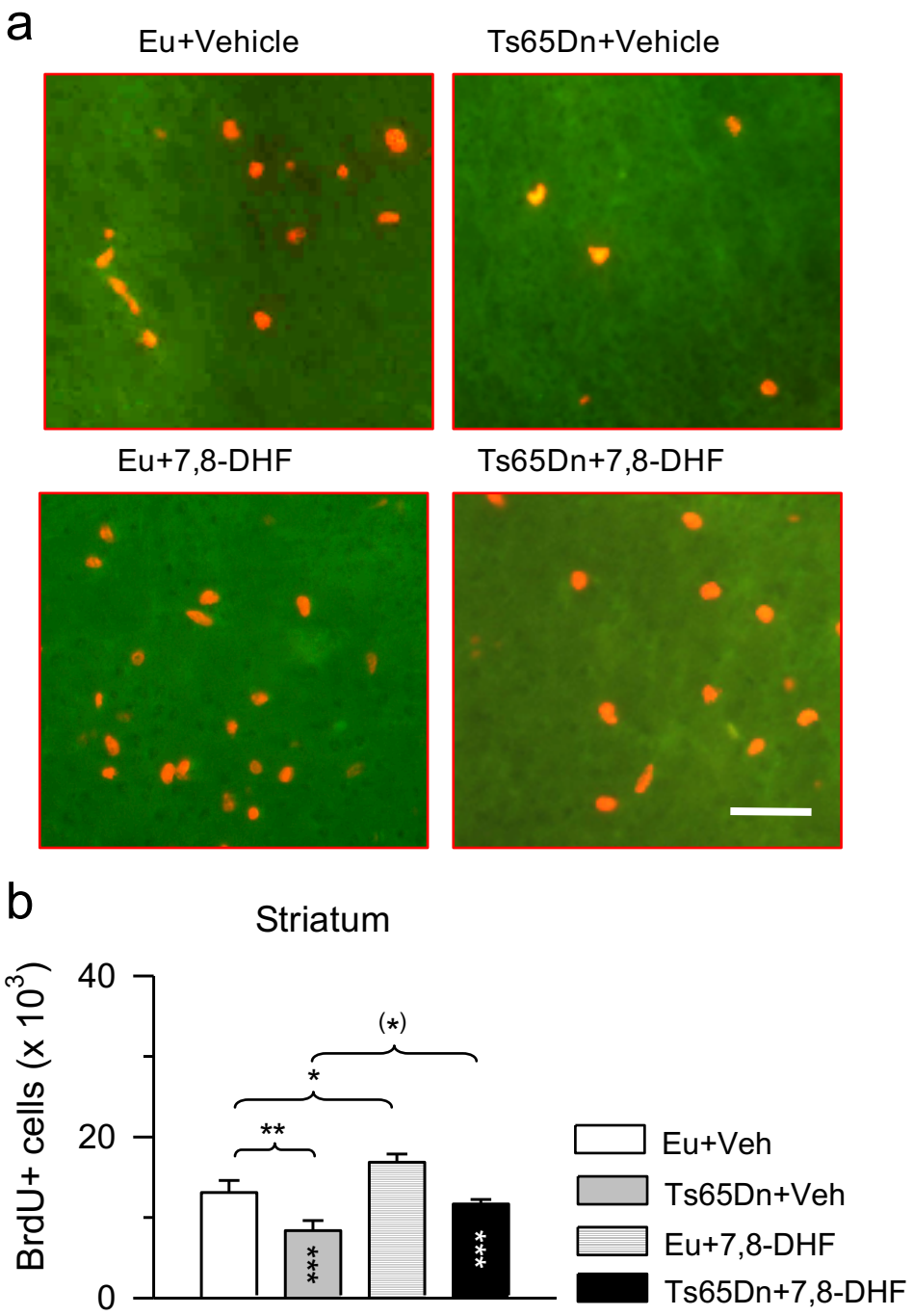

Fig.17. Effect of embryonic treatment with 7,8-DHF on proliferating cells in the striatum of P2 Ts65Dn and euploid mice. *A) Examples of sections immunostained for BrdU and NeuN from the STR of an animal from each experimental group. Calibration = 50 μm. B) Total number of BrdU-positive cells in the STR of untreated euploid (n= 9) and Ts65Dn (n=7) mice and euploid (n=8) and Ts65Dn (n=10) mice treated with 7,8-DHF. Values (mean ±SE) represent totals for one hemisphere. (*) p <0.06; * p < 0.05; ** p < 0.01; *** p < 0.001 (Fisher's LSD test after two-way ANOVA). Black asterisks in the gray bar indicate a difference between untreated Ts65Dn mice and treated euploid mice. White asterisks in the black bar indicate a difference between treated Ts65Dn mice and treated euploid mice. 7,8-DHF, 7,8-dihydroxyflavone; Eu, euploid; Veh, vehicle.*

Effect of embryonic treatment with 7,8 DHF on the proliferation potency in the thalamus of Ts65Dn and euploid mice

Cells populating the thalamus derive from the MGE and LGE (Brazel, 2003). A two-way ANOVA on the number of BrdU-positive cells in the thalamus showed no genotype x treatment interaction, a main effect of genotype [F (1,20) = 4.735, p < 0.038], and no main effect of treatment. A *post hoc* Fisher's LSD test showed that untreated Ts65Dn mice had a reduced number of proliferating cells (-40%) in comparison with untreated euploid mice. Treatment did not significantly increase the number of proliferating cells in comparison with their untreated counterparts, although in absolute terms the number of proliferating cells became larger in treated (16,179 ±1582) in comparison with untreated (11,953 ±1561) Ts65Dn mice and was statistically similar to that of untreated euploid mice. No effect of treatment was found in the thalamus of euploid mice.

	df	F	Sign.
Genotype	1	4,735	**,038**
treatment	1	,169	,684
genotype x treatment	1	2,325	,138
Error	30		

Table.22. *The table reports the results of the two-way ANOVA on the effect of 7,8-DHF on the number of BrdU positive cells in the TH of euploid and Ts65Dn mice. df, degree of freedom; sign, significance.*

	Number of BrdU positive cells
	p
Eu+Veh/ Ts65Dn+Veh	**.016**
Eu+Veh/Ts65Dn+7,8-DHF	.194
Ts65Dn+Veh/Ts65Dn+7,8-DHF	.184
Eu+Veh/Eu+7,8-DHF	.434
Eu+7,8-DHF/Ts65Dn+Veh	.094
Eu+7,8-DHF/Ts65Dn+7,8-DHF	.638

Table.23. *The table reports the p value of the Fisher's LSD test after two-way ANOVA on the effect of 7,8-DHF on the number of BrdU positive cells in the thalamus of euploid and Ts65Dn mice. 7,8-DHF, 7,8-dihydroxyflavone; Eu, euploid; Veh, vehicle.*

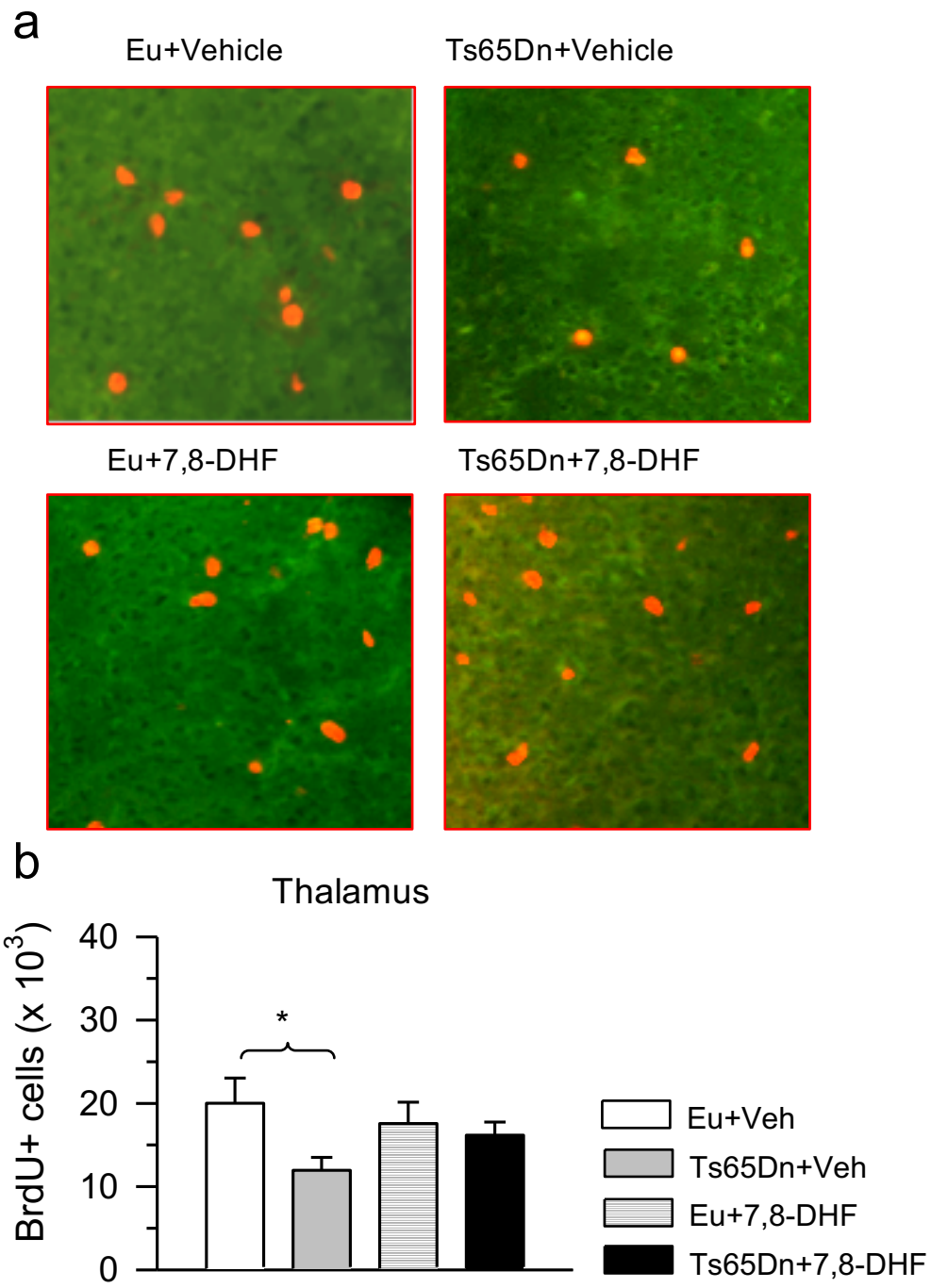

Fig.18. Effect of embryonic treatment with 7,8-DHF on proliferating cells in the thalamus of P2 Ts65Dn and euploid mice. A) Examples of sections immunostained for BrdU and NeuN from the TH of an animal from each experimental group. Calibration bar= 50 μm. B) Total number of BrdU-positive cells in the TH of untreated euploid (n=9) and Ts65Dn (n=7) mice and euploid (n=8) and Ts65Dn (n=9) mice treated with 7,8-DHF. Values (mean ± SE) represent totals for one hemisphere. * $p < 0.05$ (Fisher's LSD test after two-way ANOVA). Abbreviations: 7,8-DHF, 7,8-dihydroxyflavone; Eu, euploid; Veh, vehicle.

Effect of embryonic treatment with 7,8 DHF on the proliferation potency in the hypothalamus of Ts65Dn and euploid mice

A two-way ANOVA on the number of BrdU-positive cells in the hypothalamus showed no genotype x treatment interaction, a main effect of genotype [$F(1,20) = 7.928$, $p < 0.009$], and no main effect of treatment. A *post hoc* Fisher's LSD test showed that in untreated Ts65Dn mice the number of proliferating cells was lower (-45%) in comparison with untreated euploid mice. Treatment did not increase the number of proliferating cells in Ts65Dn mice that remained lower (-35%) in comparison with untreated euploid mice (Fig. 18).

	df	F	Sign.
genotype	1	7,928	**,009**
treatment	1	,002	,962
genotype x treatment	1	,738	,397
Error	30		

Table.24. *The table reports the results of the two-way ANOVA on the effect of 7,8-DHF on the number of BrdU positive cells in the HYP of euploid and Ts65Dn mice. df, degree of freedom; sign, significance.*

	Number of BrdU positive cells
	p
Eu+Veh/ Ts65Dn+Veh	**.017**
Eu+Veh/Ts65Dn+7,8-DHF	**.039**
Ts65Dn+Veh/Ts65Dn+7,8-DHF	.573
Eu+Veh/Eu+7,8-DHF	.523
Eu+7,8-DHF/Ts65Dn+Veh	.074
Eu+7,8-DHF/Ts65Dn+7,8-DHF	.164

Table.25. *The table reports the p value of the Fisher's LSD test after two-way ANOVA on the effect of 7,8-DHF on the number of BrdU positive cells in the hypothalamus of euploid and Ts65Dn mice. 7,8-DHF, 7,8-dihydroxyflavone; Eu, euploid; Veh, vehicle.*

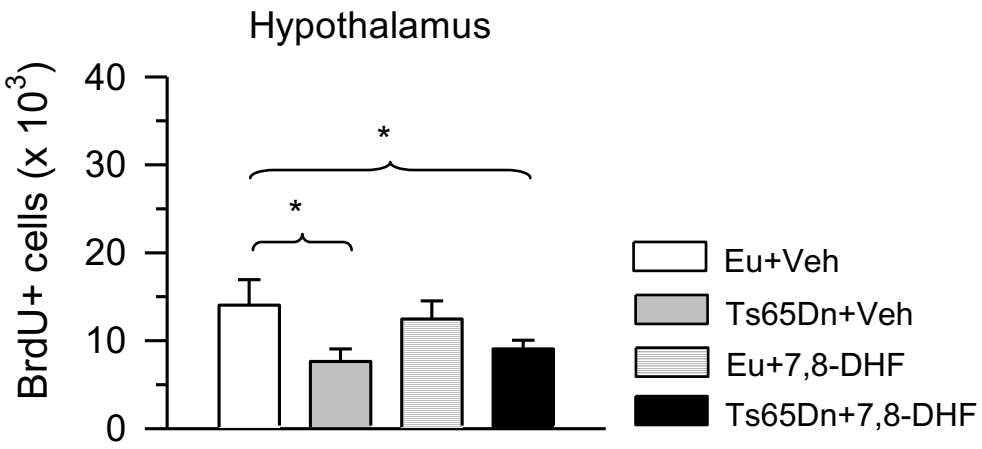

Fig.18. Effect of embryonic treatment with 7,8-DHF on proliferating cells in the hypothalamus of P2 Ts65Dn and euploid mice. *Total number of BrdU-positive cells in the HYP of untreated euploid (n= 9) and Ts65Dn (n=7) mice and euploid (n=8) and Ts65Dn (n=9) mice treated with 7,8-DHF. Values (mean ± SE) represent totals for one hemisphere. * p < 0.05 (Fisher's LSD test after two-way ANOVA). Abbreviations: 7,8-DHF, 7,8-dihydroxyflavone; Eu, euploid; Veh, vehicle.*

Effect of embryonic treatment with 7,8-DHF on cellularity in Ts65Dn and euploid mice

Considering the positive effects of prenatal treatment with 7,8-DHF on the proliferation potency in the SVZ and SGZ of Ts65Dn mice we wanted to investigate whether this effect translated into an increase in cell number. To this purpose, we evaluated the number of cells in the caudal neocortex, granule cell layer of the DG and pyramidal layer of hippocampal field CA1.

Effect of embryonic treatment with 7,8-DHF on cortical thickness in the caudal neocortex of Ts65Dn and euploid mice

A two-way ANOVA on the thickness of the caudal neocortex showed no genotype x treatment interaction, no main effect of genotype, and a main effect of treatment [$F(1,24) = 6.293$, $p = 0.019$]. A *post hoc* Fisher's LSD test showed no difference in cortical thickness between untreated Ts65Dn and untreated euploid mice, although in absolute terms the cortical thickness of untreated euploid mice was larger in comparison with that of Ts65Dn mice. Untreated Ts65Dn mice had a reduced cortical thickness in comparison with treated euploid mice. Treatment had no effect on the cortical thickness both in Ts65Dn and euploid mice.

	df	F	Sign.
genotype	1	2,842	,105
treatment	1	6,293	**,019**
genotype x treatment	1	,001	,979
Error	24		

Table.26. *The table reports the results of the two-way ANOVA on the effect of 7,8-DHF on the thickness of the cCx of euploid and Ts65Dn mice. df, degree of freedom; sign, significance.*

	Thickness
	p
Eu+Veh/ Ts65Dn+Veh	.215
Eu+Veh/Ts65Dn+7,8-DHF	.546
Ts65Dn+Veh/Ts65Dn+7,8-DHF	.063
Eu+Veh/Eu+7,8-DHF	.116
Eu+7,8-DHF/Ts65Dn+Veh	**.009**
Eu+7,8-DHF/Ts65Dn+7,8-DHF	.274

Table.27. *The table reports the p value of the Fisher's LSD test after two-way ANOVA on the effect of 7,8-DHF on the thickness of the cCx of euploid and Ts65Dn mice. 7,8-DHF, 7,8-dihydroxyflavone; Eu, euploid; Veh, vehicle.*

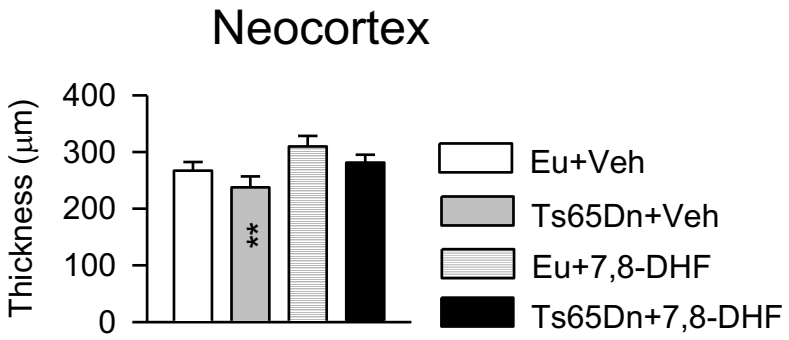

Fig.20. Effect of embryonic treatment with 7,8-DHF on cortical thickness in P2 Ts65Dn and euploid mice. *Cortical thickness (layers II-VI) in untreated euploid (n=7) and Ts65Dn (n=6 for layer II; n=7 for layer VI;) mice and euploid (n=5) and Ts65Dn (n=6 for layer II; n=8 for layer VI) mice treated with 7,8-DHF. p < 0.05; ** (Fisher's LSD test after two-way ANOVA). Black asterisks in the gray bar indicate a difference between untreated Ts65Dn mice and treated euploid mice. 7,8-DHF, 7,8-dihydroxyflavone; Eu, euploid; Veh, vehicle.*

Effect of embryonic treatment with 7,8-DHF on cell density in the caudal neocortex of Ts65Dn and euploid mice

The neocortex develops in an inside-outside fashion, with older neurons located in the deep cortical layers and younger neurons located in the more superficial layers. We wondered whether prenatal

treatment had an effect on cellularity in layer II and layer VI because these layers contain neurons with a different date of birth. Consequently, progenitors of neurons of layer II were exposed to treatment for a longer time, while progenitors of neurons of layer VI were exposed to treatment for a shorter time. A two-way ANOVA on cell density in layer II showed a genotype x treatment interaction [$F(1,20) = 14.119$, $p = 0.01$], a main effect of genotype [$F(1,20) = 21.563$, $p < 0.01$], and a main effect of treatment [$F(1,20) = 5.575$, $p = 0.028$]. A *post hoc* Fisher's LSD test showed that cell density was lower (-10%) in untreated Ts65Dn mice in comparison with untreated euploid mice. Treatment increased cell density (+8%) in Ts65Dn mice to a value similar to that of untreated euploid mice. In euploid mice treatment had no effect on cell density in layer II. Although we could not statistically compare data of layer VI cell density, because the Kruskal-Wallis test did not show a significant effect, the graph in Figure 21 shows that different groups had similar value

	gl	F	Sign.
genotype	1	21,563	**,000**
treatment	1	5,575	**,028**
genotype x treatment	1	14,119	**,001**
Error	20		

Table.28. *The table reports the results of the two-way ANOVA on the effect of 7,8-DHF on cell density of cortical layer II of euploid and Ts65Dn mice. df, degree of freedom; sign, significance.*

Chi-square	2,792
df	3
Sign	,425

Table.29. *The table reports the results of the Kruskal-Wallis test on the effect of 7,8-DHF on cell density of cortical layer IV of euploid and Ts65Dn mice. df, degree of freedom; sign, significance.*

	Cell density
	Layer II
	p
Eu+Veh/ Ts65Dn+Veh	**<.001**
Eu+Veh/Ts65Dn+7,8-DHF	.107
Ts65Dn+Veh/Ts65Dn+7,8-DHF	**<.001**
Eu+Veh/Eu+7,8-DHF	.339
Eu+7,8-DHF/Ts65Dn+Veh	**<.001**
Eu+7,8-DHF/Ts65Dn+7,8-DHF	.554

Table.30. *The table reports the p value of the Fisher's LSD test after two-way ANOVA on the effect of 7,8-DHF on the cell density of the cCx of euploid and Ts65Dn mice. 7,8-DHF, 7,8-dihydroxyflavone; Eu, euploid; Veh, vehicle*.

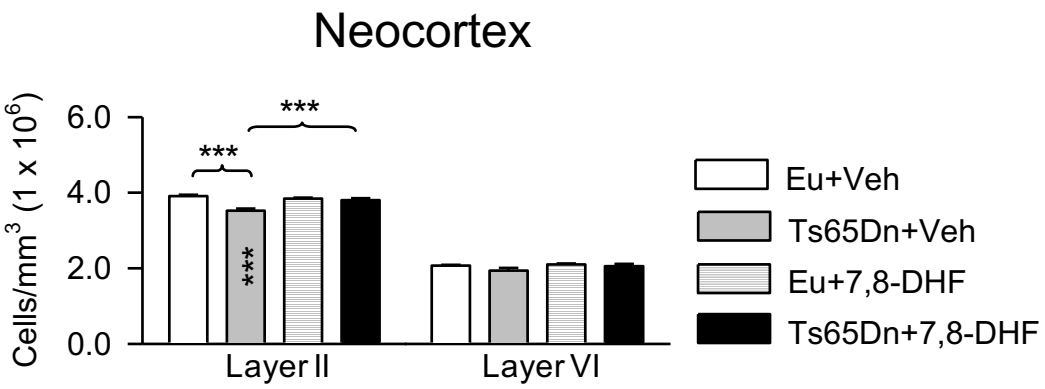

Fig. 21. Effect of embryonic treatment with 7,8-DHF on cell density in P2 Ts65Dn and euploid mice. *Cell number (cells per mm^3) in layer II and layer VI in untreated euploid (n=7) and Ts65Dn (n=6 for layer II; n=7 for layer VI;) mice and euploid (n=5) and Ts65Dn (n=6 for layer II; n=8 for layer VI) mice treated with 7,8-DHF. ; *** p < 0.001 (Fisher's LSD test after two-way ANOVA). Black asterisks in the gray bar indicate a difference between untreated Ts65Dn mice and treated euploid mice. 7,8-DHF, 7,8-dihydroxyflavone; Eu, euploid; Veh, vehicle.*

Effect of embryonic treatment with 7,8-DHF on the stereology of the dentate gyrus of the hippocampus of Ts65Dn and euploid mice

A two-way ANOVA on the volume of the DG showed no genotype x treatment interaction, a main effect of genotype [F (1,21) = 8.974, p = 0.010], and no main effect of treatment. A *post hoc* Fisher's LSD test showed that the volume of the granule cell layer of untreated Ts65Dn mice was reduced in comparison with that of untreated euploid mice. The volume of the granule cell layer of treated Ts65Dn mice became statistically similar to that of untreated euploid mice, although in absolute terms its size was smaller than that of euploid mice. The Kruskal-Wallis test showed no significant effect on granule cell density. A two-way ANOVA on total number of granule cells showed no genotype x treatment interaction, a main effect of genotype [F(1,20) = 18.973, p < 0.001], and no main effect of treatment. A *post hoc* Fisher's LSD test showed that in untreated Ts65Dn mice the number of granule cells was reduced in comparison with that of untreated euploid mice and that treatment did not restore total granule cell number that remained lower in comparison with untreated euploid mice.

	df	F	Sign.
genotype	1	8,974	**,007**
treatment	1	1,147	,296
genotype x treatment	1	,129	,723

Error	21		

Table.31. *The table reports the results of the two-way ANOVA on the effect of 7,8-DHF on the volume of the DG of euploid and Ts65Dn mice. df, degree of freedom; sign, significance.*

	Volume
	p
Eu+Veh/ Ts65Dn+Veh	**.028**
Eu+Veh/Ts65Dn+7,8-DHF	.163
Ts65Dn+Veh/Ts65Dn+7,8-DHF	.295
Eu+Veh/Eu+7,8-DHF	.638
Eu+7,8-DHF/Ts65Dn+Veh	**.013**
Eu+7,8-DHF/Ts65Dn+7,8-DHF	.075

Table.32. *The table reports the p value of the Fisher's LSD test after two-way ANOVA on the effect of 7,8-DHF on the volume of the granule cell layer of euploid and Ts65Dn mice. 7,8-DHF, 7,8-dihydroxyflavone; Eu, euploid; Veh, vehicle.*

Chi-square	2,314
df	3
Sign	,510

Table.33. *The table reports the results of the Kruskal-Wallis test on the effect of 7,8-DHF on cell density of the granule cell layer of euploid and Ts65Dn mice. df, degree of freedom; sign, significance.*

	Df	F	Sign.
genotype	1	18,973	**,000**
treatment	1	2,938	,102
genotype x treatment	1	,014	,906
Error	20		

Table.34. *The table reports the results of the two-way ANOVA on the effect of 7,8-DHF on the total number of granule cells of euploid and Ts65Dn mice. df, degree of freedom; sign, significance.*

	Total number of granule cells
	p
Eu+Veh/ Ts65Dn+Veh	**.009**
Eu+Veh/Ts65Dn+7,8-DHF	.055
Ts65Dn+Veh/Ts65Dn+7,8-DHF	.258
Eu+Veh/Eu+7,8-DHF	.223
Eu+7,8-DHF/Ts65Dn+Veh	**.001**
Eu+7,8-DHF/Ts65Dn+7,8-DHF	**.004**

Table.35. *The table reports the p value of the Fisher's LSD test after two-way ANOVA on the effect of 7,8-DHF on the total number of granule cells of euploid and Ts65Dn mice. 7,8-DHF, 7,8-dihydroxyflavone; Eu, euploid; Veh, vehicle.*

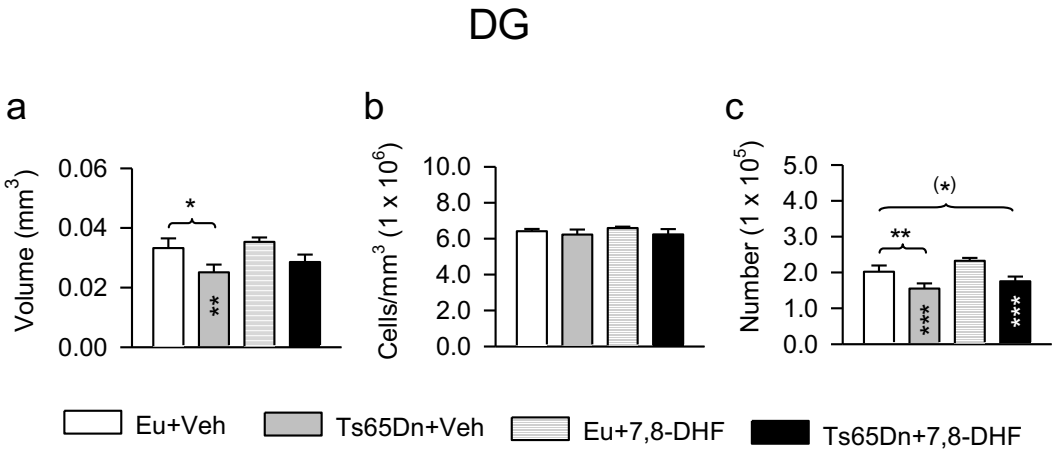

Fig.22. Effect of embryonic treatment with 7,8-DHF on the stereology of the dentate gyrus in P2 Ts65Dn and euploid mice. *Volume of the granule cell layer, density of granule cells (number per mm^3) and total number of granule cells of the DG in untreated euploid (n= 6) and Ts65Dn (n=6) mice and euploid (n=5) and Ts65Dn (n=8) mice treated with 7,8-DHF. Values (mean ± SE) refer to one hemisphere. (*) p < 0.06; * p < 0.05; ** p < 0.01; *** p < 0.001 (Fisher's LSD test after two-way ANOVA). Black asterisks in the gray bar indicate a difference between untreated Ts65Dn mice and treated euploid mice. White asterisks in the black bar indicate a difference between treated Ts65Dn mice and treated euploid mice. Abbreviations: 7,8-DHF, 7,8-dihydroxyflavone; DG, dentate gyrus; Eu, euploid; Veh, vehicle.*

Effect of embryonic treatment with 7,8-DHF on the stereology of the hippocampus of Ts65Dn and euploid mice

A two-way ANOVA on the volume of the pyramidal layer of field CA1 showed no genotype x treatment interaction, a main effect of genotype [F(1,21) = 5.447, p = 0.030], and no main effect of treatment. A *post hoc* Fisher's LSD test showed no difference between untreated Ts65Dn and euploid mice in the volume of the pyramidal layer and no effect of treatment. A two-way ANOVA on the density of pyramidal neurons showed a genotype x treatment interaction [F(1,20) = 6.360, p = 0.020], and no main effect of genotype and of treatment. A *post hoc* Fisher's LSD test showed that untreated Ts65Dn mice had a reduced cell density in comparison with untreated euploid mice and that treatment increased cell density to a value similar to that of untreated euploid mice. A two-way ANOVA on the number of pyramidal neurons showed no genotype x treatment interaction, a main effect of genotype [F(1,20) = 7.905, p = 0.011], and no main effect of treatment. A *post hoc* Fisher's LSD test showed that untreated Ts65Dn mice had a reduced number of pyramidal neurons in comparison with untreated euploid mice. Although in Ts65Dn mice treatment did not significantly increase the total number of pyramidal neurons in comparison with their untreated counterparts,

in absolute terms the number of pyramidal neurons became larger in treated (169,341±16,535) in comparison with untreated (149,690±19,064) mice and was statistically similar to that of untreated euploid mice.

	df	F	Sign.
genotype	1	5,447	**,030**
treatment	1	,020	,888
genotype x treatment	1	,003	,957
Error	21		

Table.36. *The table reports the results of the two-way ANOVA on the effect of 7,8-DHF on volume of the pyramidal layer of euploid and Ts65Dn mice. df, degree of freedom; sign, significance.*

	Volume
	p
Eu+Veh/ Ts65Dn+Veh	.124
Eu+Veh/Ts65Dn+7,8-DHF	.115
Ts65Dn+Veh/Ts65Dn+7,8-DHF	.948
Eu+Veh/Eu+7,8-DHF	.896
Eu+7,8-DHF/Ts65Dn+Veh	.112
Eu+7,8-DHF/Ts65Dn+7,8-DHF	.104

Table.37. *The table reports the p value of the Fisher's LSD test after two-way ANOVA on the effect of 7,8-DHF on volume of the pyramidal layer of euploid and Ts65Dn mice. 7,8-DHF, 7,8-dihydroxyflavone; Eu, euploid; Veh, vehicle.*

	Df	F	Sign.
Genotype	1	,526	,477
treatment	1	1,252	,276
genotype x treatment	1	6,360	**,020**
Error	20		

Table.38. *The table reports the results of the two-way ANOVA on the effect of 7,8-DHF on cell density in CA1 of euploid and Ts65Dn mice. df, degree of freedom; sign, significance.*

	CA1 cell density
	p
Eu+Veh/ Ts65Dn+Veh	**.037**
Eu+Veh/Ts65Dn+7,8-DHF	.765
Ts65Dn+Veh/Ts65Dn+7,8-DHF	**.015**
Eu+Veh/Eu+7,8-DHF	.347
Eu+7,8-DHF/Ts65Dn+Veh	.240
Eu+7,8-DHF/Ts65Dn+7,8-DHF	.205

Table.39. *The table reports the p value of the Fisher's LSD test after two-way ANOVA on the effect of 7,8-DHF on cell density in CA1 of euploid and Ts65Dn mice. 7,8-DHF, 7,8-dihydroxyflavone; Eu, euploid; Veh, vehicle.*

	df	F	Sign.
genotype	1	7,905	**,011**
treatment	1	,165	,689
genotype x treatment	1	,902	,354
Error	20		

Table.40. *The table reports the results of the two-way ANOVA on the effect of 7,8-DHF on the number of pyramidal neurons of euploid and Ts65Dn mice. df, degree of freedom; sign, significance.*

	Number of pyramidal neurons
	p
Eu+Veh/ Ts65Dn+Veh	**.018**
Eu+Veh/Ts65Dn+7,8-DHF	.079
Ts65Dn+Veh/Ts65Dn+7,8-DHF	.335
Eu+Veh/Eu+7,8-DHF	.713
Eu+7,8-DHF/Ts65Dn+Veh	**.047**
Eu+7,8-DHF/Ts65Dn+7,8-DHF	.190

Table.22. *The table reports the p value of the Fisher's LSD test after two-way ANOVA on the effect of 7,8-DHF on the number of pyramidal neurons of euploid and Ts65Dn mice. 7,8-DHF, 7,8-dihydroxyflavone; Eu, euploid; Veh, vehicle.*

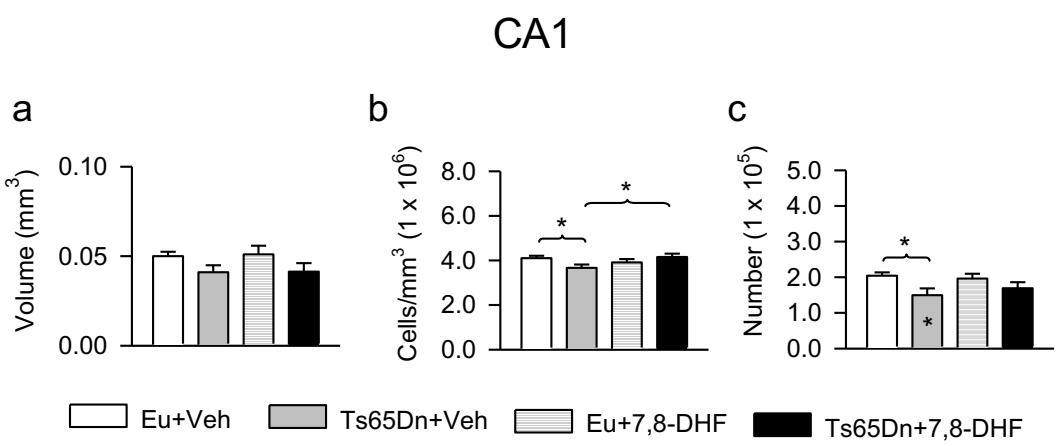

Fig.23. Effect of embryonic treatment with 7,8-DHF on the stereology of the hippocampal field CA1 in P2 Ts65Dn and euploid mice. *Volume of the pyramidal layer, density of pyramidal neurons (number per mm^3) and total number of pyramidal neurons of field CA1 in untreated euploid (n= 6) and Ts65Dn (n=6) mice and euploid (n=5) and Ts65Dn (n=8) mice treated with 7,8-DHF. Values (mean ± SE) refer to one hemisphere. * p < 0.05; (Fisher's LSD test after two-way ANOVA). Black asterisks in the gray bar indicate a difference between untreated Ts65Dn mice and treated euploid mice. 7,8-DHF, 7,8-dihydroxyflavone; CA1, hippocampal field; Eu, euploid; Veh, vehicle.*

DISCUSSION

In this study, consistently with previous evidence (Guidi, 2014), we observed a reduced proliferation potency in all the examined forebrain regions of Ts65Dn mice aged two days (P2). Prenatal treatment with 7,8-DHF was able to increase the number of proliferating cells in the SVZ of the Ts65Dn mice both in the rostral and caudal part. However, the magnitude of the effect was different between the two regions of the SVZ. While in the caudal part the number of proliferating cells in treated Ts65Dn mice became similar to that of untreated euploid mice, in the rostral part the number of proliferating cells in treated Ts65Dn mice remained lower in comparison with untreated euploid mice. In the SGZ of Ts65Dn mice treatment increased the pool of proliferating cells to a number similar to that of untreated euploid mice. In the rCX, STR and TH treatment enhanced the number of proliferating cells to a number statistically similar to that of untreated euploid mice although, in absolute terms, their number did not reach the value of euploid mice. At variance with the other examined regions the number of proliferating cells in the cCx and HYP of treated Ts65Dn mice was not increased by treatment. The embryonic VZ/SVZ of the lateral ventricle are the neurogenic niches from which the progenitors of neurons and glia cells that will constitute the telencephalon arise. The finding that in the SVZ of Ts65Dn mice treatment increased the number of proliferating cells indicates that 7,8-DHF positively enhances the proliferative potency of progenitor cells located in the SVZ. Considering that neurogenesis is mainly a prenatal event this suggests a positive effect of 7,8-DHF on the production of telencephalic neurons (and glia).

The production of neurons and glia occurs at discrete time points during fetal brain development. Gliogenesis follows neurogenesis and persists long after neurogenesis has ceased. During the early postnatal period, the SVZ of the lateral ventricle gives origin to glial cells, initially astrocytes and then oligodendrocytes, destined to the cortex and striatum (Brazel, 2003; Miller, 2007). Therefore, the proliferating cells found in the CX and STR of P2 mice are cells (most likely glioblasts) derived from the SVZ that have retained proliferative capacity during their migration. The low number of actively dividing cells found in CX and STR of untreated Ts65Dn mice is in agreement with the reduced proliferation potency observed in the SVZ of untreated Ts65Dn mice. The increase in the number of proliferating cells in the CX and STR of Ts65Dn mice after embryonic treatment with 7,8-DHF is consistent with the increase induced by treatment in the number of progenitors in the SVZ. In the cCX, at variance with rCX, treatment did not increase the number of proliferating cells. The molecular processes regulating astrocyte and oligodendrocyte precursor migration in DS remain poorly defined. However, the migration of cells from germinative zones not only depends on the

proliferation potency of the progenitor cells but is also under the control of environmental attractive/repulsive chemical signals (Brazel, 2003). The lack of an increase in the number of glioblasts in the cCX may be explained by lack of signals favoring cells migration.

Cells in the SGZ are the progenitors of neurons and astrocytes forming the hippocampal DG. The reduced number of proliferating cells found in the SGZ of untreated Ts65Dn mice indicates that the formation of the DG is impaired from the earliest phases of development. The finding that prenatal administration of 7,8-DHF was able to completely restore the number of the progenitors of future granule cells and astrocytes in the SGZ of Ts65Dn mice indicates that those progenitors are sensitive to the effect of 7,8-DHF not only during neonatal period, as previously demonstrated (Stagni, , 2017), but also during embryonic stages.

The number of proliferating cells was also reduced in the thalamic and hypothalamic regions of Ts65Dn mice. Most of the neurons forming the thalamus and hypothalamus are born during the period E11-E19, in the time window of our treatment. The progenitors of these cells arise from the VZ/SVZ laying the III ventricles (Wang, 2011). The reduced proliferation potency observed in P2 untreated Ts65Dn mice suggests that this reduction may be due to an impaired proliferation in the VZ/SVZ surrounding the III ventricle. This is consistent with the finding that aged people with DS have a reduction in the number of neuronal and glial cells in thalamic nuclei (Karlsen, 2014; Perry, 2019). Although this reduction may be part of a neurodegenerative process, it is also conceivable that alteration of neurogenesis during early brain development may be a determinant of the reduced number of thalamic neurons. We found that prenatal treatment with 7,8 DHF was able to increase the number of proliferating cells in the thalamus but not in the hypothalamus of Ts65Dn mice. This suggests that prenatal treatment with 7,8-DHF exerts a positive effect on the proliferation of diencephalic neural progenitors, although this effect is limited to the progenitors of cells destined to the thalamus.

Taken together these results demonstrate that early treatment with the natural flavonoid 7,8-DHF promotes a widespread pro-proliferative effect in the forebrain of the Ts65Dn mice. The magnitude of this pro-proliferative effects was different according to the brain region. 7,8-DHF specifically binds the TrkB receptor mimicking the action of the BDNF (Jang, 2010). Conflicting evidence exists concerning the pro-proliferative effect of the BDNF/TrkB system (Foltran, 2016; Vilar, 2016). Our previous study suggests that 7,8-DHF may influence proliferation in a non-cell autonomous manner (Stagni, 2017). The environment of the neurogenic niche and/or of the final destination of migrating

neuroblasts/glioblasts may explain the differences in the strength and distribution of the pro-proliferative effect of 7,8-DHF observed here.

P2 Ts65Dn mice displayed a reduced cell density in cortical layer II, but the number of cells in layer VI is similar to euploid mice, which is partially in agreement with our previous findings (Guidi, 2014). Embryonic treatment with 7,8-DHF in Ts65Dn mice was able to restore the number of cells of layer II and had no effect in layer VI. The restoration of cell density in layer II in treated Ts65Dn mice is coherent with the pro-proliferative effects of 7,8-DHF in the SVZ. Corticogenesis follow an inside-outside pattern, earlier born neurons settle into the deeper layers while later born neurons migrate past them and colonize more superficial layers. Projection neurons of the deeper layers arise from the VZ, while projection neurons of the outer layers arise from the SVZ. Corticogenesis in mice begins approximately on E10 (Brazel, 2003), at the time we initiated the embryonic treatment. Thus, the progenitors of layer II neurons had been exposed to treatment for a longer period in comparison with the progenitor giving origin to layer VI neurons. The necessity of a relatively long exposure to 7,8-DHF for the improvement of cell proliferation may explain the positive effect exerted by 7,8-DHF on cellularity of layer II but not of layer VI.

Since the hippocampus is a brain region seriously damaged in DS and exerts a critical role in learning and memory, we were interested in establishing whether prenatal treatment with 7,8-DHF was able to improve hippocampal development. Consistently with our previous study (Guidi, 2014), we found a reduced number of neurons in the DG and hippocampal field CA1 of P2 Ts65Dn mice. Prenatal treatment did not increase total cell number in the DG of Ts65Dn mice although it was able to attenuate the difference in comparison with euploid mice. Thus, although prenatal treatment with 7,8-DHF was able to restore the number of the granule cell progenitors in the SGZ, its effect was not sufficient to restore the number of granule neurons. In the hippocampus, treatment restored cell density in field CA1 of Ts65Dn mice. The total number of pyramidal neurons, however, did not reach the value of untreated euploid mice.

Taken together these results show that prenatal treatment with 7,8-DHF enhances cortical cellularity in Ts65Dn mice, but it has moderate effects on the hippocampal formation.

From the comparison of the effects of embryonic treatment with 7,8-DHF found here and the effects of prenatal administration of fluoxetine observed in our previous study (Guidi, 2014) it clearly emerges that the effect of fluoxetine on brain development is remarkably more prominent in

comparison with 7,8-DHF. Prenatal treatment with fluoxetine restored the number of proliferating cells in the rostral and caudal SVZ, SGZ, rostral and caudal neocortex, striatum, thalamus and hypothalamus in addition to other regions not examined here. Furthermore, fluoxetine was able to restore cell density in all cortical layers, DG and hippocampus. While the beneficial effects of 7,8-DHF disappear one month after treatment cessation (Giacomini, 2019), the effect of fluoxetine are retained after treatment cessation and translate into restoration of cognitive performance in adulthood (Guidi, 2014; Stagni, 2015). Taken together, these observations suggest that a prenatal treatment with fluoxetine could be a better choice than 7,8-DHF in order to restore the development of the trisomic brain. However, the use of fluoxetine during pregnancy may pose some caveats due to possible serious side effects, while 7,8-DHF in view of its chemical nature is potentially usable during gestation. Thus, despite its milder effects the natural flavonoid 7,8-DHF may be a better choice for a prenatal therapy.

In conclusion, the current study shows that prenatal treatment with 7,8-DHF has a positive influence on prenatal neurogenesis and cortical cellularity in a mouse model of DS. Since 7,8-DHF is orally bioavailable, a food supplementation with this flavonoid during pregnancy and in the early postnatal period may be considered as a safe preventive therapy for an overall improvement of brain development in DS.

REFERENCES

Aldridge, K., Reeves, R. H., Olson, L. E., & Richtsmeier, J. T. (2007). Differential effects of trisomy on brain shape and volume in related aneuploid mouse models. *American Journal of Medical Genetics, Part A*, *143*(10), 1060–1070. https://doi.org/10.1002/ajmg.a.31721

Alldred, M. J., Chao, H. M., Lee, S. H., Beilin, J., Powers, B. E., Petkova, E., … Ginsberg, S. D. (2019). Long-term effects of maternal choline supplementation on CA1 pyramidal neuron gene expression in the Ts65Dn mouse model of Down syndrome and Alzheimer's disease. *FASEB Journal*, *33*(9), 9871–9884. https://doi.org/10.1096/fj.201802669RR

Altman J. and Bayer S. (n.d.). MosaicOrgamzation of the Hippocampal NeuroepitheEumandthe Multiple GennimlSourcesofDentateG m d eCells, *342*, 325–342.

Altman, J., & Bayer, S. A. (n.d.). Migration and distribution of two populations of hippocampal granule cell precursors during the perinatal and postnatal periods. *Journal of Comparative Neurology*, *301*(3), 365–381. https://doi.org/10.1002/cne.903010304

Andersen, S. L. (2003). Trajectories of brain development: Point of vulnerability or window of opportunity? *Neuroscience and Biobehavioral Reviews*, *27*(1–2), 3–18. https://doi.org/10.1016/S0149-7634(03)00005-8

Antonarakis, S. E. (2017, March 1). Down syndrome and the complexity of genome dosage imbalance. *Nature Reviews Genetics*. Nature Publishing Group. https://doi.org/10.1038/nrg.2016.154

Antonarakis, S. E., Skotko, B. G., Rafii, M. S., Strydom, A., Pape, S. E., Bianchi, D. W., … Reeves, R. H. (2020). Down syndrome. *Nature Reviews Disease Primers*, *6*(1), 1–20. https://doi.org/10.1038/s41572-019-0143-7

Arumugam, A., Raja, K., Venugopalan, M., Chandrasekaran, B., Kovanur Sampath, K., Muthusamy, H., & Shanmugam, N. (2016). Down syndrome—A narrative review with a focus on anatomical features. *Clinical Anatomy*, *29*(5), 568–577. https://doi.org/10.1002/ca.22672

Ash, J. A., Velazquez, R., Kelley, C. M., Powers, B. E., Ginsberg, S. D., Mufson, E. J., & Strupp, B. J. (2014). Maternal choline supplementation improves spatial mapping and increases basal forebrain cholinergic neuron number and size in aged Ts65Dn mice. *Neurobiology of Disease*, *70*, 32–42. https://doi.org/10.1016/j.nbd.2014.06.001

Asim, A., Kumar, A., Muthuswamy, S., Jain, S., & Agarwal, S. (2015). "down syndrome: An insight of the disease." *Journal of Biomedical Science*, *22*(1), 1–9. https://doi.org/10.1186/s12929-015-0138-y

Aziz, N. M., Guedj, F., Pennings, J. L. A., Olmos-Serrano, J. L., Siegel, A., Haydar, T. F., & Bianchi, D. W. (2018). Lifespan analysis of brain development, gene expression and behavioral phenotypes in the Ts1Cje, Ts65Dn and Dp(16)1/Yey mouse models of Down syndrome. *DMM Disease Models and Mechanisms*, *11*(6). https://doi.org/10.1242/dmm.031013

Baburamani, A. A., Patkee, P. A., Arichi, T., & Rutherford, M. A. (2019). New approaches to studying early brain development in Down syndrome. *Developmental Medicine and Child Neurology*, *61*(8), 867–879. https://doi.org/10.1111/dmcn.14260

Barriga, G. G. D., Giralt, A., Anglada-Huguet, M., Gaja-Capdevila, N., Orlandi, J. G., Soriano, J., … Alberch, J. (2017). 7,8-dihydroxyflavone ameliorates cognitive and motor deficits in a Huntington's disease mouse model through specific activation of the PLCγ1 pathway. *Human Molecular Genetics*, *26*(16), 3144–3160. https://doi.org/10.1093/hmg/ddx198

Bartesaghi, R., Guidi, S., & Ciani, E. (2011). Is it possible to improve neurodevelopmental abnormalities in Down syndrome? *Reviews in the Neurosciences*, *22*(4), 419–455. https://doi.org/10.1515/RNS.2011.037

Baxter, L. L. (2000). Discovery and genetic localization of Down syndrome cerebellar phenotypes using the Ts65Dn mouse. *Human Molecular Genetics*, *9*(2), 195–202. https://doi.org/10.1093/hmg/9.2.195

Becker, L. E., Armstrong, D. L., & Chan, F. (1986). Dendritic atrophy in children with Down's syndrome. *Annals of Neurology*, *20*(4), 520–526. https://doi.org/10.1002/ana.410200413

Belicenko. (2007). Synaptic and Cognitive Abnormalities in Mouse Models of Down Syndrome: Exploring Genotype-Phenotype Relationships. *Journal of Comparative Neurology*, *346*(October 2007), 339–346. https://doi.org/10.1002/cne

Belichenko, P. V., Masliah, E., Kleschevnikov, A. M., Villar, A. J., Epstein, C. J., Salehi, A., & Mobley, W. C. (2004). Synaptic structural abnormalities in the Ts65Dn mouse model of Down syndrome. *Journal of Comparative Neurology*, *480*(3), 281–298. https://doi.org/10.1002/cne.20337

Benavides-Piccione, R., Ballesteros-Yáñez, I., Martínez De Lagrán, M., Elston, G., Estivill, X., Fillat, C., … Dierssen, M. (2004). On dendrites in Down syndrome and DS murine models: A spiny way to learn. *Progress in Neurobiology*, *74*(2), 111–126. https://doi.org/10.1016/j.pneurobio.2004.08.001

Bianchi, P., Ciani, E., Guidi, S., Trazzi, S., Felice, D., Grossi, G., … Bartesaghi, R. (2010). Early pharmacotherapy restores neurogenesis and cognitive performance in the Ts65Dn mouse model for down syndrome. *Journal of Neuroscience*, *30*(26), 8769–8779. https://doi.org/10.1523/JNEUROSCI.0534-10.2010

Blehaut, H., Mircher, C., Ravel, A., Conte, M., De Portzamparc, V., Poret, G., … Sturtz, F. G. (2010). Effect of leucovorin (folinic acid) on the developmental quotient of children with down's syndrome (trisomy 21) and influence of thyroid status. *PLoS ONE*, *5*(1), 1–9. https://doi.org/10.1371/journal.pone.0008394

Boada, R., Hutaff-Lee, C., Schrader, A., Weitzenkamp, D., Benke, T. A., Goldson, E. J., & Costa, A. C. S. (2012). Antagonism of NMDA receptors as a potential treatment for Down syndrome: A pilot randomized controlled trial. *Translational Psychiatry*, *2*(7), e141-11. https://doi.org/10.1038/tp.2012.66

Boltaev, U., Meyer, Y., Tolibzoda, F., Jacques, T., Gassaway, M., Xu, Q., … Sames, D. (2017). Multiplex quantitative assays indicate a need for re-evaluating reported small-molecule TrkB agonists. *Science Signaling*, *10*(493). https://doi.org/10.1126/scisignal.aal1670

Brazel, C. Y., Romanko, M. J., Rothstein, R. P., & Levison, S. W. (2003). Roles of the mammalian subventricular zone in brain development. *Progress in Neurobiology*, *69*(1), 49–69. https://doi.org/10.1016/S0301-0082(03)00002-9

Brumwell, C. L., & Curran, T. (2006). Developmental mouse brain gene expression maps. *Journal of Physiology*, *575*(2), 343–346. https://doi.org/10.1113/jphysiol.2006.112607

Bull, M. J., Saal, H. M., Braddock, S. R., Enns, G. M., Gruen, J. R., Perrin, J. M., … Spire, P. (2011). Clinical report - Health supervision for children with Down syndrome. *Pediatrics*, *128*(2), 393–406. https://doi.org/10.1542/peds.2011-1605

Buxhoeveden, D., Fobbs, A., Roy, E., & Casanova, M. (2002). Quantitative comparison of radial cell columns in children with Down's syndrome and controls. *Journal of Intellectual Disability Research*, *46*(1), 76–81. https://doi.org/10.1046/j.1365-2788.2002.00362.x

Bystron, I., Blakemore, C., & Rakic, P. (2008). Development of the human cerebral cortex: Boulder Committee revisited. *Nature Reviews Neuroscience*, *9*(2), 110–122. https://doi.org/10.1038/nrn2252

Calis, Z., Mogulkoc, R., & Baltaci, A. K. (2019). The roles of Flavonoles/Flavonoids in Neurodegeneration and Neuroinflammation. *Mini-Reviews in Medicinal Chemistry*, *19*. https://doi.org/10.2174/1389557519666190617150051

Chakrabarti, L., Best, T. K., Cramer, N. P., Carney, R. S. E., Isaac, J. T. R., Galdzicki, Z., & Haydar, T. F.

(2010). Olig1 and Olig2 triplication causes developmental brain defects in Down syndrome. *Nature Neuroscience*, *13*(8), 927–934. https://doi.org/10.1038/nn.2600

Chakrabarti, L., Galdzicki, Z., & Haydar, T. F. (2007). Defects in embryonic neurogenesis and initial synapse formation in the forebrain of the Ts65Dn mouse model of Down syndrome. *Journal of Neuroscience*, *27*(43), 11483–11495. https://doi.org/10.1523/JNEUROSCI.3406-07.2007

Chan, C. B., Tse1, M. C. L., Liu, X., Zhang, S., Schmidt, R., Otten, R., … Ye1, K. (2015). Activation of Muscular TrkB by its Small Molecular Agonist 7,8- Dihydroxyflavone Sex-Dependently Regulates Energy Metabolism in Diet-Induced Obese Mice. *Physiology & Behavior*, *176*(1), 139–148. https://doi.org/10.1016/j.physbeh.2017.03.040

Channell, M. M., Hahn, L. J., Rosser, T. C., Hamilton, D., Frank-Crawford, M. A., Capone, G. T., & Sherman, S. L. (2019). Characteristics Associated with Autism Spectrum Disorder Risk in Individuals with Down Syndrome. *Journal of Autism and Developmental Disorders*, *49*(9), 3543–3556. https://doi.org/10.1007/s10803-019-04074-1

Commenges, A. D., Scotet, V., Renaud, S., Dartigues, J., European, S., Apr, N., … Dartigues, J. (2016). Intake of Flavonoids and Risk of Dementia Published by : Springer Stable URL : http://www.jstor.org/stable/3581727, *16*(4), 357–363.

Conover, J. C., & Todd, K. L. (2017). Development and aging of a brain neural stem cell niche. *Experimental Gerontology*, *94*, 9–13. https://doi.org/10.1016/j.exger.2016.11.007

Contestabile, Andrea, Fila, T., Bartesaghi, R., & Ciani, E. (2009). Cell cycle elongation impairs proliferation of cerebellar granule cell precursors in the Ts65Dn mouse, an animal model for down syndrome. *Brain Pathology*, *19*(2), 224–237. https://doi.org/10.1111/j.1750-3639.2008.00168.x

Contestabile, Andrea, Fila, T., Bartesaghi, R., Contestabile, A., & Ciani, E. (2006). Choline acetyltransferase activity at different ages in brain of Ts65Dn mice, an animal model for Down's syndrome and related neurodegenerative diseases. *Journal of Neurochemistry*, *97*(2), 515–526. https://doi.org/10.1111/j.1471-4159.2006.03769.x

Contestabile, Andrea, Fila, T., Ceccarelli, C., Bonasoni, P., Bonapace, L., Santini, D., … Ciani, E. (2007). Cell Cycle Alteration and Decreased Cell Proliferation in the Hippocampal Dentate Gyrus and in the Neocortical Germinal Matrix of Fetuses With Down Syndrome and in Ts65Dn Mice.

Contestabile, Antonio, Ciani, E., & Contestabile, A. (2008). The place of choline acetyltransferase activity measurement in the "cholinergic hypothesis" of neurodegenerative diseases. *Neurochemical Research*, *33*(2), 318–327. https://doi.org/10.1007/s11064-007-9497-4

Cooper, J. D., Salehi, A., Delcroix, J. D., Howe, C. L., Belichenko, P. V., Chua-Couzens, J., … Mobley, W. C. (2001). Failed retrograde transport of NGF in a mouse model of Down's syndrome: Reversal of cholinergic neurodegenerative phenotypes following NGF infusion. *Proceedings of the National Academy of Sciences of the United States of America*, *98*(18), 10439–10444. https://doi.org/10.1073/pnas.181219298

Corrales, A., Vidal, R., García, S., Vidal, V., Martínez, P., García, E., … Rueda, N. (2014). Chronic melatonin treatment rescues electrophysiological and neuromorphological deficits in a mouse model of Down syndrome. *Journal of Pineal Research*, *56*(1), 51–61. https://doi.org/10.1111/jpi.12097

Cunha, C., Brambilla, R., & Thomas, K. L. (2010). A simple role for BDNF in learning and memory? *Frontiers in Molecular Neuroscience*, *3*(February), 1–14. https://doi.org/10.3389/neuro.02.001.2010

D. Hamlett, E., A. Boger, H., Ledreux, A., M. Kelley, C., J. Mufson, E., F. Falangola, M., … E. Granholm, A.-C. (2015). Cognitive Impairment, Neuroimaging, and Alzheimer Neuropathology in Mouse Models of Down Syndrome. *Current Alzheimer Research*, *13*(1), 35–52. https://doi.org/10.2174/1567205012666150921095505

Dang, V., Medina, B., Das, D., Moghadam, S., Martin, K. J., Lin, B., … Salehi, A. (2014). Formoterol, a long-acting β2 adrenergic agonist, improves cognitive function and promotes dendritic complexity in a mouse model of down syndrome. *Biological Psychiatry*, *75*(3), 179–188. https://doi.org/10.1016/j.biopsych.2013.05.024

Das, I., Park, J., Shin, J. H., Jeon, S. K., Lorenzi, H., David, J., … Reeves, R. H. (2013). Hedgehog agonist therapy corrects structural and cognitive deficits in a Down syndrome mouse model, *5*(201), 1–20. https://doi.org/10.1126/scitranslmed.3005983.Hedgehog

Das, I., & Reeves, R. H. (2011). The use of mouse models to understand and improve cognitive deficits in down syndrome. *DMM Disease Models and Mechanisms*, *4*(5), 596–606. https://doi.org/10.1242/dmm.007716

de Graaf-Peters, V. B., & Hadders-Algra, M. (2006). Ontogeny of the human central nervous system: What is happening when? *Early Human Development*, *82*(4), 257–266. https://doi.org/10.1016/j.earlhumdev.2005.10.013

de la Torre, R., de Sola, S., Hernandez, G., Farré, M., Pujol, J., Rodriguez, J., … Freixas, R. (2016). Safety and efficacy of cognitive training plus epigallocatechin-3-gallate in young adults with Down's syndrome (TESDAD): A double-blind, randomised, placebo-controlled, phase 2 trial. *The Lancet Neurology*, *15*(8), 801–810. https://doi.org/10.1016/S1474-4422(16)30034-5

De la Torre, R., De Sola, S., Pons, M., Duchon, A., de Lagran, M. M., Farré, M., … Dierssen, M. (2014). Epigallocatechin-3-gallate, a DYRK1A inhibitor, rescues cognitive deficits in Down syndrome mouse models and in humans. *Molecular Nutrition and Food Research*, *58*(2), 278–288. https://doi.org/10.1002/mnfr.201300325

Dey, A., Bhowmik, K., Chatterjee, A., Chakrabarty, P. B., Sinha, S., & Mukhopadhyay, K. (2013). Down Syndrome Related Muscle Hypotonia: Association with COL6A3 Functional SNP rs2270669. *Frontiers in Genetics*, *4*(April), 1–8. https://doi.org/10.3389/fgene.2013.00057

Dierssen, M. (2012). Down syndrome: The brain in trisomic mode. *Nature Reviews Neuroscience*, *13*(12), 844–858. https://doi.org/10.1038/nrn3314

Driscoll, D. A., & Gross, S. (2009). Prenatal screening for aneuploidy. *New England Journal of Medicine*, *360*(24), 2556. https://doi.org/10.1056/NEJMcp0900134

Duchon, A., Raveau, M., Chevalier, C., Nalesso, V., Sharp, A. J., & Herault, Y. (2011). Identification of the translocation breakpoints in the Ts65Dn and Ts1Cje mouse lines: Relevance for modeling down syndrome. *Mammalian Genome*, *22*(11–12), 674–684. https://doi.org/10.1007/s00335-011-9356-0

Ellis, J. M., Hooi, K. T., Gilbert, R. E., Muller, D. P. R., Henley, W., Moy, R., … Logan, S. (2008). Supplementation with antioxidants and folinic acid for children with Down's syndrome: Randomised controlled trial. *Bmj*, *336*(7644), 594–597. https://doi.org/10.1136/bmj.39465.544028.AE

Emili, M., Stagni, F., Elisa, M., Uguagliati, B., Giacomini, A., & Guidi, S. (2020). Neurobiology of Disease Neonatal therapy with clenbuterol and salmeterol restores spinogenesis and dendritic complexity in the dentate gyrus of the Ts65Dn model of Down syndrome. *Neurobiology of Disease*, *140*(January), 104874. https://doi.org/10.1016/j.nbd.2020.104874

Fabian Fernandez, Jonathan C. Trinidad, Martina Blank, Dong-Dong Feng, A. L. B., & Garner, C. C. (2008). Normal protein composition of synapses in Ts65Dn mice, a mouse model of Down syndrome. *Bone*, *23*(1), 1–7. https://doi.org/10.1038/jid.2014.371

Fernandez, F., Morishita, W., Zuniga, E., Nguyen, J., Blank, M., Malenka, R. C., & Garner, C. C. (2007). Pharmacotherapy for cognitive impairment in a mouse model of Down syndrome. *Nature Neuroscience*, *10*(4), 411–413. https://doi.org/10.1038/nn1860

Ferrara, B. T., & Thompson, E. P. (2019). A method for visualizing fluorescence of flavonoid therapeutics in vivo in the model eukaryote Dictyostelium discoideum. *BioTechniques*, *66*(2),

65–71. https://doi.org/10.2144/btn-2018-0084
Foltran, R. B., & Diaz, S. L. (2016). BDNF isoforms: a round trip ticket between neurogenesis and serotonin? *Journal of Neurochemistry*, 204–221. https://doi.org/10.1111/jnc.13658
Foulkes, L., & Blakemore, S. J. (2018). Studying individual differences in human adolescent brain development. *Nature Neuroscience*, *21*(3), 315–323. https://doi.org/10.1038/s41593-018-0078-4
Fujita, S. (1967). Quantitative analysis of cell proliferation and differentiation in the cortex of the postnatal mouse cerebellum. *The Journal of Cell Biology*, *32*(2), 277–287. https://doi.org/10.1083/jcb.32.2.277
García-Cerro, S., Rueda, N., Vidal, V., Puente, A., Campa, V., Lantigua, S., … Martínez-Cué, C. (2020). Prenatal Administration of Oleic Acid or Linolenic Acid Reduces Neuromorphological and Cognitive Alterations in Ts65dn Down Syndrome Mice. *The Journal of Nutrition*. https://doi.org/10.1093/jn/nxaa074
Gardiner, K. J. (2014). Pharmacological approaches to improving cognitive function in down syndrome: Current status and considerations. *Drug Design, Development and Therapy*, *9*, 103–125. https://doi.org/10.2147/DDDT.S51476
Giacomini, A., Stagni, F., Emili, M., Uguagliati, B., Rimondini, R., Bartesaghi, R., & Guidi, S. (2019). Timing of Treatment with the Flavonoid 7,8-DHF Critically Impacts on its effects on learning and memory in the Ts65Dn Mouse. *Antioxidants*, *8*(6), 1–19. https://doi.org/10.3390/antiox8060163
Giacomini, A., Stagni, F., Trazzi, S., Guidi, S., Emili, M., Brigham, E., … Bartesaghi, R. (2015). Inhibition of APP gamma-secretase restores Sonic Hedgehog signaling and neurogenesis in the Ts65Dn mouse model of Down syndrome. *Neurobiology of Disease*, *82*, 385–396. https://doi.org/10.1016/j.nbd.2015.08.001
Girard, N., Koob, M., & Brunel, H. (2016). Normal development. *Handbook of Clinical Neurology*, *136*, 1091–1119. https://doi.org/10.1016/B978-0-444-53486-6.00057-0
Godfrey, M., & Lee, N. R. (2018). Memory profiles in Down syndrome across development: A review of memory abilities through the lifespan. *Journal of Neurodevelopmental Disorders*, *10*(1). https://doi.org/10.1186/s11689-017-9220-y
Gonzalez, A., Moya-Alvarado, G., Gonzalez-Billaut, C., & Bronfman, F. C. (2016). Cellular and molecular mechanisms regulating neuronal growth by brain-derived neurotrophic factor. *Cytoskeleton*, *73*(10), 612–628. https://doi.org/10.1002/cm.21312
Grieco, J., Pulsifer, M., Seligsohn, K., Skotko, B., & Schwartz, A. (2015). Down syndrome: Cognitive and behavioral functioning across the lifespan. *American Journal of Medical Genetics, Part C: Seminars in Medical Genetics*, *169*(2), 135–149. https://doi.org/10.1002/ajmg.c.31439
Guidi, S., Bonasoni, P., Ceccarelli, C., Santini, D., Gualtieri, F., Ciani, E., & Bartesaghi, R. (2008). Neurogenesis impairment and increased cell death reduce total neuron number in the hippocampal region of fetuses with Down syndrome. *Brain Pathology*, *18*(2), 180–197. https://doi.org/10.1111/j.1750-3639.2007.00113.x
Guidi, S., Ciani, E., Bonasoni, P., Santini, D., & Bartesaghi, R. (2011). Widespread proliferation impairment and hypocellularity in the cerebellum of fetuses with down syndrome. *Brain Pathology*, *21*(4), 361–373. https://doi.org/10.1111/j.1750-3639.2010.00459.x
Guidi, S., Giacomini, A., Stagni, F., Emili, M., Uguagliati, B., Bonasoni, M. P., & Bartesaghi, R. (2018). Abnormal development of the inferior temporal region in fetuses with Down syndrome. *Brain Pathology*, *28*(6), 986–998. https://doi.org/10.1111/bpa.12605
Guidi, S., Stagni, F., Bianchi, P., Ciani, E., Giacomini, A., De Franceschi, M., … Bartesaghi, R. (2014). Prenatal pharmacotherapy rescues brain development in a Down's syndrome mouse model. *Brain*, *137*(2), 380–401. https://doi.org/10.1093/brain/awt340

Guidi, S., Stagni, F., Bianchi, P., Ciani, E., Ragazzi, E., Trazzi, S., … Bartesaghi, R. (2013). Early pharmacotherapy with fluoxetine rescues dendritic pathology in the ts65dn mouse model of down syndrome. *Brain Pathology*, *23*(2), 129–143. https://doi.org/10.1111/j.1750-3639.2012.00624.x

Guihard-Costa, A. M., Khung, S., Delbecque, K., Ménez, F., & Delezoide, A. L. (2006). Biometry of face and brain in fetuses with trisomy 21. *Pediatric Research*, *59*(1), 33–38. https://doi.org/10.1203/01.pdr.0000190580.88391.9a

Gupta, M., Dhanasekaran, A. R., & Gardiner, K. J. (2016). Mouse models of Down syndrome: gene content and consequences. *Mammalian Genome*, *27*(11–12), 538–555. https://doi.org/10.1007/s00335-016-9661-8

Han, X., Zhu, S., Wang, B., Chen, L., Li, R., Yao, W., & Qu, Z. (2014). Antioxidant action of 7,8-dihydroxyflavone protects PC12 cells against 6-hydroxydopamine-induced cytotoxicity. *Neurochemistry International*, *64*(1), 18–23. https://doi.org/10.1016/j.neuint.2013.10.018

Hanney, M., Prasher, V., Williams, N., Jones, E. L., Aarsland, D., Corbett, A., … Ballard, C. (2012). Memantine for dementia in adults older than 40 years with Down's syndrome (MEADOWS): A randomised, double-blind, placebo-controlled trial. *The Lancet*, *379*(9815), 528–536. https://doi.org/10.1016/S0140-6736(11)61676-0

Harada, C. N., Natelson Love, M. C., & Triebel, K. L. (2013). Normal cognitive aging. *Clinics in Geriatric Medicine*, *29*(4), 737–752. https://doi.org/10.1016/j.cger.2013.07.002

Hart, S. J., Visootsak, J., Tamburri, P., Phuong, P., Baumer, N., Hernandez, M. C., … Spiridigliozzi, G. A. (2017). Pharmacological interventions to improve cognition and adaptive functioning in Down syndrome: Strides to date. *American Journal of Medical Genetics, Part A*, *173*(11), 3029–3041. https://doi.org/10.1002/ajmg.a.38465

Hattori, M., Fujiyama, A., Taylor, T. D., Watanabe, H., Yada, T., Patterson, D., … Yaspo, M.-L. (2000). The DNA sequence of human chromosome 21 - supplement table. *Nature*, *405*(May), 7118.

Helguera, P., Pelsman, A., Pigino, G., Wolvetang, E., Head, E., & Busciglio, J. (2005). Ets-2 Promotes the Activation of a Mitochondrial Death Pathway in Down'S Syndrome Neurons. *Journal of Neuroscience*, *25*(9), 2295–2303. https://doi.org/10.1523/JNEUROSCI.5107-04.2005

Herault, Y., Delabar, J. M., Fisher, E. M. C., Tybulewicz, V. L. J., Yu, E., & Brault, V. (2017). Rodent models in Down syndrome research: Impact and future opportunities. *DMM Disease Models and Mechanisms*, *10*(10), 1165–1186. https://doi.org/10.1242/dmm.029728

Holtzman, D. M., Santucci, D., Kilbridge, J., Chua-Couzens, J., Fontana, D. J., Daniels, S. E., … Mobley, W. C. (1996). Developmental abnormalities and age-related neurodegeneration in a mouse model of Down syndrome. *Proceedings of the National Academy of Sciences of the United States of America*, *93*(23), 13333–13338. https://doi.org/10.1073/pnas.93.23.13333

Huang, E. J., & Reichardt, L. F. (2003). Trk Receptors: Roles in Neuronal Signal Transduction. *Annual Review of Biochemistry*, *72*(1), 609–642. https://doi.org/10.1146/annurev.biochem.72.121801.161629

Huang, Y. Z., Pan, E., Xiong, Z. Q., & McNamara, J. O. (2008). Zinc-Mediated Transactivation of TrkB Potentiates the Hippocampal Mossy Fiber-CA3 Pyramid Synapse. *Neuron*, *57*(4), 546–558. https://doi.org/10.1016/j.neuron.2007.11.026

Hunter, C. L., Bimonte, H. A., & Granholm, A. C. E. (2003). Behavioral comparison of 4 and 6 month-old Ts65Dn mice: Age-related impairments in working and reference memory. *Behavioural Brain Research*, *138*(2), 121–131. https://doi.org/10.1016/S0166-4328(02)00275-9

Incerti, M., Horowitz, K., Roberson, R., Abebe, D., Toso, L., Caballero, M., & Spong, C. Y. (2012). Prenatal Treatment Prevents Learning Deficit in Down Syndrome Model. *PLoS ONE*, *7*(11), 3–6. https://doi.org/10.1371/journal.pone.0050724

Insausti, A. M., Megías, M., Crespo, D., Cruz-Orive, L. M., Dierssen, M., Vallina, T. F., … Flórez, J.

(1998). Hippocampal volume and neuronal number in Ts65Dn mice: A murine model of Down syndrome. *Neuroscience Letters*, *253*(3), 175–178. https://doi.org/10.1016/S0304-3940(98)00641-7

Jang, S. W., Liu, X., Yepes, M., Shepherd, K. R., Miller, G. W., Liu, Y., … Ye, K. (2010). A selective TrkB agonist with potent neurotrophic activities by 7,8-dihydroxyflavone. *Proceedings of the National Academy of Sciences of the United States of America*, *107*(6), 2687–2692. https://doi.org/10.1073/pnas.0913572107

Jessell, T. M., & Sanes, J. R. (2000). Development: The decade of the developing brain. *Current Opinion in Neurobiology*, *10*(5), 599–611. https://doi.org/10.1016/S0959-4388(00)00136-7

Ji, Y., Lu, Y., Yang, F., Shen, W., Tang, T. T.-T., Feng, L., … Lu, and B. (2010). Acute and gradual increases in BDNF concentration elicit distinct signaling and functions in hippocampal neurons. *Physiology & Behavior*, *176*(1), 139–148. https://doi.org/10.1016/j.physbeh.2017.03.040

Kafitz, K. W., Rose, C. R., Thoenen, H., & Konnerth, A. (1999). Neurotrophin-evoked rapid excitation through TrkB receptors. *Nature*, *401*(6756), 918–921. https://doi.org/10.1038/44847

Karlsen, A. S., Korbo, S., Uylings, H. B. M., & Pakkenberg, B. (2014). A stereological study of the mediodorsal thalamic nucleus in Down syndrome. *Neuroscience*, *279*, 253–259. https://doi.org/10.1016/j.neuroscience.2014.08.046

Kelley, C. M., Ash, J. A., Powers, B. E., Velazquez, R., Alldred, M. J., Ikonomovic, M. D., … Mufson, E. J. (2016). Effects of Maternal Choline Supplementation on the Septohippocampal Cholinergic System in the Ts65Dn Mouse Model of Down Syndrome HHS Public Access. *Curr Alzheimer Res. Curr Alzheimer Res*, *13*(1), 84–96.

Kelley, C. M., Ginsberg, S. D., Alldred, M. J., Strupp, B. J., & Mufson, E. J. (2019). Maternal Choline Supplementation Alters Basal Forebrain Cholinergic Neuron Gene Expression in the Ts65Dn Mouse Model of Down Syndrome. *Developmental Neurobiology*, *79*(7), 664–683. https://doi.org/10.1002/dneu.22700

Kelley, C. M., Powers, B. E., Velazquez, R., Ash, J. A., Ginsberg, S. D., Strupp, B. J., & Mufson, ad E. J. (2015). Maternal choline supplementation differentially alters the basal forebrain cholinergic system of young-adult Ts65Dn and disomic mice, *522*(6), 1390–1410. https://doi.org/10.1002/cne.23492.Maternal

Kempermann, G., & Gage, F. H. (2002). Genetic influence on phenotypic differentiation in adult hippocampal neurogenesis. *Developmental Brain Research*, *134*(1–2), 1–12. https://doi.org/10.1016/S0165-3806(01)00224-3

Khundrakpam, B. S., Lewis, J. D., Zhao, L., Chouinard-Decorte, F., & Evans, A. C. (2016). Brain connectivity in normally developing children and adolescents. *NeuroImage*, *134*, 192–203. https://doi.org/10.1016/j.neuroimage.2016.03.062

Kishnani, P. S., Heller, J. H., Spiridigliozzi, G. A., Lott, I., Escobar, L., Richardson, S., … McRae, T. (2010). Donepezil for treatment of cognitive dysfunction in children with Down syndrome aged 10-17. *American Journal of Medical Genetics, Part A*, *152 A*(12), 3028–3035. https://doi.org/10.1002/ajmg.a.33730

Kishnani, P. S., Sommer, B. R., Handen, B. L., Seltzer, B., Capone, G. T., Spiridigliozzi, G. A., … McRae, T. (2009). The efficacy, safety, and tolerability of donepezil for the treatment of young adults with Down syndrome'. *American Journal of Medical Genetics, Part A*, *149*(8), 1641–1654. https://doi.org/10.1002/ajmg.a.32953

Kleschevnicov, A. M., Belichenko, P. V., Villar, A. J., Epstein, C. J., Malenka, R. C., & Mobley, W. C. (2004). Hippocampal long-term potentiation suppressed by increased inhibition in the Ts65Dn mouse, a genetic model of down syndrome. *Journal of Neuroscience*, *24*(37), 8153–8160. https://doi.org/10.1523/JNEUROSCI.1766-04.2004

Levison, S. W., & Goldman, J. E. (1993). Both oligodendrocytes and astrocytes develop from

progenitors in the subventricular zone of postnatal rat forebrain. *Neuron*, *10*(2), 201–212. https://doi.org/10.1016/0896-6273(93)90311-E

Liu, C., Chan, C. B., & Ye, K. (2016). 7,8-dihydroxyflavone, a small molecular TrkB agonist, is useful for treating various BDNF-implicated human disorders. *Translational Neurodegeneration*, *5*(1), 1–9. https://doi.org/10.1186/s40035-015-0048-7

Liu, X., Chan, C. B., Jang, S. W., Pradoldej, S., Huang, J., He, K., … Ye, K. (2010). A synthetic 7,8-dihydroxyflavone derivative promotes neurogenesis and exhibits potent antidepressant effect. *Journal of Medicinal Chemistry*, *53*(23), 8274–8286. https://doi.org/10.1021/jm101206p

Liu, X., Chan, C. B., Qi, Q., Xiao, G., Luo, H. R., He, X., & Ye, K. (2012). Optimization of a small tropomyosin-related kinase B (TrkB) agonist 7,8-dihydroxyflavone active in mouse models of depression. *Journal of Medicinal Chemistry*, *55*(19), 8524–8537. https://doi.org/10.1021/jm301099x

Liu, X., Obiany, O., Chan, C. B., Huang, J., Xue, S., Yang, J. J., … Ye, K. (2014). Biochemical and biophysical investigation of the brain-derived neurotrophic factor mimetic 7,8-dihydroxyflavone in the binding and activation of the trkb receptor. *Journal of Biological Chemistry*, *289*(40), 27571–27584. https://doi.org/10.1074/jbc.M114.562561

Liu, X., Qi, Q., Xiao, G., Li, J., Luo, H. R., & Ye, and K. (2013). O-Methylated Metabolite of 7,8-Dihydroxyflavone Activates TrkB Receptor and Displays Antidepressant Activity. *Pharmacology*, *91*(3–4), 185–200. https://doi.org/10.1016/j.physbeh.2017.03.040

López-Hidalgo, R., Ballestín, R., Vega, J., Blasco-Ibáñez, J. M., Crespo, C., Gilabert-Juan, J., … Varea, E. (2016). Hypocellularity in the murine model for down syndrome Ts65Dn is not affected by adult neurogenesis. *Frontiers in Neuroscience*, *10*(MAR). https://doi.org/10.3389/fnins.2016.00075

Lorenzi, H. A., & Reeves, R. H. (2006). Hippocampal hypocellularity in the Ts65Dn mouse originates early in development. *Brain Research*, *1104*(1), 153–159. https://doi.org/10.1016/j.brainres.2006.05.022

Lott, I. T. (2012). Neurological phenotypes for Down syndrome across the life span. *Progress in Brain Research*, *197*(714), 101–121. https://doi.org/10.1016/B978-0-444-54299-1.00006-6

Lott, I. T., & Dierssen, M. (2010). Cognitive deficits and associated neurological complications in individuals with Down's syndrome. *The Lancet Neurology*, *9*(6), 623–633. https://doi.org/10.1016/S1474-4422(10)70112-5

Lott, I. T., Doran, E., Nguyen, V. Q., Tournay, A., Head, E., & Gillen, D. L. (2011). Down syndrome and dementia: A randomized, controlled trial of antioxidant supplementation. *American Journal of Medical Genetics, Part A*, *155*(8), 1939–1948. https://doi.org/10.1002/ajmg.a.34114

Lu, J., Lian, G., Zhou, H., Esposito, G., Steardo, L., Delli-Bovi, L. C., … Sheen, V. (2012). OLIG2 over-expression impairs proliferation of human down syndrome neural progenitors. *Human Molecular Genetics*, *21*(10), 2330–2340. https://doi.org/10.1093/hmg/dds052

Luo, Y., Smith, J. V., Paramasivam, V., Burdick, A., Curry, K. J., Buford, J. P., … Butko, P. (2002). Inhibition of amyloid-β aggregation and caspase-3 activation by the Ginkgo biloba extract EGb761. *Proceedings of the National Academy of Sciences of the United States of America*, *99*(19), 12197–12202. https://doi.org/10.1073/pnas.182425199

Maki, T., Okamoto, Y., Carare, R. O., Hase, Y., Hattori, Y., Hawkes, C. A., … Ihara, M. (2014). Phosphodiesterase III inhibitor promotes drainage of cerebrovascular β-amyloid. *Annals of Clinical and Translational Neurology*, *1*(8), 519–533. https://doi.org/10.1002/acn3.79

Malberg, J. E., Eisch, A. J., Nestler, E. J., & Duman, R. S. (2000). Chronic antidepressant treatment increases neurogenesis in adult rat hippocampus. *Journal of Neuroscience*, *20*(24), 9104–9110. https://doi.org/10.1523/jneurosci.20-24-09104.2000

Manach, C., Scalbert, A., Morand, C., Rémésy, C., & Jiménez, L. (2004). Polyphenols: Food sources

and bioavailability. *American Journal of Clinical Nutrition*, *79*(5), 727–747. https://doi.org/10.1093/ajcn/79.5.727

Marin-Padilla, M. (1976). Pyramidal cell abnormalities in the motor cortex of a child with Down's syndrome. A Golgi study. *Journal of Comparative Neurology*, *167*(1), 63–81. https://doi.org/10.1002/cne.901670105

Marshall, C. A. G., Suzuki, S. O., & Goldman, J. E. (2003). Gliogenic and neurogenic progenitors of the subventricular zone: Who are they, where did they come from, and where are they going? *Glia*, *43*(1), 52–61. https://doi.org/10.1002/glia.10213

Martínez-Cué, C., Martínez, P., Rueda, N., Vidal, R., García, S., Vidal, V., … Hernández, M. C. (2013). Reducing GABAA α5 receptor-mediated inhibition rescues functional and neuromorphological deficits in a mouse model of down syndrome. *Journal of Neuroscience*, *33*(9), 3953–3966. https://doi.org/10.1523/JNEUROSCI.1203-12.2013

Marzban, H., Del Bigio, M. R., Alizadeh, J., Ghavami, S., Zachariah, R. M., & Rastegar, M. (2015). Cellular commitment in the developing cerebellum. *Frontiers in Cellular Neuroscience*, *8*(JAN), 1–26. https://doi.org/10.3389/fncel.2014.00450

Massarwa_2013_neural plate mouse.pdf. (n.d.).

Mattson, M. P., & Arumugam, T. V. (2018). Hallmarks of Brain Aging: Adaptive and Pathological Modification by Metabolic States. *Cell Metabolism*, *27*(6), 1176–1199. https://doi.org/10.1016/j.cmet.2018.05.011

McElyea, S. D., Starbuck2, J. M., Brink, D. T., Harrington, E., Blazek, J. D., Ghonemia, A., … Roper, and R. J. (2016). Influence of Prenatal EGCG Treatment and Dyrk1a Dosage Reduction on Craniofacial Features Associated with Down Syndrome, (317).

Miale, I. L., & Sidman, R. L. (1961). An autoradiographic analysis of histogenesis in the mouse cerebellum. *Experimental Neurology*, *4*(4), 277–296. https://doi.org/10.1016/0014-4886(61)90055-3

Miller, F. D., & Gauthier, A. S. (2007). Timing Is Everything: Making Neurons versus Glia in the Developing Cortex. *Neuron*, *54*(3), 357–369. https://doi.org/10.1016/j.neuron.2007.04.019

Minichiello, L. (2009). TrkB signalling pathways in LTP and learning. *Nature Reviews Neuroscience*, *10*(12), 850–860. https://doi.org/10.1038/nrn2738

Mircher, C., Sacco, S., Bouis, C., Gallard, J., Pichot, A., Le Galloudec, E., … Sturtz, F. G. (2020). Thyroid hormone and folinic acid in young children with Down syndrome: the phase 3 ACTHYF trial. *Genetics in Medicine*, *22*(1), 44–52. https://doi.org/10.1038/s41436-019-0597-8

Moon, J., Maclean, K. N., Chen, M., U., S. G., Strawderman, M., Cornell, D. A. L., & Cornell, B. J. S. (2010). Perinatal Choline Supplementation Improves Cognitive Functioning and Emotion Regulation in the Ts65Dn Mouse Model of Down Syndrome.

Mukai, Y., & Sato, S. (2011). Polyphenol-containing azuki bean (Vigna angularis) seed coats attenuate vascular oxidative stress and inflammation in spontaneously hypertensive rats. *Journal of Nutritional Biochemistry*, *22*(1), 16–21. https://doi.org/10.1016/j.jnutbio.2009.11.004

Necchi, D., Lomoio, S., & Scherini, E. (2008). Axonal abnormalities in cerebellar Purkinje cells of the Ts65Dn mouse. *Brain Research*, *1238*, 181–188. https://doi.org/10.1016/j.brainres.2008.08.010

Nery, S., Fishell, G., & Corbin, J. G. (2002). The caudal ganglionic eminence is a source of distinct cortical and subcortical cell populations. *Nature Neuroscience*, *5*(12), 1279–1287. https://doi.org/10.1038/nn971

Olmos-Serrano J.L, Tyler W. A., Cabral H. J., and H. T. F. (2006). Longitudinal measures of cognition in the Ts65Dn mouse: refining windows and defining modalities for therapeutic intervention in Down syndrome. *Physiology & Behavior*, *176*(1), 139–148.

https://doi.org/10.1016/j.physbeh.2017.03.040
Olson, L. E., Roper, R. J., Sengstaken, C. L., Peterson, E. A., Aquino, V., Galdzicki, Z., … Reeves, R. H. (2007). Trisomy for the Down syndrome "critical region" is necessary but not sufficient for brain phenotypes of trisomic mice. *Human Molecular Genetics*, *16*(7), 774–782. https://doi.org/10.1093/hmg/ddm022
Pangalos, C., Avramopoulos, D., Blouin, J. L., Raoul, O., DeBlois, M. C., Prieur, M., … Antonarakis, S. E. (1994). Understanding the mechanism(s) of mosaic trisomy 21 by using DNA polymorphism analysis. *American Journal of Human Genetics*, *54*(3), 473–481.
Papavassiliou, P., York, T. P., Gursoy, N., Hill, G., Vanner, L., Sundaram, U., … Jackson-cook, C. (2013). Present in Different Tissues, *0*(4), 573–583. https://doi.org/10.1002/ajmg.a.32729.The
Pérez-Cremades, D., Hernández, S., Blasco-Ibáñez, J. M., Crespo, C., Nacher, J., & Varea, E. (2010). Alteration of inhibitory circuits in the somatosensory cortex of Ts65Dn mice, a model for Down's syndrome. *Journal of Neural Transmission*, *117*(4), 445–455. https://doi.org/10.1007/s00702-010-0376-9
Pérez-Hernández, J., Zaldívar-Machorro, V. J., Villanueva-Porras, D., Vega-Ávila, E., & Chavarría, A. (2016). A Potential Alternative against Neurodegenerative Diseases: Phytodrugs. *Oxidative Medicine and Cellular Longevity*, *2016*. https://doi.org/10.1155/2016/8378613
Perez-Vizcaino, F., & Fraga, C. G. (2018). Research trends in flavonoids and health. *Archives of Biochemistry and Biophysics*, *646*(March), 107–112. https://doi.org/10.1016/j.abb.2018.03.022
Perry, J. C., Pakkenberg, B., & Vann, S. D. (2019). Striking reduction in neurons and glial cells in anterior thalamic nuclei of older patients with Down syndrome. *Neurobiology of Aging*, *75*, 54–61. https://doi.org/10.1016/j.neurobiolaging.2018.11.009
Pradhan, J., Noakes, P. G., & Bellingham, M. C. (2019). The Role of Altered BDNF/TrkB Signaling in Amyotrophic Lateral Sclerosis. *Frontiers in Cellular Neuroscience*, *13*(August), 1–16. https://doi.org/10.3389/fncel.2019.00368
Rachidi, M., & Lopes, C. (2008). Mental retardation and associated neurological dysfunctions in Down syndrome: A consequence of dysregulation in critical chromosome 21 genes and associated molecular pathways. *European Journal of Paediatric Neurology*, *12*(3), 168–182. https://doi.org/10.1016/j.ejpn.2007.08.010
Rafii, M. S., Skotko, B. G., McDonough, M. E., Pulsifer, M., Evans, C., Doran, E., … Lott, I. T. (2017). A Randomized, Double-Blind, Placebo-Controlled, Phase II Study of Oral ELND005 (scyllo - Inositol) in Young Adults with Down Syndrome without Dementia. *Journal of Alzheimer's Disease*, *58*(2), 401–411. https://doi.org/10.3233/JAD-160965
Rantamäki, T. (2019). TrkB neurotrophin receptor at the core of antidepressant effects, but how? *Cell and Tissue Research*, *377*(1), 115–124. https://doi.org/10.1007/s00441-018-02985-6
Reinholdt, L. G., Ding, Y., Gilbert, G. J., Czechanski, A., Jeffrey, P., Roper, R. J., … Harbor, B. (2011). Molecular Characterization of the Translocation Breakpoints in the Down Syndrome Mouse Model, Ts65Dn, *22*(Chr 16), 685–691. https://doi.org/10.1007/s00335-011-9357-z.Molecular
Rendeiro, C., Rhodes, J. S., & Spencer, J. P. E. (2015). The mechanisms of action of flavonoids in the brain: Direct versus indirect effects. *Neurochemistry International*, *89*, 126–139. https://doi.org/10.1016/j.neuint.2015.08.002
Rice, D., & Barone, S. (2000). Critical periods of vulnerability for the developing nervous system: Evidence from humans and animal models. *Environmental Health Perspectives*, *108*(SUPPL. 3), 511–533. https://doi.org/10.2307/3454543
Roizen, N. J., & Patterson, D. (2003). Down ' s syndrome, *361*, 1281–1289.
Roncacé, V., Burattini, C., Stagni, F., Guidi, S., Giacomini, A., Emili, M., … Bartesaghi, R. (2017). Neuroanatomical alterations and synaptic plasticity impairment in the perirhinal cortex of the

Ts65Dn mouse model of Down syndrome. *Neurobiology of Disease*, *106*, 89–100. https://doi.org/10.1016/j.nbd.2017.06.017

Roper, R. J., Baxter, L. L., Saran, N. G., Klinedinst, D. K., Beachy, P. A., & Reeves, R. H. (2006). Defective cerebellar response to mitogenic Hedgehog signaling in Down's syndrome mice. *Proceedings of the National Academy of Sciences of the United States of America*, *103*(5), 1452–1456. https://doi.org/10.1073/pnas.0510750103

Roper, R. J., & Reeves, R. H. (2006). Understanding the basis for Down syndrome phenotypes. *PLoS Genetics*, *2*(3), 0231–0236. https://doi.org/10.1371/journal.pgen.0020050

Roper, R. J., St. John, H. K., Philip, J., Lawler, A., & Reeves, R. H. (2006). Perinatal loss of Ts65Dn Down syndrome mice. *Genetics*, *172*(1), 437–443. https://doi.org/10.1534/genetics.105.050898

Rosenbloom, M., Barclay, T., Johnsen, J., Erickson, L., Svitak, A., Pyle, M., … Hanson, L. R. (2020). Double-Blind Placebo-Controlled Pilot Investigation of the Safety of a Single Dose of Rapid-Acting Intranasal Insulin in Down Syndrome. *Drugs in R and D*, *20*(1), 11–15. https://doi.org/10.1007/s40268-020-00296-2

Rueda, N., Flórez, J., & Martínez-Cué, C. (2012). Mouse models of down syndrome as a tool to unravel the causes of mental disabilities. *Neural Plasticity*, *2012*. https://doi.org/10.1155/2012/584071

Ruparelia, A., Pearn, M. L., & Mobley, W. C. (2013). Aging and intellectual disability: Insights from mouse models of down syndrome. *Developmental Disabilities Research Reviews*, *18*(1), 43–50. https://doi.org/10.1002/ddrr.1127

Ryu, M. J., Kang, K. A., Piao, M. J., Kim, K. C., Zheng, J., Yao, C. W., … Hyun, J. W. (2014). Effect of 7, 8-dihydroxyflavone on the up-regulation of Nrf2-mediated heme oxygenase-1 expression in hamster lung fibroblasts. *In Vitro Cellular and Developmental Biology - Animal*, *50*(6), 549–554. https://doi.org/10.1007/s11626-014-9735-4

Sansom, S. N., & Livesey, F. J. (2009). Gradients in the brain: the control of the development of form and function in the cerebral cortex. *Cold Spring Harbor Perspectives in Biology*, *1*(2), 1–16. https://doi.org/10.1101/cshperspect.a002519

Sasi, M., Vignoli, B., Canossa, M., & Blum, R. (2017). Neurobiology of local and intercellular BDNF signaling. *Pflugers Archiv : European Journal of Physiology*, *469*(5–6), 593–610. https://doi.org/10.1007/s00424-017-1964-4

Seidl, R., Bidmon, B., Bajo, M., Yoo, B. C., Lubec, G., Cairns, N., & LaCasse, E. C. (2001). Evidence for apoptosis in the fetal Down syndrome brain. *Journal of Child Neurology*, *16*(6), 438–442. https://doi.org/10.1177/088307380101600610

Shichiri, M., Yoshida, Y., Ishida, N., Hagihara, Y., Iwahashi, H., Tamai, H., & Niki, E. (2011). α-Tocopherol suppresses lipid peroxidation and behavioral and cognitive impairments in the Ts65Dn mouse model of Down syndrome. *Free Radical Biology and Medicine*, *50*(12), 1801–1811. https://doi.org/10.1016/j.freeradbiomed.2011.03.023

Sillitoe, R. V., & Joyner, A. L. (2007). Morphology, Molecular Codes, and Circuitry Produce the Three-Dimensional Complexity of the Cerebellum. *Annual Review of Cell and Developmental Biology*, *23*(1), 549–577. https://doi.org/10.1146/annurev.cellbio.23.090506.123237

Spencer, J. P. E. (2007). The interactions of flavonoids within neuronal signalling pathways. *Genes and Nutrition*, *2*(3), 257–273. https://doi.org/10.1007/s12263-007-0056-z

Spencer, J. P. E. (2009). Flavonoids and brain health: Multiple effects underpinned by common mechanisms. *Genes and Nutrition*, *4*(4), 243–250. https://doi.org/10.1007/s12263-009-0136-3

Spencer, J. P. E., Abd El Mohsen, M. M., & Rice-Evans, C. (2004). Cellular uptake and metabolism of flavonoids and their metabolites: Implications for their bioactivity. *Archives of Biochemistry and Biophysics*, *423*(1), 148–161. https://doi.org/10.1016/j.abb.2003.11.010

Spiridigliozzi, G. A., Hart, S. J., Heller, J. H., Schneider, H. E., Baker, J. A., Weadon, C., … Kishnani, P. S. (2016). Safety and efficacy of rivastigmine in children with Down syndrome: A double blind placebo controlled trial. *American Journal of Medical Genetics, Part A*, *170*(6), 1545–1555. https://doi.org/10.1002/ajmg.a.37650

Stagni, F. (2018). Stagni_2018_subiculum .pdf.

Stagni, F., Giacomini, A., Emili, M., Guidi, S., & Bartesaghi, R. (2018a). Neurogenesis impairment: An early developmental defect in Down syndrome. *Free Radical Biology and Medicine*, *114*(July 2017), 15–32. https://doi.org/10.1016/j.freeradbiomed.2017.07.026

Stagni, F., Giacomini, A., Emili, M., Guidi, S., & Bartesaghi, R. (2018b). Neurogenesis impairment: An early developmental defect in Down syndrome. *Free Radical Biology and Medicine*, *114*(June 2017), 15–32. https://doi.org/10.1016/j.freeradbiomed.2017.07.026

Stagni, F., Giacomini, A., Emili, M., Trazzi, S., Guidi, S., Sassi, M., … Bartesaghi, R. (2016). Short- and long-term effects of neonatal pharmacotherapy with epigallocatechin-3-gallate on hippocampal development in the Ts65Dn mouse model of Down syndrome. *Neuroscience*, *333*, 277–301. https://doi.org/10.1016/j.neuroscience.2016.07.031

Stagni, F., Giacomini, A., Emili, M., Uguagliati, B., Bonasoni, M. P., Bartesaghi, R., & Guidi, S. (2019). Subicular hypotrophy in fetuses with Down syndrome and in the Ts65Dn model of Down syndrome. *Brain Pathology*, *29*(3), 366–379. https://doi.org/10.1111/bpa.12663

Stagni, F., Giacomini, A., Guidi, S., Ciani, E., & Bartesaghi, R. (2015). Timing of therapies for downsyndrome: The sooner, the better. *Frontiers in Behavioral Neuroscience*, *9*(OCT). https://doi.org/10.3389/fnbeh.2015.00265

Stagni, F., Giacomini, A., Guidi, S., Ciani, E., Ragazzi, E., Filonzi, M., … Bartesaghi, R. (2015). Long-term effects of neonatal treatment with fluoxetine on cognitive performance in Ts65Dn mice. *Neurobiology of Disease*, *74*, 204–218. https://doi.org/10.1016/j.nbd.2014.12.005

Stagni, F., Giacomini, A., Guidi, S., Emili, M., Uguagliati, B., Salvalai, M. E., … Bartesaghi, R. (2017). A flavonoid agonist of the TrkB receptor for BDNF improves hippocampal neurogenesis and hippocampus-dependent memory in the Ts65Dn mouse model of DS. *Experimental Neurology*, *298*(March), 79–96. https://doi.org/10.1016/j.expneurol.2017.08.018

Stagni, F., Magistretti, J., Guidi, S., Ciani, E., Mangano, C., Calzà, L., & Bartesaghi, R. (2013). Pharmacotherapy with Fluoxetine Restores Functional Connectivity from the Dentate Gyrus to Field CA3 in the Ts65Dn Mouse Model of Down Syndrome. *PLoS ONE*, *8*(4). https://doi.org/10.1371/journal.pone.0061689

Stagni, F., Raspanti, A., Giacomini, A., Guidi, S., Emili, M., Ciani, E., … Bartesaghi, R. (2017). Long-term effect of neonatal inhibition of APP gamma-secretase on hippocampal development in the Ts65Dn mouse model of Down syndrome. *Neurobiology of Disease*, *103*, 11–23. https://doi.org/10.1016/j.nbd.2017.03.012

Stagni, F., Salvalai, M. E., Giacomini, A., Emili, M., Uguagliati, B., Xia, E., … Guidi, S. (2019). Neonatal treatment with cyclosporine A restores neurogenesis and spinogenesis in the Ts65Dn model of Down syndrome. *Neurobiology of Disease*, *129*(May), 44–55. https://doi.org/10.1016/j.nbd.2019.05.005

Stiles, J., & Jernigan, T. L. (2010). The basics of brain development. *Neuropsychology Review*, *20*(4), 327–348. https://doi.org/10.1007/s11065-010-9148-4

Suzuki, S., Numakawa, T., Shimazu, K., Koshimizu, H., Hara, T., Hatanaka, H., … Kojima, M. (2004). BDNF-induced recruitment of TrkB receptor into neuronal lipid rafts: Roles in synaptic modulation. *Journal of Cell Biology*, *167*(6), 1205–1215. https://doi.org/10.1083/jcb.200404106

Takashima, S., Becker, L. E., Armstrong, D. L., & Chan, F. (1981). Abnormal neuronal development in the visual cortex of the human fetus and infant with down's syndrome. A quantitative and

qualitative golgi study. *Brain Research*, *225*(1), 1–21. https://doi.org/10.1016/0006-8993(81)90314-0

TAKASHIMA, S., IIDA, K., MITO, T., & ARIMA, M. (1994). Dendritic and histochemical development and ageing in patients with Down's syndrome. *Journal of Intellectual Disability Research*, *38*(3), 265–273. https://doi.org/10.1111/j.1365-2788.1994.tb00394.x

Teipel, S. J., & Hampel, H. (2006). Neuroanatomy of Down syndrome in vivo: A model of preclinical Alzheimer's disease. *Behavior Genetics*, *36*(3), 405–415. https://doi.org/10.1007/s10519-006-9047-x

Terahara, N. (2015). Flavonoids in foods: A review. *Natural Product Communications*, *10*(3), 521–528. https://doi.org/10.1177/1934578x1501000334

Toso, L., & Cameroni, I. (2008). Prevention of Developmental Delays in a. *Obstetrics & Gynecology*, *112*(6), 1242–1251.

Tozuka, Y., Fukuda, S., Namba, T., Seki, T., & Hisatsune, T. (2005). GABAergic excitation promotes neuronal differentiation in adult hippocampal progenitor cells. *Neuron*, *47*(6), 803–815. https://doi.org/10.1016/j.neuron.2005.08.023

Tsuji, M., Ohshima, M., Yamamoto, Y., Saito, S., Hattori, Y., Tanaka, E., … Ogawa, Y. (2020). Cilostazol, a Phosphodiesterase 3 Inhibitor, Moderately Attenuates Behaviors Depending on Sex in the Ts65Dn Mouse Model of Down Syndrome. *Frontiers in Aging Neuroscience*, *12*(April), 1–12. https://doi.org/10.3389/fnagi.2020.00106

V., P., & M., A. (2011). Deficiency of Adult Neurogenesis in the Ts65Dn Mouse Model of Down Syndrome. *Genetics and Etiology of Down Syndrome*. https://doi.org/10.5772/24585

Vacca, R. A., Bawari, S., Valenti, D., Tewari, D., Nabavi, S. F., Shirooie, S., … Nabavi, S. M. (2019). Down syndrome: Neurobiological alterations and therapeutic targets. *Neuroscience and Biobehavioral Reviews*, *98*(October 2018), 234–255. https://doi.org/10.1016/j.neubiorev.2019.01.001

Velazquez, R., Ash, J. A., Powers, B. E., Kelley, C. M., Strawderman, M., Luscher, Z. I., … Strupp, B. J. (2013). Maternal choline supplementation improves spatial learning and adult hippocampal neurogenesis in the Ts65Dn mouse model of Down syndrome. *Neurobiology of Disease*, *58*, 92–101. https://doi.org/10.1016/j.nbd.2013.04.016

Versacci, P., Di Carlo, D., Digilio, M. C., & Marino, B. (2018). Cardiovascular disease in Down syndrome. *Current Opinion in Pediatrics*, *30*(5), 616–622. https://doi.org/10.1097/MOP.0000000000000661

Vicari, S. (2006). Motor development and neuropsychological patterns in persons with Down syndrome. *Behavior Genetics*, *36*(3), 355–364. https://doi.org/10.1007/s10519-006-9057-8

Vilar, M., & Mira, H. (2016). Regulation of neurogenesis by neurotrophins during adulthood: Expected and unexpected roles. *Frontiers in Neuroscience*, *10*(FEB), 1–9. https://doi.org/10.3389/fnins.2016.00026

VINK, J., INCERTI, M., TOSO, L., ROBERSON, R., ABEBE, D., & SPONG, C. Y. (2009). Prenatal NAP+SAL Prevents Developmental Delay in Down Syndrome through affects on NMDA and GABA receptors. *Physiology & Behavior*, *176*(1), 139–148. https://doi.org/10.1016/j.physbeh.2017.03.040

Visu-Petra, L., Benga, O., Ţincaş, I., & Miclea, M. (2007). Visual-spatial processing in children and adolescents with Down's syndrome: A computerized assessment of memory skills. *Journal of Intellectual Disability Research*, *51*(12), 942–952. https://doi.org/10.1111/j.1365-2788.2007.01002.x

Wang, L., Bluske, K. K., Dickel, L. K., & Nakagawa, Y. (2011). Basal progenitor cells in the embryonic mouse thalamus - their molecular characterization and the role of neurogenins and Pax6. *Neural Development*, *6*(1). https://doi.org/10.1186/1749-8104-6-35

Whittle, N., Sartori, S. B., Dierssen, M., Lubec, G., & Singewald, N. (2007). Fetal Down syndrome brains exhibit aberrant levels of neurotransmitters critical for normal brain development. *Pediatrics*, *120*(6). https://doi.org/10.1542/peds.2006-3448

Williams, R. J., Spencer, J. P. E., & Rice-Evans, C. (2004). Flavonoids: Antioxidants or signalling molecules? *Free Radical Biology and Medicine*, *36*(7), 838–849. https://doi.org/10.1016/j.freeradbiomed.2004.01.001

Yin, X., Jin, N., Shi, J., Zhang, Y., Wu, Y., Gong, C. X., … Liu, F. (2017). Dyrk1A overexpression leads to increase of 3R-tau expression and cognitive deficits in Ts65Dn Down syndrome mice. *Scientific Reports*, *7*(1), 1–12. https://doi.org/10.1038/s41598-017-00682-y

Yu, T., Liu, C., Belichenko, P., Clapcote, S. J., Li, S., Pao, A., … Yu, Y. E. (2010). Effects of individual segmental trisomies of human chromosome 21 syntenic regions on hippocampal long-term potentiation and cognitive behaviors in mice. *Brain Research*, *1366*, 162–171. https://doi.org/10.1016/j.brainres.2010.09.107

Zeng, Y., Liu, Y., Wu, M., Liu, J., & Hu, Q. (2012). Activation of TrkB by 7,8-dihydroxyflavone prevents fear memory defects and facilitates amygdalar synaptic plasticity in aging. *Journal of Alzheimer's Disease*, *31*(4), 765–778. https://doi.org/10.3233/JAD-2012-120886

WEB SITES

https://clinicaltrials.gov
https://www.anzctr.org.au